Photochemistry and photophysics of lanthanide complexes

Lisa Marie Bushby

PHOTOCHEMISTRY AND PHOTOPHYSICS OF LANTHANIDE COMPLEXES

Lisa Marie Bushby

Department of Chemistry,

University of Durham, Durham

Submitted in partial fulfilment of the requirements for the degree of Doctor of Philosophy, University of Durham.

September 2001

DECLARATION

The work described in this thesis was carried out in the Chemistry Department of the University of Durham between October 1998 and September 2001. This thesis is the work of the author except where acknowledged by reference, and has not been submitted for any other degree.

STATEMENT OF COPYRIGHT

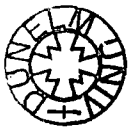

ABSTRACT

Luminescent lanthanide complexes have proven to be a productive area of research due in essence to their unique emission properties enabling their use in a variety of applications.

A major drawback to using lanthanides is their low extinction coefficients, so that the antenna effect is often used to overcome this problem. In this way, the antenna chromophore absorbs incoming radiation and transfers the energy to the ion, leading to indirect excitation of the lanthanide. Understanding this mechanism of energy transfer is of fundamental importance both for the theory of the photophysical processes, and for the development of more efficient materials. In this thesis, many of the areas of both the population and the deactivation of the lanthanide excited states are discussed.

The time resolved data of the Tm^{3+} ion in a variety of solvents and chelate systems have been measured, and the effects of deuteration on the decay kinetics investigated.

The mechanism of energy transfer is followed by detailed kinetic measurements of a complex with a benzophenone containing chromophore. The calculation of the pure radiative lifetime allowed the efficiency of each of the steps involved in the sensitisation process to be determined for the first time. Changing the coordination environment around the ion, even slightly, by the addition of a single CH_2 group into the arm of the ligand affects the oscillator strength of the hypersensitive transitions in both the Eu^{3+} and Tb^{3+} complexes, and influences the efficiency of energy transfer.

Intramolecular sensitisation of Eu^{3+} ions by acetophenone containing ligands was investigated in a series with increasing electron donating ability of the chromophore. It was found that the efficiency of energy transfer increases with the polarity of the antenna, but that in the case of a dimethylamino substituted ligand, the solvent also has a profound effect on the intensity of Eu^{3+} emission.

Energy transfer to bound Eu^{3+} and Tb^{3+} ions in aqueous micellar systems is demonstrated, with the process dependent on the hydrophobic properties of the chromophore and the properties of the surfactant.

Photoinduced electron transfer reactions are found to occur in ethoxybenzyl substituted complexes with the emission from the chromophore and from the lanthanide ion dependent upon the lanthanide reduction potential and the ΔG value of both the forward and backward electron transfer reactions.

ACKNOWLEDGMENTS

I would like to thank my supervisor, Dr Andy Beeby, to whom I am exceptionally grateful for the guidance he has given and the patience he has shown me throughout the whole of my Ph.D.

For helping me out in the lab and making sure my time there has been an enjoyable one, I would like to thank the former and present occupants of CG 7 who've all become good friends Allison, Simon, and Sylvia.
For ensuring my brief visits to Oxford were good fun as well as informative and productive, I would like to thank everyone I met there, especially Kai Look and Zhenjia Wang.

I would like to acknowledge the kind donation of complexes by Schering AG (ethoxybenzyl), Dr J. A. G. Williams (benzophenone and acetophenone) and Dr I. A. Fallis, (micelles). Simon again I thank for proof reading this thesis, for providing more computing assistance than the IT service ever believed possible, and for spending copious amounts of precious brain power time on lanthanide luminescence. I would also like to thank Dr J. A. G. Williams for several helpful discussions.

I am grateful for the financial support given by the EPSRC and Opsys displays Ltd. allowing this project to take place.

Finally, I would like to say a special thank you to my family and friends, especially Dad, Mum, and Victoria.

CONTENTS

LIST OF FIGURES

CHAPTER 1

CHAPTER 5

CHAPTER 6

CHAPTER 7

APPENDIX A

LIST OF TABLES

CHAPTER 7

APPENDIX A

Ln = lanthanide

M = metal

λ_{em} = emission wavelength / nm

λ_{ex} = excitation wavelength / nm

λ_{max} = wavelength (band) maximum / nm

T = temperature

FWHM = full width at half maximum

IR = infrared

uv = ultraviolet

E = energy

h = Planck's constant = 6.626×10^{-34} J s

c= speed of light = 2.998×10^{8} m s^{-1}

N_A = Avogadro's number = 6.022×10^{23} mol^{-1}

1.1 The Lanthanides

The lanthanides[1] comprise 14 elements from cerium to lutetium, but often also include lanthanum with the consecutive addition of electrons into one of the 7 4f orbitals (^{57}La[Xe]6s^{2}5d^{1}4f^0 → ^{71}Lu[Xe]6s^{2}5d^{1}4f^{14}).

The first three ionisation enthalpies of the lanthanides are low so that in solution and in the solid state compounds and complexes are usually found in their 3+ oxidation state. Other states, Ln^{4+} and Ln^{2+}, do exist however, for example, Ce can also give Ce^{4+}. Sm, Eu, and Yb, are all known as metastable M^{2+} ions in aqueous solutions, organic complexes, and in the solid state[2], due to the stabilising effect of the electronic configuration; Sm^{2+} 4f^6, Eu^{2+} 4f^7, and Yb^{2+} 4f^{14}. The standard reduction potential, E^θ of the $Eu^{3+} + e^- \rightarrow Eu^{2+}$ reduction = - 0.35 V, and Eu^{2+} has been shown to persist for times of the order of minutes to hours in dilute acid solution[3].

The lanthanides are characterised by an incompletely filled 4f shell. The 4f orbitals lie close to the nucleus and are shielded from the surroundings by the filled 5s^2 and 5p^6 orbitals. Therefore the influence of the chemical environment, specifically the effect of the ligands on the 4f^n configuration is small.

The ionic radii of the lanthanide(III) ions reduces from 1.17 Å in La^{3+} to 1.00 Å in Lu^{3+}, in a phenomenon known as the lanthanide contraction. The 4f electrons are rather ineffective at screening the nucleus from the peripheral electrons, hence as the nuclear charge increases there is a subsequent contraction in ionic radius[1].

Due to the large ionic radii of the Ln^{3+} ions and the fact that the 4f electrons constitute inner shells and are therefore unavailable for bonding, the lanthanides act as 'hard' cations resembling the alkali and alkaline earth metals e.g. Ca^{2+} / Na^+, and form few complexes. Those complexes that do form generally do so with 'hard' ligands, and normally bond to oxygen or nitrogen containing ligands such as phosphinates and carboxylates[4].

1.2 Electronic structure of Ln^{3+} ions

The Ln^{3+} ions in their ground state configuration, contain the closed shell electronic structure of the noble gas xenon,

$$1s^2\ 2s^2\ 2p^6\ 3s^2\ 3p^6\ 3d^{10}\ 4s^2\ 4p^6\ 4d^{10}\ 5s^2\ 5p^6 = \{Xe\}$$

and have 2 or 3 external electrons ($6s^2$ / $5d6s^2$), in addition to their complement of $4f^n$ electrons.

1.2.1 Term symbols

The distribution of the electrons around the nucleus of a Ln^{3+} ion can be described by a wavefunction that is specified by 4 quantum numbers, n, L, S and J.

n = principal quantum number
L = orbital angular momentum quantum number
S = spin angular momentum quantum number
J = spin orbit coupling quantum number

The electronic energy levels of the Ln^{3+} ions are described by their term symbols being given by $^{2S+1}L_J$, where 2S+1 is the multiplicity of the state[12].
The electrons in the 4f orbitals give rise to a number of different energy levels due to the distinct interactions occurring within the shell.
The largest of the interactions which separates the configuration into the ^{2S+1}L terms is the Coulombic repulsion between the electrons in the 4f orbitals. The terms are then split by the spin and orbital angular momenta (spin-orbit coupling) yielding the electronic energy levels described by the term symbols shown in fig. 1-1. Finally, any further splitting (seen as fine structure in the absorption and emission spectra and labelled "sublevels" in fig. 1-2) observed is due to the small, but significant ligand field. In the case of the Ln^{3+} ions the 4f orbitals are well shielded by the outer 5s and 5p shells and the influence of the ligand field is very small compared to that observed in the d-d transitions of transition metals amounting to only 10^2 cm^{-1}. The interactions and their corresponding contributions to the splittings observed are shown schematically in fig. 1-2 using the Eu^{3+} ion as an example.

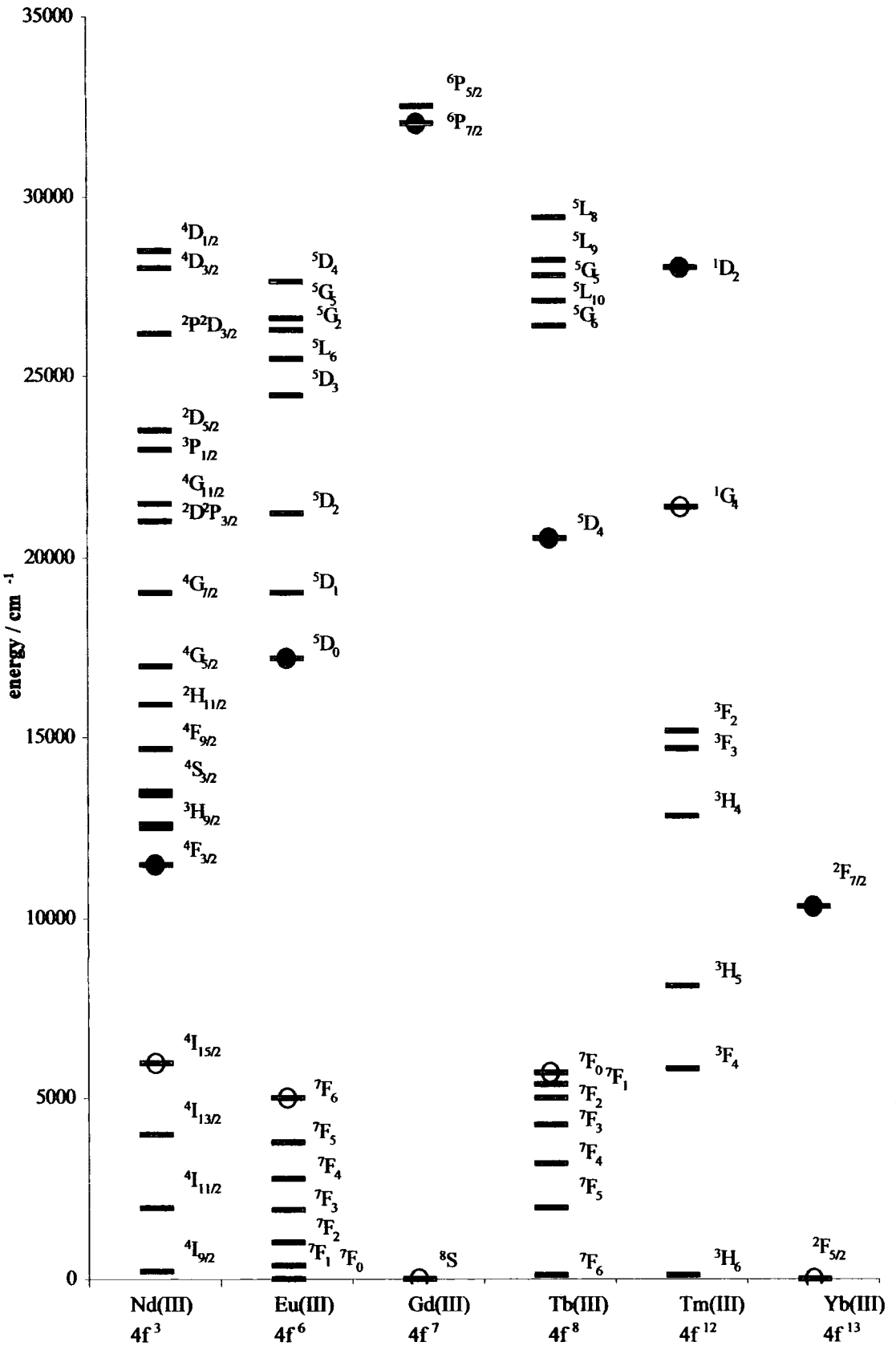

Figure 1-1 *Electronic energy levels of several lanthanide ions. The commonly observed luminescent state(s) have been marked with a filled circle, an open circle indicates the highest non-luminescent state. Adapted from J. Chem. Phys.,* **1974**, *62*, 208[5].

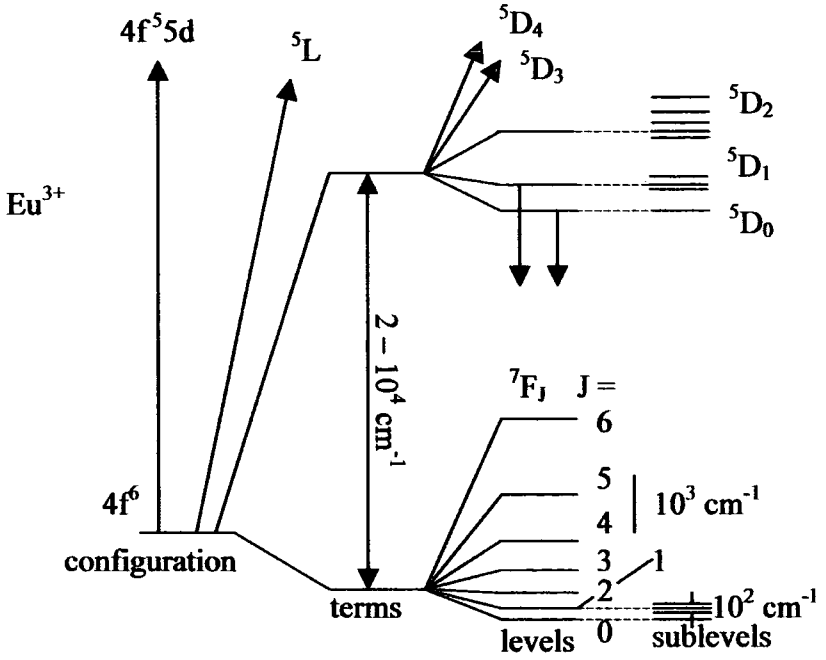

***Figure 1-2** Schematic diagram showing the splitting of the energy levels belonging to the [Xe] $4f^6$ $5d^0$ configuration of Eu^{3+} taken from Inorg. Chim. Acta, **1987**, 139, 219* [6]

1.2.2 f-d transitions

The parity allowed optical transitions of the Ln^{3+} ions are inter-configurational ($4f^n \rightarrow 4f^{n-1}5d$) and are more prevalent in the Ln^{3+} ions which are most easily oxidised to their 4+ states, Ce^{3+}, Pr^{3+} and Tb^{3+}. These f-d transitions are higher in energy (see fig. 1-3) than the f-f transitions, occurring mainly in the uv region as broad bands. Conversely, the f-d transitions are most energetic for those ions which are easily reduced to their 2+ states, Sm^{3+}, Eu^{3+} and Yb^{3+} and occur in the short wavelength region of the uv spectrum.

The electronic absorption and emission spectra for most of the Ln^{3+} ions at wavelengths > 200 nm, involve only transitions within the $4f^n$ configuration. f-d transitions are discussed in more detail in ref. [7].

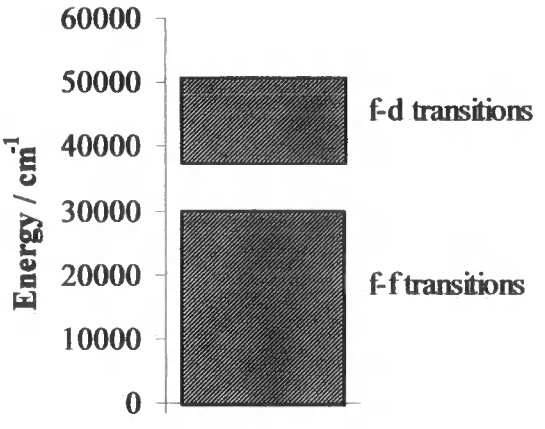

Figure 1-3 *Energy level diagram showing relative energies of Tb^{3+} f-f and f-d transitions. Data taken from J. Phys. Soc. Japan,* **1971**, *31*, 828 [8]

1.2.3 f-f transitions

The luminescence from the lanthanide ions is typically of interest due to particular properties of the electronic transitions shown by some of the ions. As described earlier, transitions within the f-f electronic energy levels of the Ln^{3+} ions results in characteristic narrow absorption and emission bands. An example of a Tb^{3+} emission spectrum is displayed in fig. 1-4. Due to the shielding of the f electrons from the surrounding ligands by the outer orbitals[9] the electronic transitions show more similarity to those shown by isolated atoms than the much broader bands seen in the f-d transitions and those observed in organic molecules. The f-f transitions of the gas phase lanthanides are much narrower, $< 1\ cm^{-1}$, but there is still some small ligand effect.

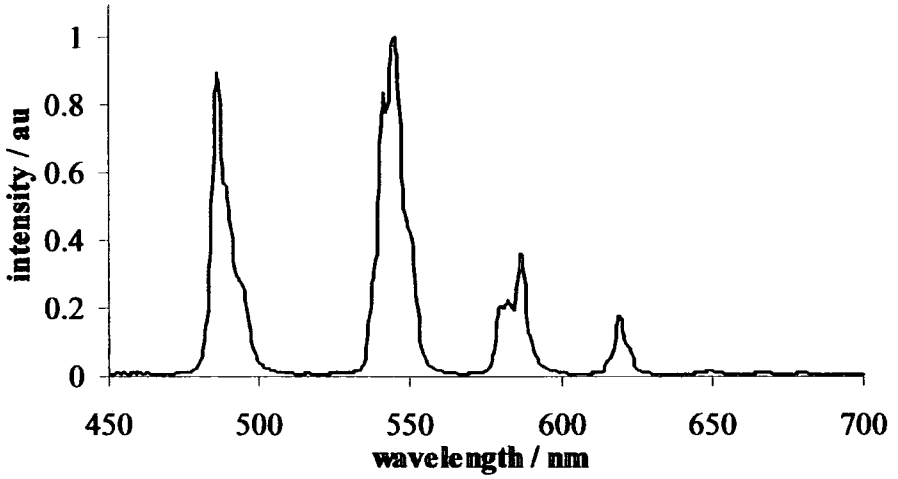

Figure 1-4 *Steady state emission spectrum of a* Tb^{3+} *complex,* $\lambda_{ex} = 300$ *nm bandpass = 1 nm, emission bandpass = 1 nm*

The f orbitals are *ungerade* so that any f-f transitions are formally 'forbidden' by the Laporte selection rules since they involve a change in multiplicity, resulting in low ε values[2] (typically ≤ 1 mol^{-1} dm^3 cm^{-1}). A consequence of low oscillator strengths is low k_f values (k_f = rate of fluorescence) and long pure radiative lifetimes. The Ln^{3+} ions therefore also exhibit long pure radiative lifetimes, with certain ions (e.g. Eu^{3+} and Tb^{3+}) also showing relatively long luminescent lifetimes of the order of ms[10,11].

1.2.3.1 Luminescence

Luminescence is the term given to describe the radiative decay process and an excited electronic state. It is a more general term than fluorescence or phosphorescence in which the change in spin ΔS upon relaxation is zero or non-zero respectively[12]. Formally, processes with $\Delta S \neq 0$ are forbidden, however, in the case of the lanthanides, the transitions $\Delta S = 0$ and $\Delta S \neq 0$ are both equally allowed. For this reason, the term luminescence is used to describe their emission.

For organic molecules, fluorescence usually occurs from the lowest vibrational level of the S_1 state, and as a spin allowed transition, occurs quickly, typically on the ns time scale; phosphorescence occurs after intersystem crossing (ISC) from an excited singlet state to an excited triplet state. This process is spin forbidden, and consequently, the timescale is much longer ca. ms-s. ISC occurs where the potential energy curves of the singlet and

triplet states intersect. The rate of ISC, k_{ISC} is governed by the energy gap and the electronic configuration of the states undergoing ISC. See fig. 1-5.

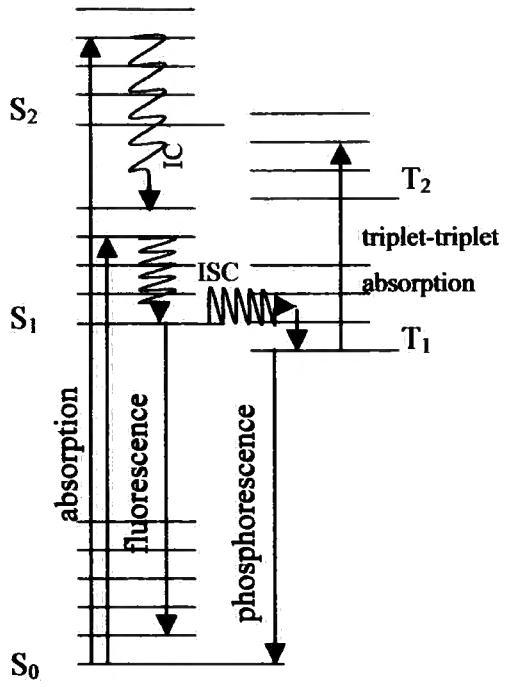

***Figure 1-5** Jablonski diagram showing absorption and deactivation processes of organic molecules*

1.3 The nature of the f-f transitions

1.3.1 Background

In general, atomic spectra have to obey the following selection rules:

$\Delta S = 0$, the spin selection rule forbids electronic transitions between levels with different spin states

$\Delta L = 0, \pm 1$, with $\Delta l = \pm 1$, the orbital angular momentum of an individual electron must change during the transition

$\Delta J = 0, \pm 1$, $J = 0$ to $J = 0$ is forbidden

The parity selection rule, forbids electronic (electric-dipole) transitions between levels with the same parity (e.g. f-f transitions)

The relaxation of the selection rules is connected to wavefunction mixing from the original unperturbed wavefunctions. This can be due to several physical phenomena, such as spin-orbit coupling or electronic vibrational coupling.
The ligand field in transition metal complexes relaxes the influence of the parity selection rule preventing d-d transitions; however, since the f orbitals are only weakly affected by the ligand field, the parity selection rule still holds for f-f transitions.

Since the f-f transitions are strictly forbidden by the parity selection rule, a number of studies have concentrated on the factors that govern the intensity observed in the f-f transitions. After Van Vleck in 1937[13] ruled out the possibility of the lines seen in the Ln^{3+} spectra being due to f-d transitions (he calculated that these transitions would be more energetic), and then a series of papers published in the 1940s[14] studying the possible nature of the intensity of the f-f transitions with regards to forced electric dipole, magnetic dipole, and electric quadrupole mechanisms, considerable interest in the intensities of certain bands in the absorption and emission spectra of the Ln^{3+} ions has developed.

1.3.2 Magnetic and forced electric dipole transitions

Two mechanisms by which the f-f transitions within Ln^{3+} ions can gather intensity have since been established - magnetic dipole (MD) and induced (or forced) electric dipole $(ED)^2$.
In general, electronic transitions arise from an interaction between the electrons in the molecule or ion with the oscillating electric dipole moment associated with the electromagnetic radiation, and the magnetic dipole moment has little influence. However, according to certain selection rules, electronic transitions induced by the MD component also become allowed. Certain transitions within the 4f configuration obey the $\Delta J = 0, \pm 1$ selection rule and are such MD transitions. They are unaffected by the environment around the ion, and have constant, though low, oscillator strengths[15].
The uneven components of the ligand field which are present in sites without inversion symmetry mix small amounts of opposite parity wavefunctions. A Ln^{3+} ion in a vacuum would display only absorption and emission bands with MD intensity, but in coordinating environments forced ED transitions occurring with no change in the parity, as opposed to true ED transitions, become allowed by the mixing of opposite parity wavefunctions (5d into 4f). i.e. the ED transitions "borrow" intensity from the allowed 4f-5d transitions with approximately the same oscillator strength as MD transitions and represent a relaxation of

the parity selection rule. Since both MD and ED transitions have oscillator strengths of the same magnitude, both can be observed in the spectra of Ln^{3+} ions.

1.3.3 Judd-Ofelt theory

In 1962 Judd[16] and Ofelt[17] independently derived expressions for the calculation of the oscillator strengths associated with electric dipole (ED) f-f intensities in the absorption spectra of lanthanide ions.

It was found that the oscillator strength, D_{ED}, of an electric dipole transition can be determined from only three factors Ω_λ, $\lambda = 2, 4, 6$.

$$D_{ED} = e^2 \sum_{\lambda=2,4,6} \Omega_\lambda \left| \langle J \| U^{(\lambda)} \| J' \rangle \right|^2 \qquad 1\text{-}1$$

e = elementary charge, 4.803×10^{-10} esu

The Ω_λ parameters belong to the particular combination of the lanthanide ion and its coordinating environment, and are usually calculated from experimentally determined oscillator strengths.

The term $|\langle J||U^{(\lambda)}||J'\rangle|$ is the squared reduced matrix element, and has values which are independent of the chemical environment of the ion, they can be found in the literature[18,19].

1.3.4 Hypersensitivity

Despite the fact that the f electrons are well shielded from the ligand field and are not significantly influenced by the environment around the ion, certain ED transitions display particular sensitivity to the coordination environment. Jørgensen and Judd referred to these as *hypersensitive* transitions[20]. It was found that Ω_2 unlike Ω_4 and Ω_6 varies considerably with the environment around the Ln^{3+} ion, and is determined by the crystal field parameters $A_{t,p}$.

Jørgensen and Judd[20] noted that all hypersensitive transitions rigidly obey the selection rules $|\Delta J| \leq 2$, $|\Delta L| \leq 2$, and $\Delta S = 0$, and that these are just the selection rules on the squared reduced matrix in Judd's final equation for the calculation of D_{ED}. Judd later determined in a subsequent paper[21] that the only way Ω_2 can be altered without a corresponding change in Ω_4 or Ω_6 is through the A_{1p} crystal field parameters, concluding that the intensities of the hypersensitive transitions are determined by the symmetry of the

ion, with asymmetric sites having more oscillator strength in ED transitions. Some hypersensitive absorption and emission bands are presented in table 1-1.

Lanthanide ion	Transition
Eu^{3+}	$^5D_0 \rightarrow {}^7F_2$
Tb^{3+}	$^5D_4 \rightarrow {}^7F_5$
Dy^{3+}	$^4F_{9/2} \rightarrow {}^6H_{13/2}$
Pr^{3+}	$^3D_0 \rightarrow {}^7F_2$

***Table 1-1** Examples of some hypersensitive Ln^{3+} absorption and emission transitions*

The intensities of hypersensitive transitions may be up to 200 times larger than the corresponding transition of the free ion[22]. One well known example of a hypersensitive emission transition is the $^5D_0 \rightarrow {}^7F_2$ ($\Delta J = 2$) transition of Eu^{3+}. β-diketonates of Eu^{3+} are highly asymmetric around the Eu^{3+} ion and the emission spectra are dominated by the $\Delta J = 2$ transition. Other less well known hypersensitive emission transitions include the $^5D_4 \rightarrow {}^7F_5$ transition of Tb^{3+}, although this transition shows a lesser degree of hypersensitivity than the $\Delta J = 2$ transition of Eu^{3+}, possibly due to the fact that the transitions of Tb^{3+} are composed of both MD and ED intensity.

An excellent review of the intensities of f-f transitions in Ln^{3+} ions is given by Peacock[22].

1.3.5 Eu^{3+} emission spectral features

The emission spectrum of Eu^{3+} provides an excellent illustration of the features of Ln^{3+} spectra. The bands comprise of pure MD, ED and entirely forbidden transitions. The theory of ED transitions[16] yields a selection rule in case the initial level has $J = 0$; transitions to levels with uneven J are forbidden. Furthermore, the $J = 0 \rightarrow J = 0$ transition is forbidden, because the orbital momentum does not change. This restricts the spectrum to the $\Delta J = 1$ transition, a MD transition, the $\Delta J = 2$ transition, a hypersensitive ED emission band, and the $\Delta J = 4, 6$ transitions which are weak ED transitions. The transitions $\Delta J = 0, 3$ and 5 are forbidden by both MD and ED schemes and if they are observed, and they frequently are, they are said to "borrow" their intensity from the $\Delta J = 2$ transition[23] through a j-j mixing mechanism. Studying the emission spectra of Eu^{3+} complexes can

provide useful information on the symmetry and structural nature of the coordinating environment around the ion. Several authors[24,25] now use the recognised method of the ratio of intensity of the $\Delta J = 2$ transition to $\Delta J = 1$ transition as being a measure of the degree of symmetry in the electric field surrounding the ion. In centrosymmetric environments, the MD $\Delta J = 1$ transition is the most intense. In asymmetric environments the hypersensitive ED $\Delta J = 2$ transition of Eu^{3+} dominates, and can be increased by many times[22]. Other details can also be gained from a study of the spectrum. This information is mainly acquired from the splitting associated with a particular band. Since both the $^5D_0$ and $^7F_0$ states in europium are degenerate[26], every independent Eu^{3+} environment will have a unique $\Delta J = 0$ band. Thus, if any splitting is observed in the $^5D_0 \rightarrow {}^7F_0$ transition in Eu^{3+}, then it means that there is more than one Eu^{3+} site although conversely, if there is no observed splitting, this is not necessarily indicative of there being a single Eu^{3+} site. Splitting in $\Delta J = 1$[27] for one individual Eu^{3+} site can at most give 3 separate components, and the presence of more than 5 components in the $\Delta J = 2$ band is also indicative of more than one Eu^{3+} site by the rule $2J + 1$. A relatively intense $\Delta J = 0$ band indicates that the Eu^{3+} ion experiences a strong linear crystal field component[26].

1.4 Population of lanthanide excited states

The lanthanide ions can be excited directly, however, they have low molar absorption extinction coefficients, ε, ≤ 1 mol^{-1} dm^3 cm^{-1} requiring the use of highly concentrated solutions[28].

1.4.1 The antenna effect

The problem of low extinction coefficients can be overcome by utilising what is known as the *antenna effect.*[29,30] See fig. 1-6. A chromophore with a high molar extinction coefficient absorbs the incoming radiation, generating an excited state which subsequently transfers this energy to the emissive states of the lanthanide ion. The lanthanide then loses energy either by the emission of a photon or via a non-radiative pathway ultimately producing heat (phonons). The sensitisation process is often extremely efficient, and high emission quantum yields for Ln^{3+} ions, especially for Eu^{3+} and Tb^{3+} ions, can be achieved[31].

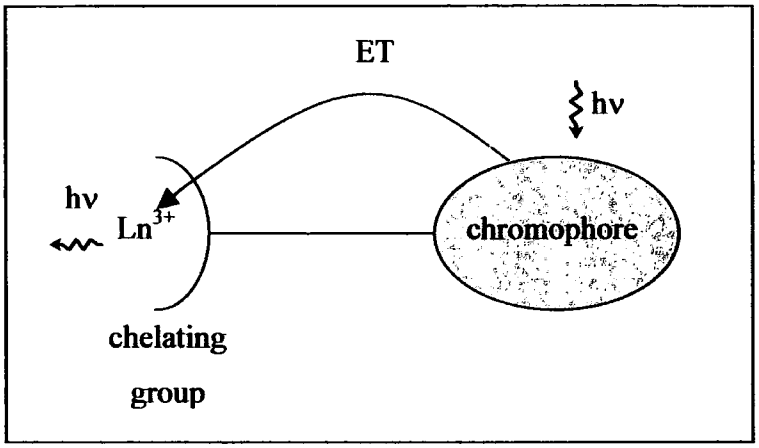

Figure 1-6 *Schematic representation of the antenna effect in lanthanide complexes*

There are many examples in the literature of both the antenna moiety coordinated directly to the lanthanide ion[32], e.g. β-diketonates, or covalently bonded to a chelating ligand[33], e.g. macrocyclic complexes, leading to inter and intra-molecular sensitisation.

Other than the reabsorption of radiation by an acceptor, following emission by a donor, known as "trivial" energy transfer[34], there are two main theories of energy transfer between donor and acceptor species, those described by Förster and Dexter.

1.4.2 Förster theory

Förster[35] expressed a long-range through space dipole-dipole theory of energy transfer from a donor, D, to an acceptor, A, in which the efficiency of transfer depends upon the energy matching between the D and A excited and ground states. Förster showed that for allowed transitions (between the singlet excited states of organic chromophores) the rate constant of energy transfer, k_{ET}, is related to the spatial distance between A and D by $^1/_r^6$ and the donor lifetime, τ_0 in the absence of A:

$$k_{ET} = \left(\frac{1}{\tau_0}\right)\left(\frac{R_0}{r}\right)^6 \qquad 1\text{-}2$$

R_0 = the critical distance for energy transfer, defined as the intermolecular separation between donor and acceptor at which $k_{ET} = k_R$ (rate of radiative decay)

$$R_0 = 8.78 \times 10^{-2}.\kappa^2.\Phi_D.n^{-4}J \qquad 1\text{-}3$$

κ^2 = an orientation factor, which for randomly oriented molecules (dilute solutions) = $^2/_3$

Φ_D = the quantum yield of the donor emission in the absence of A

n = the refractive index of the solvent

J = the spectral overlap integral of the absorption spectrum of the acceptor and the emission spectrum of the donor

Förster described the Coulombic interaction between the D* (donor excited state) and A groups resulting in the transfer of energy between the two moieties. This can occur if the condition of $\Delta E(A \rightarrow A^*) \leq \Delta E(D^* \rightarrow D)$ is satisfied.

Förster suggested that other terms must be considered when the dipole-dipole interaction is weak because of forbidden optical transitions in D or A. Forbidden optical transitions with $\Delta S \neq 0$; if $\Delta S \neq 0$ for $D^* \rightarrow D$ and $\Delta S = 0$ for $A \rightarrow A^*$, then the Förster theory still holds since the slower k_{ET} is compensated by a longer τ_D. Where $\Delta S = 0$ for $D^* \rightarrow D$, but $\Delta S \neq 0$ for $A \rightarrow A^*$, energy transfer may only occur over short distances (i.e. Förster forbidden). For symmetry forbidden transititons, Förster suggested that energy transfer might be determined by dipole-quadrupole interactions with $^1/_r^8$ dependence. Indeed k_{ET} through resonance coupling actually has a $^1/_r^n$ dependence with n = 6, 8, or 10 for dipole-dipole, dipole-quadrupole and quadrupole-quadrupole interactions respectively[36].

1.4.3 Dexter theory

Dexter[37] calculated k_{ET} for an electron exchange interaction between donor and acceptor at short inter-spatial distance:

$$k_{ET} = K.J.\exp\left(\frac{-2r}{L}\right) \qquad 1\text{-}4$$

K α specific orbital interactions

J = spectral overlap integral, normalised for the absorption coefficient of the acceptor

r = distance between D and A

L = D-A separation relative to their van der Waals radii

Dexter described that this mechanism of energy transfer, which is strongly distance dependent, occurs in a collision complex where the electrons clouds of D* and A overlap, ground and excited state electrons are simultaneously exchanged and that the rate of energy transfer decreases exponentially as the distance between D and A increases. However, this can only occur when the Wigner spin correlation rule is obeyed. This states that if S_1 and S_2 are the initial total spins of the electrons in the colliding species (D and A), the resultant total spins of the two systems taken together must have one of the values $|S_1 + S_2|$, $|S_1 + S_2 - 1|$, $|S_1 + S_2 - 2|$,... $|S_1 - S_2|$.

Unlike the Förster theory which is greatly influenced by J and Φ_D, the Dexter theory of energy transfer has normalised values of J, reducing its significance. Thus, the amount of energy transferred does not significantly depend on the extinction coefficient of the acceptor and therefore it is possible to observe efficient sensitisation of many Ln^{3+} compounds[38,39].

The proximity of D and A is the crucial parameter in Dexter energy transfer, and the properties of A and D themselves (the transition dipole moments, and the spectral overlap of D emission and A absorption) as well as the spatial distance are important parameters in Förster energy transfer.

1.4.4 Energy transfer in lanthanide complexes

1.4.4.1 Background

It was Weissman in 1942[40] who first identified energy transfer in lanthanide chelates after observing that absorption of uv sunlight by organic ligands resulted in the emission characteristic of Ln^{3+} ions.

Since then, much work has resulted in both utilising sensitised emission for applications and an effort to determine the mechanism of energy transfer in order to increase sensitised efficiency.

1.4.4.2 Triplet state studies

Results from various groups have indicated that energy transfer takes place from the triplet state of the ligand to the Ln^{3+} excited state[41,42,43]. More specifically, a Dexter mechanism, i.e. an electron exchange process is believed to be the dominant transfer mechanism occurring[36]. Studies on the variation of the triplet energy of the chromophore and the observation of sensitised emission provide convincing evidence that the triplet state is

indeed an intermediate in the energy transfer process. Watson *et al.*[41] reported steady state and time-resolved data for several Eu^{3+} and Tb^{3+} complexes. For europium(III)-hydroxyquinolate whose chromophore triplet state lies between the $^5D_1$ and $^5D_0$ states of Eu^{3+}, emission from the lanthanide was only detected from the Eu^{3+} $^5D_0$ state. Tb^{3+} hydroxyquinolate does not show sensitised emission as the triplet state is below the excited $^5D_4$ state of Tb^{3+}. The ligand triplet state of europium(III)tris(dibenzoylmethide) lies above both the $^5D_1$ and $^5D_0$ states of europium, and Eu^{3+} emission was observed from both $^5D_1$ and $^5D_0$ states.

De Sá *et al.*[38] recently investigated ligand-Ln^{3+} energy transfer mechanisms and their associated selection rules. It was determined that the selection rules for the Förster mechanism are $|J - J'| \leq \lambda \leq J + J'$ ($J' = J = 0$ excluded) and $\Delta J = 0 \pm 1$ ($J' = J = 0$ excluded) for the Dexter mechanism. Thus, direct energy transfer to the $^5D_0$ level is a forbidden process, but it was noted that the selection rules may be relaxed by J-mixing effects and the thermal population of the $^7F_1$ level.

A comprehensive study on the correlation of the triplet state energy of the chromophore with the observation of sensitised emission was conducted by Latva *et al.*[44]. In a study involving a large number of Eu^{3+} and Tb^{3+} complexes the triplet energies for each of the ligands and the Ln^{3+} emission quantum yield were determined. They found that for optimal Ln^{3+} emission, the triplet state should be ~ 2000 cm^{-1} above a Ln^{3+} excited state. In the case of Tb^{3+}, there was a clear correlation between the two factors, and it was seen that energy transfer does not occur when the triplet state of the ligand is below the $^5D_4$ Tb^{3+} level. In the case of Eu^{3+}, they suggested that there are two triplet state energies which will yield most efficient Eu^{3+} sensitisation; ~ 2000 cm^{-1} above the europium $^5D_1$ and $^5D_2$ levels respectively.

1.4.4.3 Singlet state energy transfer

Studies, first by Kleinerman[45] in the 1950s and more recently by Malta *et al.*[46,47] have suggested that the process of direct energy transfer from a chromophore singlet state to the Ln^{3+} excited state is theoretically possible and should not be excluded. However, it has never been demonstrated experimentally, in particular, because other competing processes such as ISC and fluorescent emission by the chromophore are more favourable.

It can then be shown that the established mechanism leading to lanthanide(III) sensitised emission is:

$$S_1 \rightarrow T_1 \rightarrow Ln^{3+*} \rightarrow Ln^{3+} + h\upsilon$$

1.4.4.4 Properties of suitable chromophores

Assuming the above mechanism to be correct, there are two main properties for the singlet state of the ligand to possess. Firstly the chromophore should have a high extinction coefficient such that the S_1 state is readily populated, and secondly the intersystem crossing yield should be high, preferably unity, since the quantum yield of lanthanide emission can be described by

$$\Phi_{tot} = \Phi_T . \eta_{ET} . \eta_{Ln} \qquad 1\text{-}5$$

Φ_{tot} = quantum yield of observed emission

Φ_T = triplet yield of chromophore

η_{ET} = efficiency of energy transfer

η_{Ln} = efficiency of metal centred luminescence

The main condition on the triplet state is that it is ≥ 1500 cm^{-1} above the receiving energy level of the lanthanide ion. If it is any higher, then the efficiency of energy transfer is compromised, if it is any lower, then thermally activated back energy transfer from the Ln^{3+} excited state to the ligand becomes probable (see section 1.5.3).

1.4.5 Heavy atom effect

1.4.5.1 Spin orbit coupling

The heavy atom effect aids spin orbit coupling between states with different muliplicities[48]. Since this increases Φ_T (the chromophore singlet → triplet ISC process) and η_{ET}, the sensitisation of lanthanide emission is often enhanced. The spin-orbit coupling effect is negligible however, in systems which possess n,π* triplet states[49], e.g. aromatic ketones. This is because the triplet state already possesses a high degree of spin-orbit coupling so that any effect induced externally (by the presence of a heavy nucleus) is insignificant.

1.4.5.2 The paramagnetic effect

All the lanthanide ions from Ce^{3+} to Yb^{3+} inclusive are paramagnetic (they have one or more unpaired electrons) and those of La^{3+} and Lu^{3+} are diamagnetic (no unpaired electrons)[1].

Yuster and Weissman[50] investigated a series of dibenzoylmethane derivative complexes with the metal ions of Al^{3+}, Sc^{3+}, Y^{3+}, La^{3+}, Gd^{3+}, and Lu^{3+}. They found that the complex of the only paramagnetic ion, Gd^{3+} behaved differently to the other ion complexes. The phosphorescence lifetime was significantly shorter and there was no detectable fluorescence. In a series of papers Tobita *et al.*[51] verified this *paramagnetic* effect for the $T_1 \rightarrow S_0$ radiative process by the quantitative determination of k_R in Ln^{3+} complexes with benzoyltrifluoroacetone and methylsalicylate as antenna chromophores. The Φ_f values were found to be much smaller for the complexes of paramagnetic Gd^{3+} and Tb^{3+} ions than those of the diamagnetic La^{3+} and Lu^{3+}. In addition, the fluorescence lifetime of the Gd^{3+} complex was about an order of magnitude shorter than that of the analogous La^{3+} and Lu^{3+} complexes.

Tobita *et al.* determined that the singlet-triplet mixing between the electronic states of the ligand is enhanced by the inhomogeneous magnetic field caused by the close proximity of the paramagnetic ion.

1.4.6 Electron transfer reactions

Crosby and Kasha[52] in 1958 found that energy transfer to Yb^{3+} can occur despite there being negligible spectral overlap between the emission spectrum of the dibenzoylmethane group and the absorption spectrum of the Yb^{3+} ion in a tris-dibenzoylmethane Yb^{3+} complex. Both the Förster and Dexter theories of energy transfer describe that the rate of energy transfer is directly proportional to the spectral overlap integral. Though in the Dexter theory the significance of this parameter is reduced.

Horrocks *et al.*[53] studied the photophysical properties of Ln^{3+} ions in the Ca^{2+} binding site of codfish parvalbumin. They found that the emission from the fluorescent tryptophan group was being quenched by the presence of this ion and that the Yb^{3+} ion was being sensitised despite there being no spectral overlap between the chromophore emission and the Yb^{3+} ion absorption spectra. They concluded that an alternative mechanism must be responsible for energy transfer in this complex, and proposed an electron transfer reaction in which the Yb^{3+} ion is reduced. In addition, they observed Yb^{3+} emission, but emission from the Eu^{3+} ion in the Ca^{2+} site was negligible. It was determined that since the Eu^{3+} and

Yb^{3+} ions are the most easily reduced Ln^{3+} ions with E^{θ} values of -0.35 V, and -1.05 V respectively, an electron transfer (eT) process was occurring between the metal ion and the tryptophan group in the protein.

$$Trp + Ln^{3+} \rightarrow Trp^{+\bullet} + Ln^{2+}$$

Back eT re-establishes the initial system (i.e. the reaction is reversible).
However, the driving forces, $-\Delta G^{\theta}$ for the Eu^{3+} and Yb^{3+} eT reactions are different.

$$\Delta G = E(Ant^{+\bullet} / Ant) - E_{Ant^*} - E(Ln^{3+} / Ln^{2+})$$

So that if $-\Delta G$ is greater than the Ln^{3+} excited state, then the back eT reaction may lead to Ln^{3+} emission. However if $-\Delta G$ is lower than the Ln^{3+} excited state, then the Ln^{3+} is re-formed in its ground state and cannot emit. For this reason, Eu^{3+} emission was not observed in the Horrocks system, whereas Yb^{3+} emission was. They later[54] investigated the mechanism of eT further in a more comprehensive study.
Absualeh and Meares[55] had suggested that an electron transfer mechanism was responsible for the observed quenching of indole by Eu^{3+} and Yb^{3+} some 13 years earlier. Several authors[56,57] since then have suggested this mechanism of quenching in systems with surprisingly low Eu^{3+} sensitisation and where the formation of radical cations is possible.

1.5 Quenching

Radiative emission from the excited state to the ground state of an excited species is not the only possibile mechanism of energy loss, nonradiative processes always compete in a general process known as quenching.

1.5.1 Energy gap law and the Franck-Condon factor

Deuteration of a solvent can have the effect of increasing the fluorescence lifetime of organic molecules[58], and this effect is highly significant in Ln^{3+} ions. In a series of papers Kropp and Windsor investigated the effect of O-H oscillators on the luminescence of lanthanide ions[59,60,61]. They studied europium in various H_2O:D_2O ratio mixtures and concluded that energy transfer from the Eu^{3+} ion excited state to O-H oscillators is extremely efficient, and that the radiative lifetime of the Eu^{3+} ion is significantly reduced

as a result. Energy transfer from Eu^{3+} to O-D oscillators is much less efficient, and the lifetime is correspondingly longer.

Experimentally determined lifetimes for the lanthanide(III) ions are significantly shorter than the pure radiative lifetimes (by 3 or more orders of magnitude)[62]. In 1975 Stein and Würzberg[5] conducted a study of the perchlorates of several Ln^{3+} ions and related the quenching effect by O-H oscillators to the energy of the Ln^{3+} excited state. The lower in energy the excited state, the more efficient the quenching. Thus, Eu^{3+} ions are quenched more than Tb^{3+} ions by O-H oscillators. The origins of this energy gap law lie in the Franck-Condon factor - the lower in energy the excited state, the more efficient the overlap between one of the vibrational levels of an O-H oscillator and hence the more efficient the quenching. More recently however, it has been shown that not only do O-H oscillators have the abililty to effectively deactivate the excited state of the lanthanide ion, but C-H and N-H oscillators can also enhance non-radiative quenching[63,64].

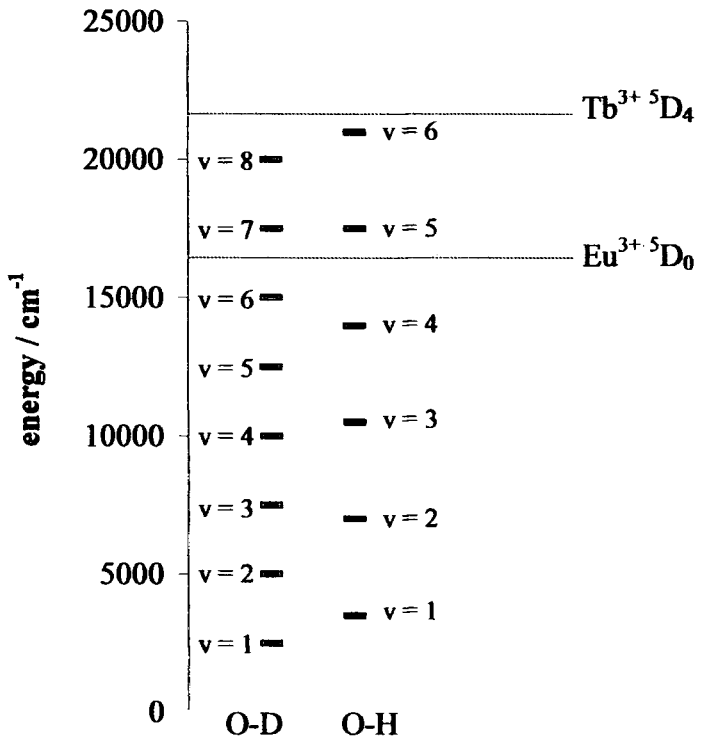

***Figure 1-7** Schematic representation of the energies of the O-H and O-D vibrational levels. The energies of the Tb^{3+} and Eu^{3+} emissive states are included for reference*

As the energy gap between the Ln^{3+} ion excited and ground states increases, the level of the vibrational overtone of the oscillator (O-H/O-D) to which energy transfer will occur also increases, see fig. 1-7. The higher the level, the less coupling between the energy of

the Ln^{3+} ion and the oscillator. Since O-D vibrates at a lower frequency than O-H, the vibrational overtone coupling with the Ln^{3+} ion is of a lower level and it is the amount of coupling between the Ln^{3+} ion and the oscillator which governs the quenching. The difference between the O-H and O-D coupling is reflected for instance, in the empirically derived A value given to the lanthanide ions for the calculation of q-values (see section 1.5.2).

Voloshin *et al.*[65,66] have noted that the emission of concentrated (> 10^{-4} mol l^{-1}) toluene solutions of Eu^{3+}, Sm^{3+} and Tb^{3+} tris β-diketonates is enhanced by the addition of H_2O. In concentrated solutions, the chelate is partially dimerised and the emission quantum yield of the dimer is significantly lower than the monomer due to a quenching in the ligand and cross-relaxation of Ln^{3+}. Addition of H_2O shifts the equilibrium to the monomer and enhances the Ln^{3+} quantum yield despite the presence of extra O-H oscillators.

1.5.2 q-values

Horrocks *et al.*[67] showed that the Eu^{3+} and Tb^{3+} lifetimes could be measured in dilute solutions (~1 x 10^{-6} mol l^{-1}) and that by measuring these values in both H_2O and D_2O, the number of bound/coordinated water molecules, q could be determined. The method they employed was later further refined by Horrocks and Sudnick[68] in a study of crystalline materials in which the actual number of Ln^{3+} ion-coordinated water molecules was known from X-ray crystallographic data.

Plots of the difference in reciprocal excited state lifetimes $\tau_{H2O}^{-1} - \tau_{D2O}^{-1} = \Delta\tau^{-1}$ vs. q, were linear with high correlation coefficients, thus validating the method.

For a given lanthanide ion, q is given by

$$q_{Ln} = A_{Ln}\left(\tau_{H_2O}^{-1} - \tau_{D_2O}^{-1}\right) \qquad 1\text{-}6$$

A_{Ln} = constant reflecting quenching sensitivity

τ^{-1} = observed decay rate constant / ms^{-1}

Equation 1-6 accounts for non-radiative deactivation by the bound water molecules - but it has been found that non-bound water, in the second sphere coordination shell can also have a quenching effect. In an Yb^{3+} complex with no coordinated water molecules (determined by x-ray crystallography), a difference in the observed lifetime in H_2O and

D_2O was recorded. Beeby *et al.*[69] assigned the quenching to a contribution from second sphere unbound water molecules. They reported a modified method for determining the number of H_2O molecules bound to Yb^{3+} using equation 1-7.

$$q_{Ln} = A_{Ln}\left(\tau_{H_2O}^{-1} - \tau_{D_2O}^{-1}\right) - B \qquad 1\text{-}7$$

B = constant representing the quenching effect of the outer sphere water molecules

This method has since been applied to other lanthanide ions Nd(III)[70], Dy(III)[71], and Sm(III)[71].

The reported literature values for the lanthanides are shown in table 1-2.

Ln^{3+}	A	B
Yb	1.0 μs	0.2 ms
Eu	1.07 ms	
Tb	4.03 ms	
Nd	360 ns	
Sm	25.4 μs	0.37 ms
Dy	2.11 μs	0.60 ms

***Table 1-2** The A and B literature values used in the calculation of the number of bound water molecules, q*

1.5.3 Back energy transfer

A further quenching mechanism to be considered and occasionally encountered in the study of Ln^{3+} emission by sensitisation is that of back energy transfer[72,73]. This process is most likely to occur if the Ln^{3+} excited state is of similar energy ± 1500 cm^{-1} to an energy level of the antenna chromophore. See fig. 1-8.

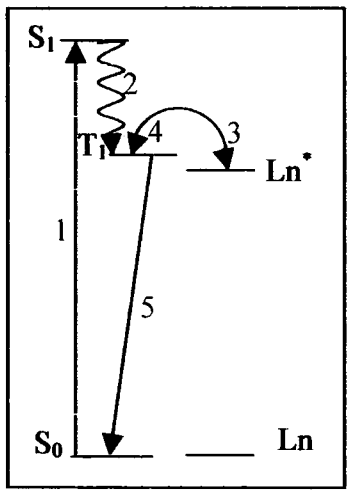

Figure 1-8 *Schematic representation of the back energy transfer process from a* Ln^{3+} *excited state to the antenna triplet state*

An increase in temperature makes this process more favourable because the thermal energy possessed by the complex, kT, allows the energy gap between the antenna and Ln^{3+} excited states to be bridged. The observation of sensitivity to oxygen in lanthanide emission can also indicate back energy transfer unlike the process of phosphorescence in organic molecules [74]. The luminescence from Ln^{3+} ions is not affected by the presence of O_2, because the f electrons are buried deep in the core of the nucleus and are well shielded by the outer 5s and 5p orbitals[75]. Since the triplet state of the organic chromophore is deactivated by O_2, if back energy transfer occurs to the chromophore triplet state, then the Ln^{3+} excited state may be quenched indirectly by O_2.

1.5.4 Energy transfer to the ground state of Ln^{3+} *ions*

In an interesting study involving the ligand emission from lanthanide complexes with the chromophores benzoylacetonate and dibenzoylmethide and 10 Ln^{3+} ions by Whan and Crosby[76], it was suggested that there is a relationship between the number of Ln^{3+} electronic energy levels below the chromophore triplet state and the efficiency of energy transfer direct to Ln^{3+} ground states. That is, the efficiency of energy transfer is dependent upon the number of available levels to accept energy from the antenna. They investigated the effect of the metal ion on the emission (fluorescence and phosphorescence) from the ligand (benzoylacetonate and dibenzoylmethide). In three main groups of ions, the first containing Lu^{3+}, La^{3+}, and Gd^{3+}, showed no energy transfer, they had no energy levels below the chromophore triplet state. The second group including Yb^{3+}, Nd^{3+}, and Tm^{3+}

with 1, 4, and 7 states respectively below the triplet state of the chromophore showed ligand emission efficiency in the order $Yb^{3+} > Nd^{3+} > Tm^{3+}$. Finally, the third group of Ln^{3+} ions showed the least amount of chromophore emission, the ions included Eu^{3+} and Tb^{3+}.

1.5.5 Quenching by a second Ln^{3+} ion

If two metal sites are populated by two different and properly chosen Ln^{3+} ions (e.g. Eu^{3+}-Er^{3+}, Eu^{3+}-Ho^{3+}, Tb^{3+}-Nd^{3+}) part of the excitation energy of the first ion can be transferred to the other, resulting in a decrease in the lifetime of the excited state. The yield of the energy transfer η_{ET} is related to both the lifetimes of the donor ion in the presence τ and absence τ_0 of the acceptor, see equation 1-8.[77,6]

$$\eta_{ET} = 1 - \left(\frac{\tau}{\tau_0}\right) = \frac{1}{\left(1 + \frac{r^6}{R_0^6}\right)} \qquad 1\text{-}8$$

R_0 = critical distance for 50 % energy transfer

r = distance between the two metal ion sites

1.6 Luminescent lanthanide complexes

1.6.1 Complexation

The luminescence from Ln^{3+} ions is reduced by the vibronic coupling to solvent molecules, so ligands are often designed as "cages" to encapsulate the Ln^{3+} ion, and protect the ion from solvent molecules. Since the coordination number of the lanthanides is most commonly 8 or 9[78,79], the ligands generally have 8 or 9 donor atoms, to prevent coordination of the solvent. Other Ln^{3+} coordination numbers, from 3 – 12 have all been reported[79].

Due to the unavailability of the f-orbitals for bonding purposes, the lanthanides form few complexes, unlike the s and d block metals, and they require hard bases, for example oxygen and nitrogen containing donors to coordinate.

The luminescent complexes studied so far have focused on Eu^{3+} and Tb^{3+} ions as the emitting materials, but the near-IR emitting Ln^{3+} ions of Yb^{3+}, Nd^{3+}, and Er^{3+} have also recently become popular due to the ability of these ions to be excited by visible light absorbing chromphores[80,81].

1.6.2 β-diketonates

The most widely studied group of lanthanide(III) complexes are that of the β-diketonates.[82,83,84] See fig. 1-9.

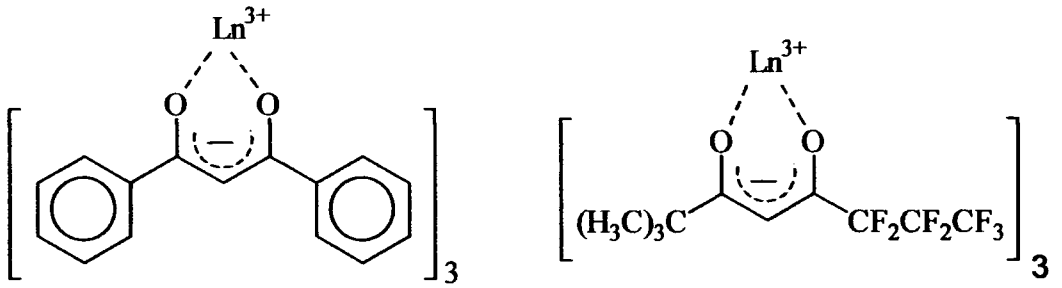

***Figure 1-9** Examples of some Ln^{3+} β-diketonate complexes*

These complexes are readily hydrolysed in aqueous solution, which makes them unsuitable for some applications. The main feature of the europium-tris(β-diketonates) is that they have strong $\Delta J = 2$ emission bands resulting from the asymmetric environment of the Eu^{3+} ion. The $^5D_0 \rightarrow {}^7F_2$ hypersensitive transition gains a large amount of oscillator strength in unsymmetric systems, so that this band frequently features strongly in the spectrum producing virtually monochromatic light[85]. See fig. 1-10.

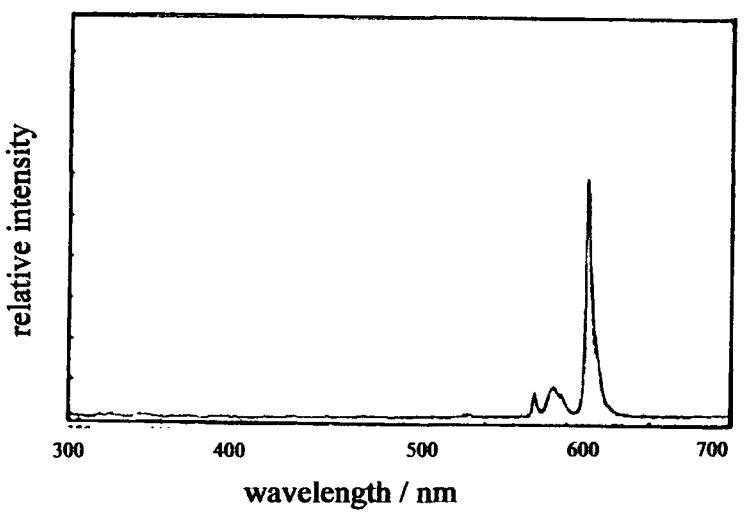

***Figure 1-10** Emission spectrum of europium tris(thenoyltrifluoroacetonate)-1,10-phenanthroline adapted from J. Am. Chem. Soc., 1971, 6286* [85].

Incorporation of a second coordinating group (known as an auxiliary ligand) into the system, for example mixing solutions of $Eu(fod)_3$* and Michler's ketone† (giving $Mk:Eu(fod)_3$) leads to a bathochromically shifted MLCT absorption band in the visible region of the absorption spectrum, and shows very efficient sensitisation[86]. This is the effect of the charge on the metal ion and its related electric field on the complex. Usually this perturbation is small and highly distance dependent, but in the case of a compound which can show strong charge-transfer character such as $Mk:Eu(fod)_3$ the effect becomes significant.

1.6.3 Macrocycles

Another significant group of Ln^{3+} complexes are octadentate macrocycles based on 1,4,7,10-tetraazacyclododecane[87,88]. See fig. 1-11.

This type of complex shields the ion very effectively by offering the lanthanide ion 8 donor atoms, with the final coordination site free for occupation by a solvent molecule[4]. The complex also allows the incorporation of an antenna enabling intramolecular energy transfer for sensitisation. These ligand systems display extremely stable kinetic[89] and thermodynamic properties[90].

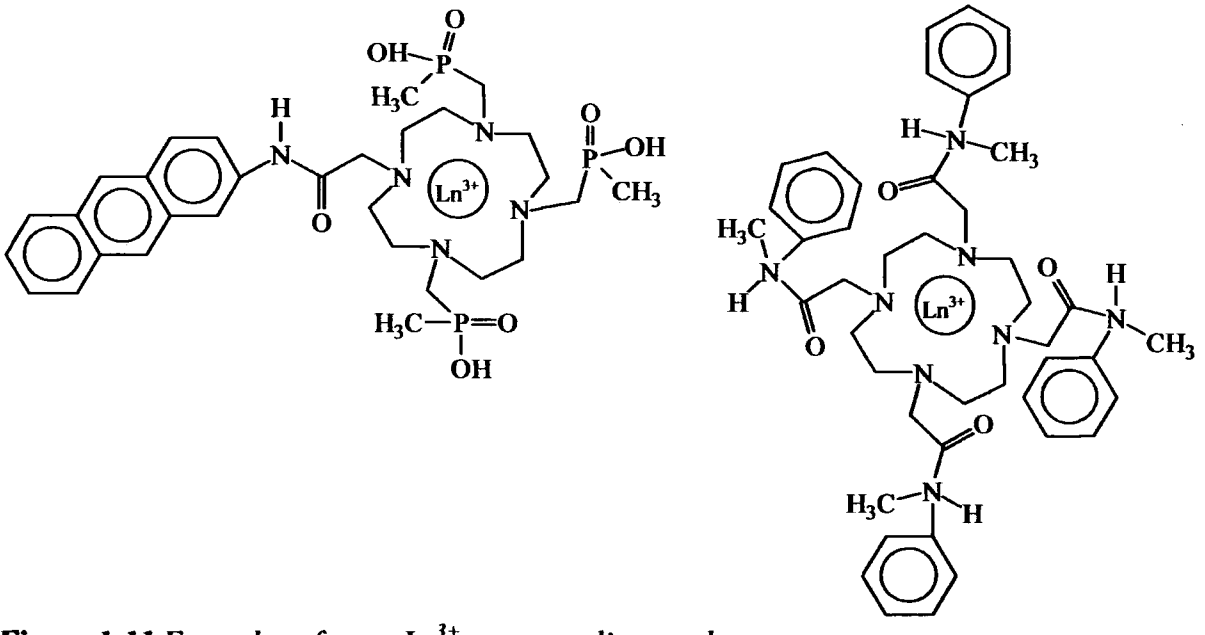

***Figure 1-11** Examples of some Ln^{3+} macrocyclic complexes*

* $Eu(fod)_3$ = europium tris(6,6,7,7,8,8,8-heptafluoro-2,2-dimethylocante-3,5-dione)

† Michler's ketone = 4,4'-bis(*N,N*-dimethylamino)benzophenone

1.6.4 Other complexes

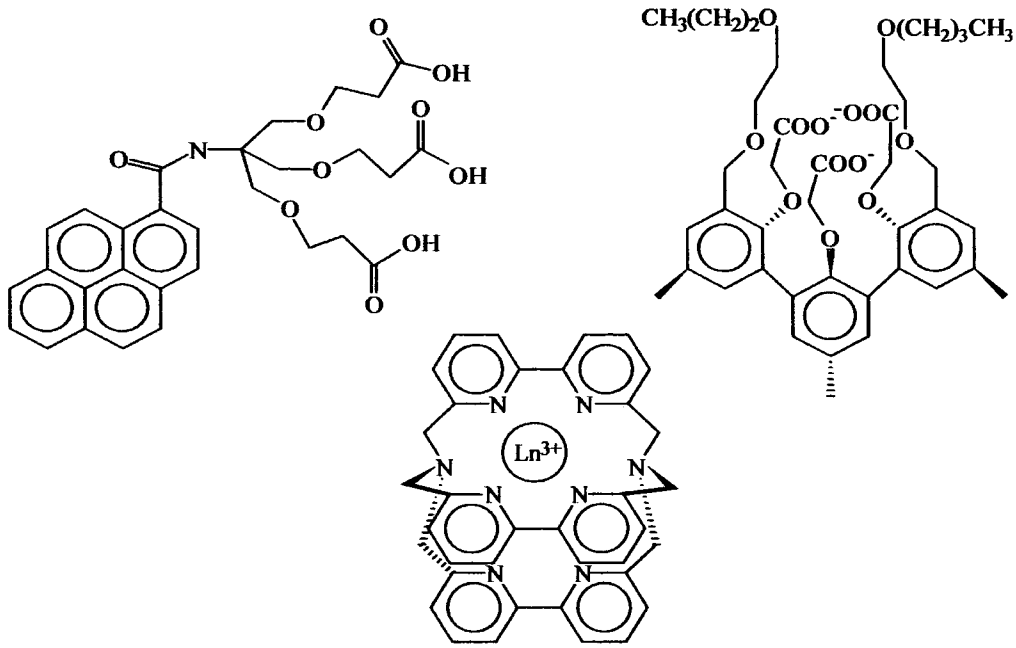

***Figure 1-12** Examples of some Ln^{3+} coordination ligands and complexes*

Examples of other types of lanthanide containing complexes include hemispherands[91], calix[4]arenes[92], calix[8]arenes[93], DTPA/EDTA complexes[94,95], and dendrimers[96]. Fig. 1-12 shows more examples of Ln^{3+} complexes.

1.6.5 Micellar systems

Micelles provide a unique, controlled environment in which the study of energy transfer can be employed, this is because they allow the compartmentalisation of the antenna and Ln^{3+} ion. It has been demonstrated in both normal[97,98] and reverse[99] micelles that energy transfer from a suitable chromophore to the Ln^{3+} ions is possible.

1.7 Applications

Due to the interesting properties of lanthanide ions, there are a large number of potential and current uses for them in solution and solid states.

1.7.1 Biological

The Ln^{3+} ions have been used as spectroscopic probes for Ca^{2+} ions in bioinorganic chemistry by exploiting the similar chemical properties of these ions. They have a similar size ca. 1.1 Å, both are hard cations with a preference for O and N donors, they have

similar coordination numbers, and the replacement of Ca^{2+} ions by Ln^{3+} ions does not significantly perturb the biological system[6].

Lanthanides have also found similar use in fluoroimmunoassay systems, this is a method used in immunology in order to detect biomolecules. The method is superior to those using radioactive materials both in terms of sensitivity and specificity. Fluoroimmunoassays exploit the long lived luminescence of Ln^{3+} ions[100,101,102] in this process, the Ln^{3+} ion binds to the biological species of interest, which is then excited, some of the energy can be transferred to the Ln^{3+} excited state. The fluorescence arising from the biological species (often referred to as autofluorescence) is short lived in comparison, and so by delaying the time between the excitation pulse and the measurement of emission, the luminescence resulting from the Ln^{3+} ion can be selectively recorded.

It has been demonstrated that luminescent lanthanide complexes can also be used as sensors, for pH, halide, hydroxide ions and oxygen[74]. The oxygen sensor utilises the fact that back energy transfer from the Ln^{3+} excited state occurs to the T_1 state of the chromophore which may be deactivated by O_2.

In a recent review article[103], the possible beneficiary effects of Ln^{3+} ions and their use as possible drugs are examined. One of the interesting possible beneficial uses is their incorporation as anti cancer agents. The molecular mechanism governing how Ln^{3+} ions increase the death rate of cancer cells is not clear, but it is thought that the Ln^{3+} ion increases the intracellular Ca^{2+} concentration, which plays an important role mediating DNA cleavage. As well as potential drugs themselves, Ln^{3+} ions can also be used in the analysis of drugs[104]. Eu^{3+} and Tb^{3+} ions coordinated to organic ligands were found to exhibit sensitised emission by certain drugs which are present in solution, allowing the determination of the latter.

In solution, the magnetic behaviour of the Ln^{3+} ions is exploited in NMR spectroscopy by using complexes as shift reagents[105] and the paramagnetic properties of gadolinium are exploited as Gd(III) complexes are often used as *in vivo* contrast agents for magnetic resonance imaging (MRI)[106,107,108].

1.7.2 Physical

A potential application for triboluminescent materials (including Eu^{3+} and Tb^{3+} complexes) has recently been highlighted[109]. Damage to the structure of the composite material used in bridges, aeroplanes, etc. can be detected using triboluminescent Ln^{3+} materials, which emit light only when fractured.

Solid state Ln^{3+} ions doped into insulating hosts find uses in a wide variety of applications[110], including phosphors for fluorescent lighting, display monitors and x-ray imaging[111].

Er^{3+} [112] and Nd^{3+} [113] are used in optical fibres for the amplification of light by stimulated emission. A large number of crystalline hosts with Ln^{3+} ions have been shown to produce efficient lasers. One of the most widely used lasers employs Nd^{3+} in hosts such as YAG or YLF[114,115,116]. The line like emission band at about 1064 nm has a high stimulated emission cross section, and allows efficient lasers to be constructed. Yb^{3+} [117], Eu^{3+} [118], Tm^{3+} [119], and Ho^{3+} [120] have all been employed in solid state lasers. In 1968 Heller[121,122] investigated a series of Ln^{3+} ions in solution with the ultimate aim of their incorporation into liquid lasers.

A recently active area of research is the development of lanthanide complexes for use in electroluminescent (EL) displays. Both Eu^{3+} [123](red) and Tb^{3+} [124](green) complexes have been shown to exhibit efficient EL emission in devices. Good EL materials have high photoluminescent (PL) efficiency, high thermal stability and charge carrier mobility[125]. Materials currently used in EL displays are mainly semiconducting (conjugated) polymers[126], but these have the problem of obtaining pure colour emission. Ideally, full colour displays (red, green and blue) are required; polymers (and small organic molecules) have broad band emission which is rarely pure in one colour requiring the use of filters[125]. The Ln^{3+} EL complexes studied are generally those of β-diketonates[123,125,127] and this is especially true of the Eu^{3+} complexes. This is because Eu^{3+} β-diketonates have intense hypersensitive $\Delta J = 2$ emission, giving the appearance of monochromatic radiation in the red region.

1.8 Aims

The work described in this thesis concerns the excited state properties of Ln^{3+} ions in various environments. The photochemistry and photophysics of Ln^{3+} ions free in solution and when complexed are studied. Understanding the mechanism of energy transfer in lanthanide(III) ions is of immediate interest to both the fundamental theory of inorganic photophysical processes and for the development of better photosensitive materials for use in various applications.

Chapter 2 describes the practical aspects of the techniques used throughout this work.

Chapter 3 discusses the luminescent properties of the Tm^{3+} ion in solution and includes the effect of simple chelates and different solvents on the photophysical behaviour of the ion.

Chapter 4 contains a study of intramolecular energy transfer to Eu^{3+}, Tb^{3+} and Yb^{3+} ions from a benzophenone chromophore. The mechanism of energy transfer is studied in detail by following the excited state kinetics. The effect of an extra CH_2 group on the arm of the ligand is investigated with respect to changes in the intensity of the hypersensitive transitions of both Eu^{3+} and Tb^{3+}. The efficiency of the energy transfer process in the Eu^{3+} complex is estimated by determination of the pure radiative lifetime using Einstein's relation for spontaneous emission.

Chapter 5 concerns the sensitisation of Eu^{3+} ions by acetophenone substituted ligands, with the substituent increasing the charge transfer nature of the complex across a series. The effect of substituent on the efficiency of energy transfer is investigated, and the crucial effect of solvent is discussed.

Chapter 6 demonstrates energy transfer to bound lanthanide ions at the surface of micelles in aqueous solution by the 2-naphthylacetic acid chromophore and considers the length of the carbon chain on the surfactant unit with respect to the degree of sensitised Ln^{3+} emission.

Chapter 7 contains a study of an ethoxybenzyl substituted DTPA ligand bound to a series of Ln^{3+} ions. The properties of the complexes are discussed in terms of electron transfer and the redox properties of the lanthanide ions.

Appendix A summarises the photophysical results obtained on some potential electroluminescent materials for use in OLEDs.

REFERENCES

[1] Cotton and Wilkinson, *Advanced Inorganic Chemistry*, **1988**, John Wiley and Sons Inc., New York

[2] Geschneider and Eyring, *Handbook on the Physics and Chemistry of the Rare Earths*, **1979**, Ch. 24, W. T. Carnall, North-Holland Publishing Company, Amsterdam

[3] H. A. Laitinen, W. A. Taebel, Europium and ytterbium in rare earth mixtures. Polarographic determination, *Ind. Eng. Chem., Anal. Ed.*, **1941**, *13*, 825

[4] D. Parker, J. A. G. Williams, Getting excited about lanthanide complexation chemistry, *J. Chem. Soc., Dalton Trans.*, **1996**, 3613

[5] G. Stein, E. Würzberg, Energy gap law in the solvent isotope effect on radiationless transitions of rare earth ions, *J. Chem. Phys.*, **1975**, *62*, 208

[6] J.-C. G. Bünzli, The europium(III) ion as a spectroscopic probe in bioinorganic chemistry, *Inorg. Chim. Acta*, **1987**, *139*, 219

[7] G. Blasse, The influence of charge-transfer and Rydberg states on the luminescence properties of lanthanides and actinides, *Struct. Bonding*, **1976**, *26*, 43

[8] T. Hoshina, S. Kuboniwa, 4f-5d transition of Tb^{3+} and Ce^{3+} in MPO_4 (M = Sc, Y and Lu), *J. Phys. Soc. Japan*, **1971**, *31*, 828

[9] B. G. Wybourne, *Spectroscopic properties of the Rare Earths*, **1965**, Wiley, New York

[10] Z. Hnatejko, S. Lis, A. Stryła, M. Elbanowski, Spectroscopic studies of the complexes formed between lanthanide ions and N-(2-hydroxyethyl)iminodiacetic acid in solution, *Photochem. Photobiol. A: Chem.*, **1998**, *119*, 109

[11] F. J. Steemers, W. Verboom, D. N. Reinhoudt, E. B. van der Tol, J. W. Verhoeven, Diazatriphenylene complexes of Eu^{3+} and Tb^{3+}; promising light converting systems with high luminescence quantum yields, *Photochem. Photobiol. A: Chem.*, **1998**, *113*, 141

[12] P. W. Atkins, *Physical Chemistry*, **1998**, Oxford University Press, Oxford

[13] H. J. Van Vleck, The puzzle of rare-earth spectra in solids, *J. Chem. Phys.*, **1937**, *41*, 67

[14] (a) P. Franzen, J. P. M. Woudenberg C. J. Gorter, The absorption of light in a solution of Sm nitrate, *Physica*, **1943**, *10*, 365, (b) J. Hoogschagen, The light absorption in the near-infrared region of praseodymium, samarium, and ytterbium solutions, *Physica*, **1946**, *11*, 513, (c) J. Hoogschagen, The absorption of light by neodymium salts in the near infrared region, *Physica*, **1946**, *11*, 513

[15] K. Binnemans, K. van Herck, C. Görller-Walrand, Influence of dipicolinate ligands on the spectroscopic properties of europium(III) in solution, *Chem. Phys. Lett.*, **1997**, *23*, 297

[16] B. R. Judd, Optical absorption intensities of rare-earth ions, *Phys. Rev.*, **1962**, *127*, 750

[17] G. S. Ofelt, Intensities of crystal spectra of rare-earth ions, *J. Chem. Phys.*, **1962**, *37*, 511

[18] W. T. Carnall, P. R. Fields, B. G. Wybourne, Spectral intensities of the trivalent lanthanides and actinides in solution. I. Pr^{3+}, Nd^{3+}, Er^{3+}, Tm^{3+}, and Yb^{3+}, *J. Chem. Phys.*, **1965**, *42*, 3797

[19] W. T. Carnall, P. R. Fields, K. Rajnak, Spectral intensities of the trivalent lanthanides and actinides in solution III. Pm^{3+}, Sm^{3+}, Eu^{3+}, Gd^{3+}, Tb^{3+}, Dy^{3+} and Ho^{3+}, *J. Chem. Phys.*, **1968**, *49*, 4412

[20] C. K. Jørgensen, B. R. Judd, Hypersensitive pseudoquadrupole transitions in lanthanides, *Mol. Phys.*, **1964**, *8*, 281

[21] B. R. Judd, Hypersensitive transitions in rare-earth ions, *J. Chem. Phys.*, **1966**, *44*, 839

[22] R. D. Peacock, The intensities of lanthanide f↔f transitions, *Struct. Bonding*, **1975**, *22*, 82

[23] A. F. Kirby, F. S. Richardson, Detailed analysis of the optical absorption and emission spectra of Eu^{3+} in the trigonal (C_3) $Eu(DBM)_3.H_2O$ system, *J. Phys. Chem.*, **1983**, *87*, 2544

[24] K. Binnemans, R. Van Deun, C. Görller-Walrand, S. R. Collinson, F. Martin, D. W. Bruce, C. Wickleder, Spectroscopic behaviour of lanthanide(III) coordination compounds with Schiff base ligands, *Phys. Chem. Chem. Phys.*, **2000**, *2*, 3753

[25] M. P. Oude Wolbers, F. C. J. M. van Veggel, J. W. Hofstraat, F. A. J. Geurts, D. N. Reinhoudt, Luminescence properties of m-terphenyl-based Eu^{3+} and Nd^{3+} complexes: visible and near-infrared emission, *J. Chem. Soc., Perkin Trans. 2*, **1997**, 2275

[26] G. Blasse, A. Bril, On the Eu^{3+} fluorescence in mixed metal oxides II. The $^5D_0 \rightarrow {}^7F_0$ emission, *Philips Res. Repts.*, **1966**, *21*, 368

[27] F. S. Richardson, Terbium(III) and europium(III) ions as luminescent probes and stains for bimolecular systems, *Chem. Rev.*, **1982**, *82*, 541

[28] N. N. Greenwood, A. Earnshaw, *Chemistry of the Elements*, **1984**, Pergamon Press, Oxford

[29] B. Alpha, R. Ballardini, V. Balzani, J.-M. Lehn, S. Perathoner and N. Sabbatini, Antenna effect in luminescent lanthanide cryptates: A photophysical study, *Photochem. Photobiol.*, **1990**, *52*, 299

[30] M. H. V. Werts, J. W. Hofstraat, F. A. J. Geurts, J. W. Verhoeven, Fluorescein and eosin as sensitising chromophores in near-infrared luminescent ytterbium(III), neodymium(III) and erbium(III) chelates, *Chem. Phys. Lett.*, **1997**, *276*, 196

[31] E. B. van der Tol, H. J. van Ramesdonk, J. W. Verhoeven, F. J. Steemers, E.. G. Kerver, W. Verboom, D. N. Reinhoudt, Tetraazatriphenylenes as extremely efficient antenna chromophores for luminescent lanthanide ions, *Chem. Eur. J.*, **1998**, *4*, 2315

[32] S. W. Magennis, S. Parsons, A. Corral, J. D. Woollins, Z. Pikramenou, Imidodiphosphinate ligands as antenna units in luminescent lanthanide complexes, *J. Chem. Soc., Chem. Commun.*, **1999**, 61

[33] M. H. V. Werts, J. W. Verhoeven and J. W. Hofstraat, Efficient visible light sensitisation of water soluble near-infrared luminescent lanthanide complexes, *J Chem. Soc., Perkin Trans. 2*, **2000**, 433

[34] F. Scandola, V. Balzani, Energy transfer processes of excited states of coordination compounds, *J. Chem. Educ.*, **1983**, *60*, 814

[35] T. Förster, Transfer mechanisms of electronic excitation (10th Spiers Memorial Lecture), *Discuss. Faraday Soc.*, **1955** *27*, 7

[36] A. Brown, F. Wilkinson, Intermolecular energy transfer in rigid matrices at 77 K. Part 1. – Quenching of triphenylene phosphorescence by aquated terpositive lanthanide ions, *J. Chem. Soc., Faraday Trans.*, **1979**, *75*, 880

[37] D. L. Dexter, A theory of sensitised luminescence in solids, *J. Chem. Phys.*, **1953**, *21*, 836

[38] G. F. de Sá, O. L. Malta, C. de Mello Donegá, A. M. Simas, R. L. Lonego, P. A. Santa Cruz, E. F. da Silva Jr, Spectroscopic properties and design of highly luminescent lanthanide coordination complexes, *Coord. Chem. Rev.*, **2000**, *196*, 165

[39] J.-E. Sohna Sohna, F. Fages, Sensitised luminescence emission of the europium(III) ion bound to a pyrene containing ligand, *Tetrahedron Lett.*, **1997**, *38*, 1381

[40] S. I. Weissman, Intramolecular energy transfer. The fluorescence of complexes of europium, *J. Chem. Phys.*, **1942**, *10*, 214

[41] W. M. Watson, R. P. Zerger, J. T. Yardley, G. D. Stucky, Examination of photophysics in rare earth chelates by laser-excited luminescence, *Inorg. Chem.*, **1975**, *14*, 2675

[42] M. Tanaka, G. Yamaguchi, J. Shikawa, C. Yamanaka, Mechanism and rate of the intramolecular energy transfer in rare earth chelates, *Bull. Chem. Soc. Japan*, **1970**, *43*, 549

[43] G. Crosby, R. Whan, R. Alire, Intramolecular energy transfer in rare earth chelates. Role of the triplet state, *J. Chem. Phys.*, **1961**, *34*, 743

[44] M. Latva, H. Takalo, V.-M. Mukkala, C. Matachescu, J. C. Rodríguez-Ubis, J. Kankare, Correlation between the lowest triplet state energy level of the ligand and lanthanide(III) luminescence quantum yield, *J. Lumin.*, **1997**, *75*, 149

[45] M. Kleinerman, Energy migration in lanthanide chelates, *J. Chem. Phys.*, **1969**, *51*, 2370

[46] O. L. Malta, Ligand-rare earth ion energy transfer in coordination compounds. A theoretical approach, *J. Lumin.*, **1997**, 229

[47] O. L. Malta, H. F. Brito, J. F. S. Menezes, G. Silva, C. de Donega, S. Alves, Experimental and theoretical emission quantum yield in the compound Eu(thenoyltrifluoroacetonate)$_3$.2(dibenzyl sulfoxide), *Chem. Phys. Lett.*, **1998**, *282*, 233

[48] A. Gilbert and J. Baggott, *Essentials of Molecular Photochemistry*, **1991**, Blackwell Scientific Publications, Oxford

[49] N. J. Turro, *Modern Molecular Photochemistry*, **1991**, Mill Valley, California

[50] P. Yuster, S. I. Weissman, Effects of perturbations on phosphorescence: luminescence of metal organic complexes, *J. Chem. Phys.*, **1949**, *17*,1182

[51] (a) S. Tobita, M. Arakawa, I. Tanaka, Electronic relaxation processes of rare-earth chelates of benzoyltrifluoroacetone, *J. Phys. Chem.*, **1984**, *88*, 2697; (b) S. Tobita, M. Arakawa, I. Tanaka, The paramagnetic metal effect on the ligand localised $S_1 \rightarrow T_1$ intersystem crossing in the rare-earth-metal complexes with methyl salicylate, *J. Phys. Chem.*, **1984**, *89*, 5649

[52] G. Crosby, M. Kasha, Intermolecular energy transfer in ytterbium organic chelates, *Spectrochim. Acta*, **1958**, *10*, 377

[53] W. D. Horrocks Jr, J. P. Bolender, W. D. Smith, R. M. Supkowski, Photosensitised near infrared luminescence of ytterbum(III) in proteins and complexes occurs via an internal redox process, *J. Am. Chem. Soc.*, **1997**, *119*, 5972

[54] R. M Supkowski, J. P. Bolender, W. D. Smith, L. E. L. Reynolds, W. DeW. Horrocks Jr, Lanthanide ions as redox probes of long-range electron transfer in proteins, *Coord. Chem. Rev.*, **1999**, *185-186*, 307

[55] A. Abusaleh and C. F. Meares, Excitation and de-excitation processes in lanthanide chelates bearing aromatic side chains, *Photochem. Photobiol.*, **1984**, *39*, 763

[56] L. Prodi, M. Meastri, R. Ziessel, V. Balzani, Luminescent Eu^{3+}, Tb^{3+} and Gd^{3+} complexes of a branched-triaazacyclononane ligand containing three 2,2'-bipyridine units, *Inorg. Chem.*, **1997**, *30*, 3798

[57] K. M. Christensen, A. Bakac, J. H. Epsenson, Quenching of the excited state of hydrated europium(III) ions by electron transfer, *Chem. Phys.*, **1993**, *176*, 359

[58] A. Beeby, A. W. Parker, M. S. C. Simpson, D. Phillips, Deuteration effects on the photophysical properties of molecules, *Photochem. Photobiol.*, **1993**, *17*, 205

[59] J. L. Kropp, M. W. Windsor, Luminescence and energy transfer in solutions of rare-earth complexes. I. Enhancement of fluorescence of deuterium substitution, *J. Chem. Phys.*, **1965**, *42*, 1599

[60] J. L. Kropp, M. W. Windsor, Comment on the fluorescence of trivalent europium in D_2O-H_2O mixtures, *J. Chem. Phys.*, **1966**, *45*, 761

[61] J. L. Kropp, M. W. Windsor, Enhancement of fluorescence yield of rare earth ions by heavy water, *J. Chem. Phys.*, **1963**, *39*, 2769

[62] Reisfeld and Jørgensen, *Lasers and Excited States of Rare Earths*, **1977**, Springer-Verlag

[63] R. S. Dickins, D. Parker, A. S. de Sousa, J. A. G. Williams, Closely diffusing O-H, amide N-H and methylene C-H oscillators quench the excited state of europium complexes in solution, *J. Chem. Soc., Chem. Commun.*, **1996**, 697

[64] A. Beeby, I. M. Clarkson, R. S. Dickins, S. Faulkner, D. Parker, L. Royle, A. S. de Sousa, J. A. G. Williams, M. Woods, Non-radiative deactivation of the excited states of europium, terbium, and ytterbium complexes by proximate energy matched O-H, N-H and C-H oscillators: an improved luminescence method for establishing solution hydration states, *J. Chem. Soc., Perkin Trans. 2*, **1999**, 493

[65] A. I. Voloshin, N. M. Shavaleev, V. P. Kazakov, Water enhances the luminescence intensity of β-diketonates of trivalent samarium and terbium in toluene solutions, *J. Photochem. Photobiol., A: Chem.*, **2000**, *134*, 111

[66] A. I. Voloshin, N. M. Shavaleev, V. P. Kazakov, Water enhances photoluminescence intensity of europium(III), terbium(III) and samarium(III) tris β-diketonates in toluene solutions and chemiluminescence, intensity of europium(III) and samarium(III) tris β-diketonates in the reaction with dioxetane, *J. Photochem. Photobiol., A: Chem.*, **2000**, *136*, 203

[67] W. de. W. Horrocks Jr, G. F. Sudnick, C. Kittrell, R. A. Bernheim, Laser induced lanthanide ion luminescence lifetime measurements by direct excitation of metal ion levels. A new class of structural probe for calcium-binding proteins and nucleic acids, *J. Am. Chem. Soc.*, **1977**, *99*, 2378

[68] W. de. W. Horrocks Jr, G. F. Sudnick, Lanthanide ion probes of structure in biology. Laser induced luminescence decay constants provide a direct measure of the number of metal-coordinated water molecules, *J. Am. Chem. Soc.*, **1979**, *101*, 334

[69] A. Beeby, R. S. Dickins, S. Faulkner, D. Parker, J. A. G. Williams, Luminescence from ytterbium(III) and its complexes in solution, *J. Chem. Soc., Chem Commun.*, 1997, 1401

[70] A. Beeby, S. Faulkner, Luminescence from neodymium(III) in solution, *Chem. Phys. Lett.*, **1997**, *266*, 116

[71] T. Kimura, Y. Kato, Luminescence study on the inner-sphere hydration number of lanthanide(III) ions in concentrated aqueous salt solutions in fluid and frozen states, *J. Alloys Compd.*, **1998**, *278*, 92

[72] J.-A. Yu, An observation of back energy transfer in complex Tb(III) with 2-naphthoate in methanol, *J. Lumin.*, **1998**, *78*, 265

[73] N. Sabbatini, M. Guardigli, J.-M. Lehn, Luminescent lanthanide complexes as photochemical supramolecular devices, *Coord. Chem. Rev.*, **1993**, *123*, 201

[74] D. Parker, P. K. Senanayake, J. A. G. Williams, Luminescent sensors for pH, pO_2, halide and hydroxide ions using phenanthridine as a photosensitiser in macrocyclic europium and terbium complexes, *J. Chem. Soc., Perkin Trans. 2*, **1998**, 2129

[75] G. Mathis, Probing molecular-interactions with homogeneous techniques based on rare-earth cryptates and fluoresecence energy transfer, *Clin. Chem.*, **1995**, *41*, 1391

[76] R. E. Whan, G. A. Crosby, Luminescence studies of rare earth complexes: Benzoyl acetonate and dibenzoylmethide chelates, *J. Mol. Spectrosc.*, **1962**, *8*, 315

[77] A. P. Snyder, D. R. Sudnick, V. A. Arkle, W. DeW. Horrocks, Jr, Lanthanide ion luminescence probes. Characterisation of metal ion binding sites and intermetal energy transfer distance measurements in calcium-binding proteins.2. Thermolysin, *Biochem.*, **1981**, *20*, 3334

[78] J. A. A. Ketelaar, The crystal structure of the ethylsulfates of the rare earths and yttrium, *Physica*, **1937**, *4*, 619

[79] J.-C. G. Bünzli, N. André, M. Elhabin, G. Muller, C. Piguet, Trivalent lanthanide ions: versatile coordination centres with unique spectroscopic and magnetic properties, *J. Alloys Compd.*, **2000**, *303-304*, 66

[80] S. I. Klink, L. Grave, D. N. Reinhoudt, F. C. J. M. van Veggel, M. H. V. Werts, F. A. J. Geurts, J. W. Hofstraat, A systematic study of the photophysical processes in polydentate triphenylene-functionalised Eu^{3+}, Tb^{3+}, Nd^{3+}, Yb^{3+}, and Er^{3+} complexes, *J. Phys. Chem. A*, **2000**, *104*, 5457

[81] A. Beeby, R. S. Dickins, S. FitzGerald, L. J. Govenlock, C. L. Maupin, D. Parker, J. P. Riehl, G. Siligardi, J. A. G. Williams, Porphyrin sensitization of circularly polarised near-IR lanthanide luminescence: enhanced emission with nucleic acid binding, *Chem. Commun.*, **2000**, 1183

[82] O. A. Serra, E. J. Nassar, P. S. Calefi, I. L. V. Rosa, Luminescence of a new Tm^{3+} β-diketonate compound, *J. Alloys Compd.*, **1998**, *275-277*, 838

[83] L. R. Melby, N. J. Rose, E. Abramson, J. C. Caris, Synthesis and fluorescence of some trivalent lanthanide complexes, *J. Am. Chem. Soc.*, **1964**, *86*, 5117

[84] A. I. Voloshin, N. M. Shavaleev, V. P. Kazakov, Singlet-singet energy transfer from ketone to lanthanide ion β-diketonates as studied by chemiluminescence quenching. First observation of infrared chemiluminescence of neodymium(III) and ytterbium(III) in solution, *J. Photochem. Photobiol. A: Chem.*, **2000**, *131*, 61

[85] P. D. Wildes, E. H. White, The dioxetane-sensitised chemiluminescence of lanthanide chelates. A chemical source of "monochromatic" light, *J. Am. Chem. Soc.*, **1971**, 6286

[86] M. H. V. Werts, M. A. Duin, J. W. Hofstraat, J. W. Verhoeven, Bathochromacity of Michler's ketone upon coordination with lanthanide(III) β-diketonates enables efficient sensitisation of Eu^{3+} for luminescence under visible light excitation, *J. Chem. Soc., Chem. Commun.*, **1999**, 799

[87] A. Beeby, D. Parker, J. A. G. Williams, Photochemical investigations of functionalised 1,4,7,10-tetraazacyclododecane ligands incorporating naphthyl chromophores, *J. Chem. Soc., Perkin Trans. 2*, **1996**, 1565

[88] G. Zucchi, R. Scopelliti, P.-A. Pittet, J.-C. Bünzli, R. D. Rogers, Structural and photophysical behaviour of lanthanide complexes with a tetraazacyclododecane featuring carbomoyl pendant arms, *J. Chem. Soc., Dalton Trans.*, **1999**, 931

[89] S. Amin, J. R. Morrow, C. H. Lake, M. R. Churchill, Lanthanide(III) tetraamide macrocyclic complexes as synthetic ribonuceases: Structure and catalytic properties of $[La(tcmc)(CF_3SO_3)(EtOH)](CF_3SO_3)_2$, *Angew. Chem. Int. Ed. Eng.*, **1994**, *33*, 773

[90] C. J. Broan, J. P. L. Cox, A. S. Craig, R. Kataky, D. Parker, A. Harrison, A. M. Randall, G. Ferguson, Structure and solution stability of indium and gallium complexes of 1,4,7-trizacyclononanetriacetate and of yttrium complexes of 1,4,7,10-tetraazacyclododecane teraacetate and related ligands: kinetically stable complexes for use in imaging and radioimmunotherapy. X-Ray molecular structure of the indium and gallium complexes of 1,4,7-triacetic acid, *J. Chem. Soc., Perkin Trans. 2*, **1991**, 87

[91] M. P. Oude Wolbers, F. C. J. M. van Veggel, B. H. M. Snellink-Ruël, J. W. Hofstraat, F. A. J. Geurts, D. N. Reinhoudt, Novel preorganised hemispherands to encapsulate rare earth ions: shielding and ligand deuteration for prolonged lifetimes of excited Eu^{3+} ions, *J. Am. Chem. Soc.*, **1997**, *119*, 138

[92] F. J. Steemers, W. Verboom, D. N. Reinhoudt, E. B. van der Tol, J. W. Verhoeven, New sensitiser – modified calix[4]arenes enabing near-uv excitation of complexed luminescent lanthanide ions, *J. Am. Chem. Soc.*, **1995**, *117*, 9408

[93] J.-C. Bünzli, F. Ihringer, Photophysical properties of lanthanide di-nuclear complexes with p-nitro-calix[8]arene, *Inorg. Chim. Acta*, **1996**, *246*, 195

[94] H. Ozaki, E. Suda, T. Nagano, H. Sawai, Sensitisation of europium(III) luminescence by DTPA derivatives, *Chem. Lett.*, **2000**, 312

[95] J. E. Rodeŕiguez-Ubis, M. T. Alonso, O. Juanes, R. Sedano, E. Brunet, The discovery of a simple ligand based on acetophenone bearing excellent quantum yields for the excitation of Eu^{3+} and Tb^{3+}, *J. Lumin.*, **1998**, *79*, 121

[96] M. Kawa, J. M. J. Fréchet, Self-assembled lanthanide-cored dendrimer complexes: enhancement of the luminescence properties of lanthanide ions through site isolation and antenna effects, *Chem. Mater.*, **1998**, *10*, 286

[97] J. R. Escabi-Perez, F. Nome, J. H. Fendler, Energy transfer in micellar systems. Steady state and time resolved luminescence of aqueous micelle solubilised naphthalene and terbium chloride, *J. Am. Chem. Soc.*, **1977**, *99*, 7749

[98] M. Almgren, F. Grieser, J. K. Thomas, Energy transfer from triplet aromatic hydrocarbons to Tb^{3+} and Eu^{3+} in aqueous micellar solutions, *J. Am. Chem. Soc.*, **1979**, *101*, 2021

[99] A. Beeby, I. M. Clarkson, J. Eastoe, S. Faulkner, B. Warne, Lanthanide – containing reversed micelles: A structural and luminescence study, *Langmuir*, **1997**, *13*, 5816

[100] S. V. Beltyukova, A. V. Egorova, Terbium chelates for fluoroimmunassays, *J. Pharm. Biomed. Anal.*, **1998**, *18*, 267

[101] M. Elbanowski, B. Makowska, The lanthanides as luminescent probes in investigations of biochemical systems, *J. Photochem. Photobiol. A:Chem.*, **1996**, *99*, 85

[102] I. Hemmilă, V.-M. Mukkala, H. Takalo, Development of luminescent lanthanide chelate labels for diagnostic assays, *J. Alloys Compds.*, **1997**, *249*, 158

[103] K. Wang, R. Li, Y. Cheng, B. Zhu, Lanthanides – the future drugs? *Coord. Chem. Rev.*, **1999**, *190-192*, 297

[104] S. V. Beltyukova, E. I. Tselik, A. V. Egorova, Use of sensitised luminescence of lanthanides in analysis of drugs, *J. Pharm. Biomed. Anal.*, **1998**, *18*, 261

[105] S. Aime, M. Botta, M. Fasano, E. Terreno, Lanthanide(III) chelates for NMR biomedical applications, *Chem. Soc. Rev.*, **1998**, *27*, 19

[106] S. Aime, F. Benetollo, G. Bombieri, S. Colla. M. Fasano, S. Paoletti, Non-ionic Ln(III) chelates as MRI contrast agents: synthesis, characterisation and ^{1}H NMR relaxometric investigations of bis (benzylamide) diethylenepentaacetic acid Ln(III) and Gd(III) chelates, *Inorg. Chim. Acta*, **1997**, *254*, 63

[107] S. W. A. Bligh, N. Choi, E. G. Evagorou, M. McPartlin, Synthesis and crystal structure of a gadolinium(III) complex of a tetraamine schiff-base macrocycle: a potential contrast agent for magnetic resonance imaging, *Polyhedron*, **1992**, *22*, 2571

[108] T. I. Smirnova, A. I. Smirnov, R. L. Belford, R. B. Clarkson, Lipid magnetic resonance imaging contrast agent interactions: a spin labeling and a multifrequency EPR study, *J. Am. Chem. Soc.*, **1998**, *120*, 5060

[109] I. Sage, Seeing the light, *Chemistry in Britain*, **2001**, *37*, 24

[110] B. M. Tissue, Synthesis and luminescence of lanthanide ions in nanoscale insulating hosts, *Chem. Mater.*, **1998**, *10*, 2837

[111] G. Blasse, B. C. Grabmaier, *Luminescent Materials*, **1994**, Springer-Verlag, New York

[112] L. H. Sloof, A. Polman, M. P. Oude Wolbers, F. C. J. M. van Veggel, D. N. Reinhoudt, J. W. Hofstraat, Optical properties of erbium-doped organic polydentate cage complexes, *J. Appl. Phys.*, **1998**, *83*, 497

[113] Q. J. Zhang, P. Wang, X. F. Sun, Y. Zhou, P. Dai, P. Yang, M. Hai, J. P. Xie, Amplified spontaneous emission of an Nd^{3+}-doped poly(methylmethacrylate) optical fiber at ambient temperature, *Appl. Phys. Lett.*, **1998**, *72*, 407

[114] D. L. Andrews, *Lasers in Chemistry*, **1997**, Springer-Verlag, London

[115] A. J. Kanellopoulos, Laser cataract surgery – A prospective clinical evaluation of 1000 consecutive laser cataract procedures using the dodick photolysis Nd:YAG system, *Ophthalmology*, **2001**, *108*, 649

[116] K. M. Du, J. Zhang, M. Quade, Y. Liao, S. Falter, M. Baumann, M. Loosen, R. Poprawe, Neodymium:YAG 30-W cw laser side pumped by three diode laser bars, *Appl. Optics*, **1998**, *37*, 2361

[117] S. A. Payne, L. D. DeLoach, L. K. Smith, W. L. Kway, J. B. Tassano, B. H. T. Chai, G. Loutts, Ytterbium-doped apatite-structure crystals: A new class of laser materials, *J. Appl. Phys.*, **1994**, *76*, 497

[118] H. Samelson, A. Lempicki, C. Brecher, V. Brophy, Room temperature operation of a europium chelate liquid laser, *Appl. Phys. Lett.*, **1964**, *5*, 173

[119] J. E. Bernard, B. G. Whitford, A. A. Madej, A Tm:YAG laser for optical frequency measurements: mixing 148 THz light with CO_2 laser radiation, *Optics Commun.*, **1997**, *140*, 45

[120] H. Pratisto, M. Ith, M. Frentz, H. P. Weber, Infrared multiwavelength laser system for establishing a surgical delivery path through water, *Appl. Phys. Lett.*, **1995**, *67*, 1963

[121] A. Heller, Liquid lasers – design of neodymium-based inorganic ionic systems *J. Mol. Spect.*, **1968**, *28*, 101

[122] A. Heller, Liquid lasers – fluorescence, absorption and energy transfer of rare earth ion solutions in selenium oxychloride, *J. Mol. Spect.*, **1968**, *28*, 208

[123] K. Okada, Y.-F. Wang, T.-M. Chem, M. Kitamura, T. Nakaya, H. Inoue, Bright red light-emitting organic electroluminescent devices based on a novel thiophene-containing europium complex as an emitting layer, *J. Mater. Chem.*, **1999**, *9*, 3023

[124] V. Christou, O. V. Salata, T. Q. Ly, S. Capecchi, N. J. Bailey, A. Cowley, A. M. Chippendale, New molecular lanthanide materials for organic electroluminescent devices, *Synth. Metals*, **2000**, *111-112*, 7

[125] M. D. McGehee, T. Bergstedt, C. Zhang, A. P. Saab, M. B. O'Regan, G. C. Bazan, V. I. Srdanov, A. J. Heeger, Narrow bandwidth luminescence from blends with energy transfer from semiconducting conjugated polymers to europium complexes, *Adv. Mater.*, **1999**, *11*, 1349

[126] D. Moses, A. Dogariu, A. J. Heeger, Mechanism of carrier generation and recombination in conjugated polymers, *Synth. Metals*, **2001**, *116*, 19

[127] Y. Miyamoto, M. Uekawa, H. Ikeda, K. Kaifu, Electroluminescent properties of a Eu-complex doped in phosphorescent materials, *J. Lumin.*, **1999**, *81*, 159

2.1 UV/Visible absorption spectroscopy

UV/Visible absorption spectra were obtained using an ATI Unicam 2-100 spectrometer and controlled using Vision software version 3.41. Absorption spectra can be obtained over the range 190 - 1100 nm. Solutions were held in quartz cuvettes, usually of 1 cm pathlength, but long or short pathlength cells were also used where necessary. The absorbances were related to the molar extinction coefficient using the Beer-Lambert law:

$$A = \varepsilon c l \qquad 2\text{-}1$$

A = absorbance

ε = molar extinction coefficient / mol^{-1} dm^3 cm^{-1}

c = concentration / mol l^{-1}

l = pathlength / cm

Equation 2-1 was also used for the determination of molar extinction coefficients.

The spectrometer was baselined by subtracting an absorption spectrum of the solvent.

2.1.1 Determination of singlet energies

Singlet state energies were estimated from the ground state absorption spectrum. The wavelength of the (0,0) transition was taken to be that at which the intensity of the absorbance was 10 % of the maximum of the first feature on the red edge of the spectrum. This wavelength was then converted into kJ mol^{-1} using equation 2-2.

$$E = \frac{N_A hc}{1000 \lambda} \qquad 2\text{-}2$$

E = energy of transition / kJ mol^{-1}

N_A = Avogadros number

2.2 Steady state luminescence spectroscopy

Luminescence emission and excitation spectra were carried out on one of 5 spectrometers. A Perkin Elmer LS-50B luminescence spectrometer, the layout of which is shown in fig. 2-1, was operated using FL Winlab 3.0 software. ISA Jobin-Yvon Horiba Fluorolog fluorimeters, FL 3-11 and FL 3-22 and an ISA Jobin-Yvon Horiba fluoromax fluorimeter, were also used for emission in the uv/visible region, controlled using Datamax software.

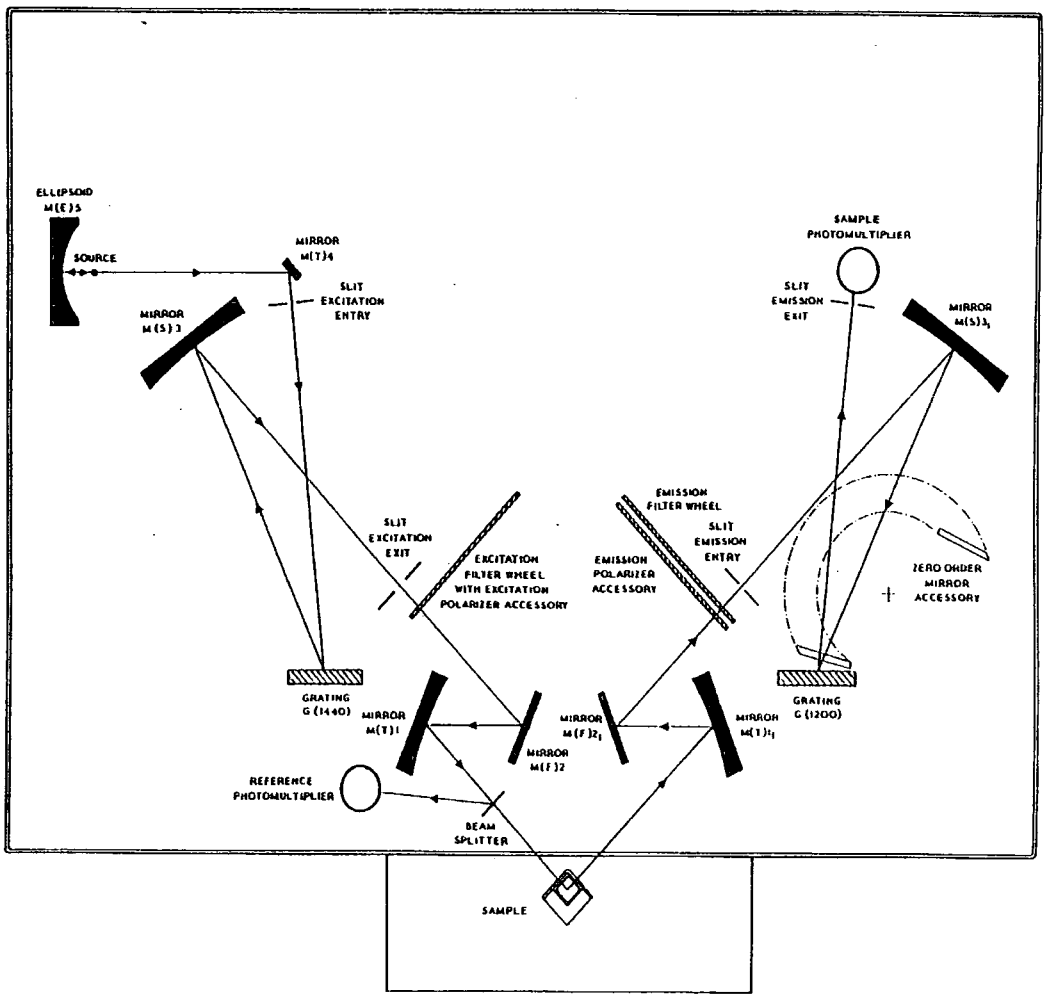

***Figure 2-1** Schematic representation of the layout of the LS-50B luminescence spectrometer*[1]

Near-infrared spectra were obtained using a homemade spectrometer, see fig. 2-2.

A 150 W Xe lamp (Bentham IL6 Illuminator) was used as the excitation source, the radiation was modulated using a chopper, and then focused into a Bentham monochromator (TM 300 V), set with a bandpass of 5 nm full width at half maximum

(FWHM) (unless otherwise stated), which selected the appropriate wavelength band of light.

Most of the energy was then transmitted onto the sample, although a small proportion of radiation was diverted onto a reference photodiode. The fluorescence emission was collected at 90° to the excitation beam and passed through an emission monochromator (Triax 320, Instruments SA, Spex) and then onto an ADC 413 germanium photodiode detector. The signal was demodulated using a lock in amplifier, and the resulting spectrum was recorded and displayed on a PC. The instrumentation was controlled using National Instruments LabVIEW programs.

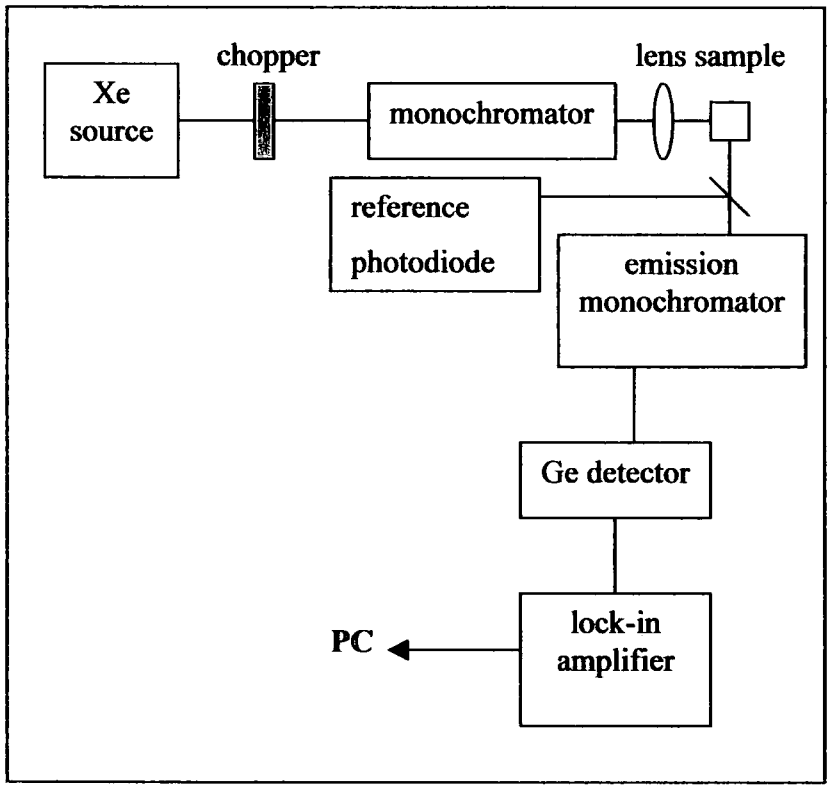

***Figure 2-2** Schematic representation of the home-built near-infrared spectrometer*

A slow scan speed of either 0.5/1.0 nm s^{-1} and narrow excitation and emission monochromator slit widths were used to increase resolution. The maximum absorbance of solutions were chosen to be < 0.2 in order to minimise inner filter effects. Optical filters were used where appropriate to cut out unwanted second or higher order emission from the monochromators.

Correction of emission spectra was achieved following the method described by Gardecki and Maroncelli[2]. The raw data obtained by the spectrometer was fully corrected for instrumental artifacts such as photomultiplier loss of sensitivity at high/low wavelength by multiplying the data by a correction factor. The correction factor was obtained by comparing the recorded spectra of standards spanning the spectral range with their published standard spectra and fitting the difference to a polynomial curve (correction factor). This factor was checked by recording the emission spectrum of a standard (not used in the production of the correction file) such as quinine bisulfate[3] and comparing the corrected spectrum (raw data multiplied by the equation of the polynomial) with the published standard spectrum[3]. An additional method of correction entailed comparing the spectral response of the spectrometer using a standard lamp which has a given output intensity at each wavelength.

2.3 Time resolved steady state emission spectroscopy

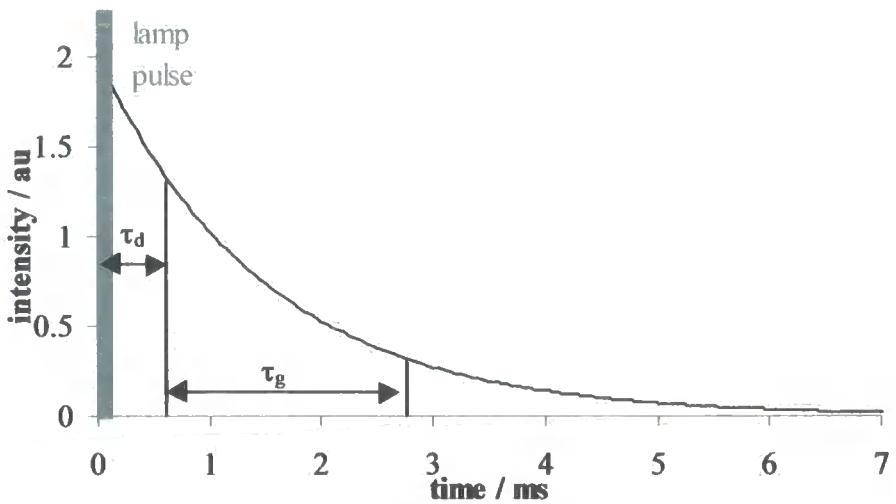

***Figure 2-3** Schematic representation of the time gating operation of the LS-50B luminescence spectrometer.*

τd = delay time / ms (detector turn on)

τg = gate time / ms (detector turn off)

The Perkin Elmer LS-50B luminescence spectrometer can be operated with time delays between the source pulse and the detection of emission. See fig. 2-3. The light source is a pulsed xenon lamp, and the detector can be set to record for a given time period after the flash by varying τd (delay time) and τg (gate time). In this way, total emission ($\tau d = 0$ ms, $\tau g = 10$ ms), fluorescence ($\tau d = 0$ ms, $\tau g = 0.1$ ms), or phosphorescence ($\tau d = 0.1$ ms, $\tau g = 10$ ms) can be recorded.

This allows short lived fluorescence to be "gated out" from long lived emission/phosphorescence.

An additional experiment can also be achieved; if a sample contains two independent emitting sites and exhibits a biexponential decay with $\tau_1 >> \tau_2$, or vice versa, the emission spectra can be recorded at different points along the decay. By recording at τd_1, τg_1, and τd_2, τg_2 so that the $2 >> 1$, if there are any differences between the emission spectra of the two species, then this experiment should allow those differences to be observed. See fig. 2-4.

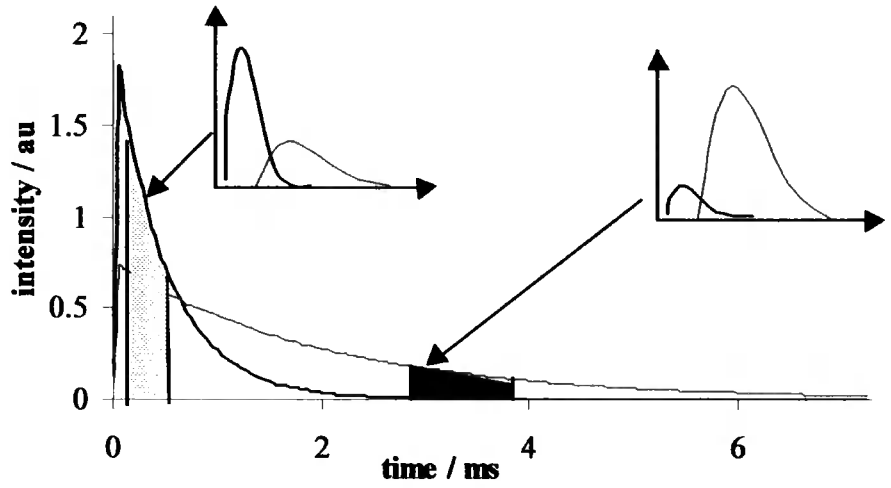

Figure 2-4 *Schematic representation of the ability of the LS-50B luminescence spectrometer to record spectra at different times of an emission decay. The insets show examples of the emission spectra of the two species at the different points along the decay*

2.4 Time resolved emission spectroscopy

The error associated with all lifetime measurements unless otherwise stated is ± 10 %.

The instrument of choice for recording emission lifetimes depends upon the approximate lifetime of the sample. For long lived species (s - hundreds of μs) the Perkin Elmer LS-50B luminescence spectrometer operating in time resolved mode via the home written program *phlemming* was used. This program utilises a pulsed source, detecting the emission for an inputted gate time after the excitation pulse. This delay time is incremented for each cycle, eventually capturing the whole decay.

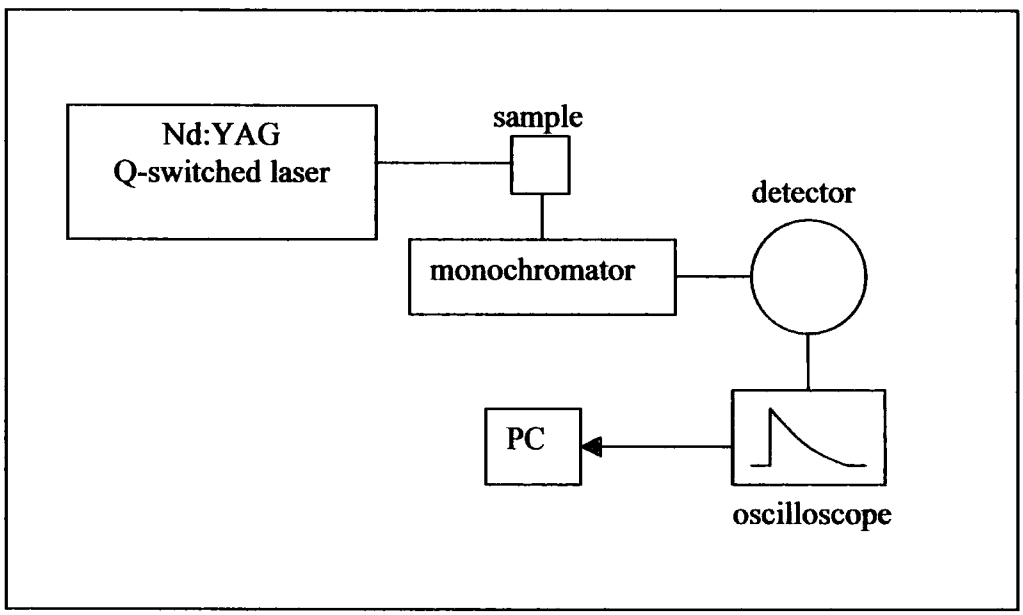

Figure 2-5 *Schematic of the instrumental set up for measuring μs - ns range luminescence lifetimes*

For lifetimes in the μs - ns range, a home made ns - laser pumped fluorimeter is used. The samples were excited by a 10 Hz train of 266, 355 or 532 nm radiation, with a typical pulse energy of 0.1-2.0 mJ per pulse and a duration of ca. 6 ns from a Q-switched Nd:YAG laser (Spectra Physics GCR 150-10). Stray radiation at 1064 nm was removed by the use of optical filters. The luminescence was collected at 90° and focussed onto the entrance slits of a 320 nm focal length monochromator (Triax 320, ISA Spex), set to a bandpass of either 2.5 or 5 nm. The radiation was monitored at the wavelength of interest using either a liquid nitrogen cooled germanium photodiode/amplifier (North Coast EO-817P) for near-infrared detection or a photomultiplier tube (Hamamatsu R928) for visible

detection. The germanium photodiode detector has a rise time of ca. 200 ns and a FWHM of 400 ns. The signal was captured and averaged by a digital storage oscilloscope (Tektronix TDS320) and transferred to a PC for analysis. The instrumental set up is shown schematically in fig. 2-5.

The emission lifetime of a single species follows an exponential decay curve. To obtain the lifetime from the data produced, the decay data is fitted to an exponential function for single species, or a biexponential function for two emitting species according to equation 2-3 either by iterative reconvolution or non linear least squares fitting[4,5].

$$I(t) = A_1.\exp\left(\frac{-t}{\tau_1}\right) + A_2.\exp\left(\frac{-t}{\tau_2}\right) \qquad 2\text{-}3$$

The best fit was determined by minimising the residuals (the difference between the calculated fit and the experimental data). Typical fits are shown in fig 2-6.

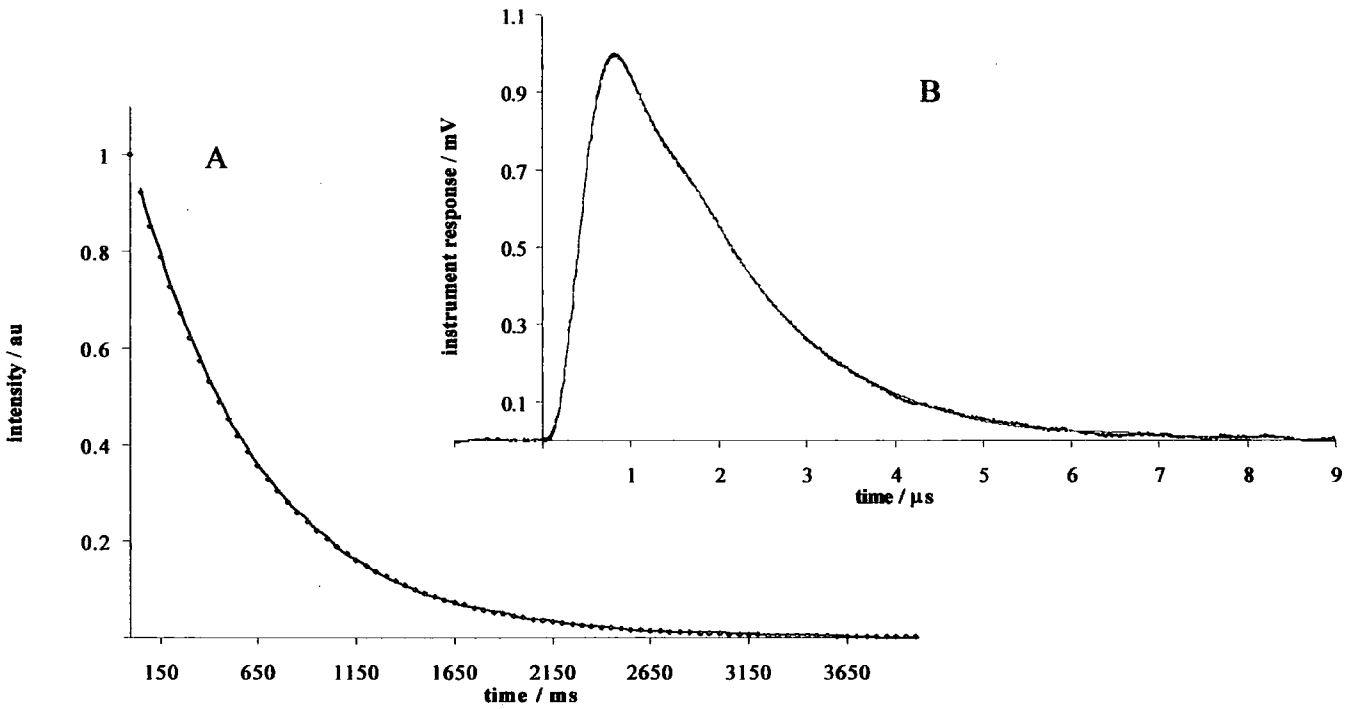

***Figure 2-6** Typical fits obtained for lifetime measurements. A: obtained using phlemming, black = decay, grey = fitted curve. B: obtained using the Nd:YAG laser and IR detection, black = decay, grey = fitted curve*

2.5 Solid state luminescence

Emission and excitation spectra (steady state and time resolved) can also be measured in the solid state. The samples prepared were either thin films (by evaporation of solvent) or in their powder form. The thin films were held on a glass slide and measurements were recorded at 60° to the excitation beam to prevent specular reflection from the film/window entering the emission port. The solid samples as powders were held in 2 mm diameter quartz tubes.

2.6 Low temperature measurements

The experiments described so far can all be carried out at room temperature, 77K or at intermediate temperatures with the aid of a variable temperature liquid nitrogen cooled cryostat (Oxford Instruments DN1 704), regulated with a temperature controller (ITC 601) to ± 0.1 K. The layout of the cryostat is shown in fig. 2-7.

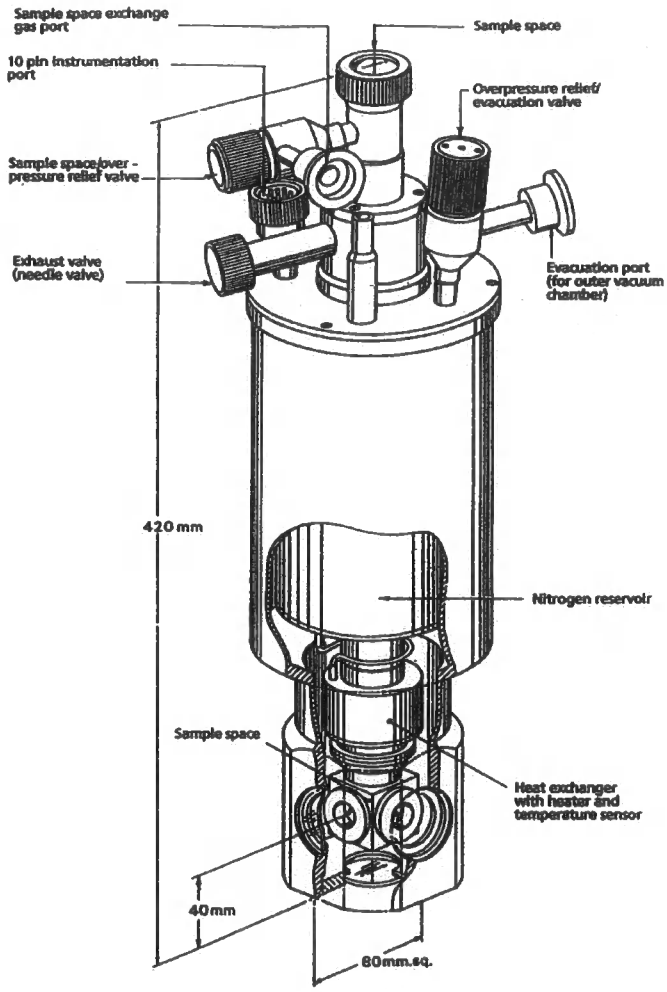

***Figure 2-7** Schematic representation of the layout of the Oxford Instruments DN 1704 Cryostat*[6]

Home built instrumentation, the Perkin Elmer LS-50B luminescence spectrometer, and the ATI Unicam UV/Visible absorption spectrometer have been specially adapted to hold the cryostat in a position such that the center of the sample is at the centre of the optical paths. Low temperature luminescence spectra were obtained at 77 K using either 2 mm diameter round quartz optical cuvettes held in a copper block, or 10 mm square quartz cuvettes. The sample is cooled by a flow of liquid nitrogen from the reservoir to a heat exchanger.
Low temperature spectra were recorded with a suitable solvent, either EPA (5:5:2 Ether:Isopentane:Ethanol) or 1:4 EtOH:MeOH, both of which form a clear glass at 77 K[7].

2.6.1 Determination of triplet energies

Triplet state energies were estimated from the phosphorescence spectra recorded at 77 K. The wavelength of the (0,0) transition was taken to be that at which the intensity of the emission at the blue edge of the band was 10 % of the maximum. This wavelength was then converted into kJ mol^{-1} using equation 2-2.

2.7 Emission quantum yields

The associated error with all quantum yield measurements (both measured and calculated) is ± 10 %

The efficiency of emission is measured by the quantum yield. The measurement of absolute quantum yields usually requires the use of integrating spheres or actinometers, but measuring the relative quantum yield is possible by comparing the emission from the sample with that of a standard compound.
By definition the emission quantum yield of a sample Φ_x expresses the proportion of optically excited molecules that deactivate by emitting a photon. It is the ratio of the number of photons emitted to the number of photons absorbed per unit time.

$$\Phi_x = \frac{\text{no. of photons emitted}}{\text{no. of photons absorbed}} \qquad 2\text{-}4$$

It can then be seen that the fluorescence quantum yield is directly related to the radiative, k_R and nonradiative, k_{NR} rate constants by:

$$\Phi_x = \frac{k_R}{(k_R + k_{NR})} \qquad 2\text{-}5$$

For recording relative emission quantum yields, the emission efficiency of a sample (x) is related to that of a standard (ref) by the equation:

$$\Phi_x = \left(\frac{A_{ref}}{A_x}\right)\left(\frac{I_x}{I_{ref}}\right)\left(\frac{n_x}{n_{ref}}\right)^2 .\Phi_{ref} \qquad 2\text{-}6$$

A = absorbance at excitation wavelength

I = integrated emission spectrum (area under fully corrected emission spectrum)

n = refractive index of solvent

The determination of a quantum yield requires the selection of an appropriate standard. A suitable standard should both absorb and emit in the same spectral region as the sample. The absorbances and emission spectra of 5 solutions each of both the sample and reference are recorded. Peak absorbances are chosen to be in the region 0.02 – 0.1 in order to minimise inner filter effects. Also, a long pathlength cell (5 or 10 cm) is used for absorption measurements to achieve a more accurate determination. The excitation and emission slits of the luminescence spectrometer were adjusted to give a satisfactory signal (not too intense to give saturation of detector, nor too weak giving a noisy signal). This setting remains unchanged throughout the experiment. The emission spectra are corrected for the instrument response and then integrated over the entire area. The gradient is found from a plot of absorbance vs. integrated emission allowing the following equation to be used for the determination of the quantum yield.

$$\Phi_x = \Phi_{ref}\left(\frac{A_{ref}}{A_x}\right)\left(\frac{slope_x}{slope_{ref}}\right)\left(\frac{n_x}{n_{ref}}\right)^2 \qquad 2\text{-}7$$

The standards used for Eu^{3+} emission were Rhodamine[8] 101 in $EtOH/H^+$ ($\Phi_f = 1.0$), Cresyl Violet[9] in MeOH ($\Phi_f = 0.54$), and for Tb^{3+} Quinine Bisulfate[10] in 1N H_2SO_4 ($\Phi_f = 0.546$), and Fluorescein[11] in $NaOH_{(aq)}$ ($\Phi_f = 0.79$).

2.8 Laser flash photolysis

Flash photolysis experiments were carried out on a modified version of the experimental set up used for the kinetic measurements (see fig. 2-5) with the addition of a Xe lamp being used to probe the sample.

The sample is excited by a pulse of laser radiation whereupon triplet states are formed via intersystem crossing. The sample then absorbs a quantity of light in a $T_1 \rightarrow T_2$ process

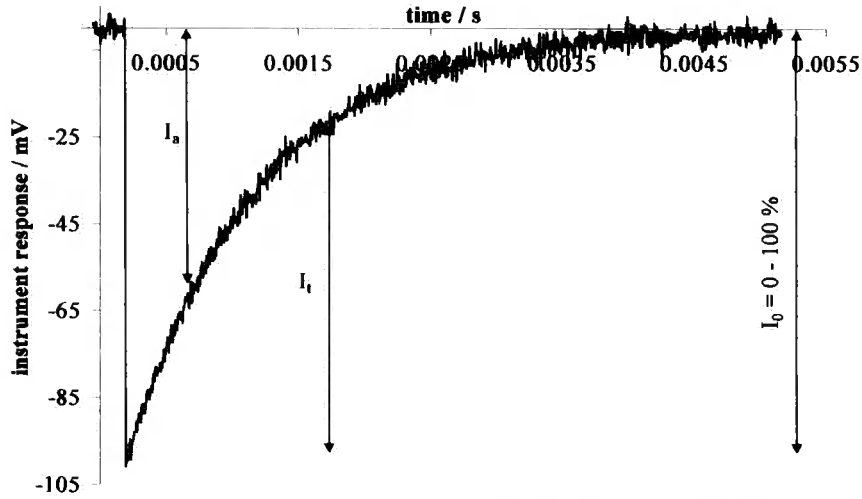

from the Xe lamp. The intensity of light passing straight through the sample is known as the 0 – 100 % voltage.

A kinetic decay is produced representing the rate of decay of the triplet-triplet absorption, as shown in fig. 2-8 and the values I_0, I_a, and I_t are determined.

The data can be converted to absorbance using equation 2-12.

$$\Delta A = \log_{10}\left(\frac{I_0}{(I_0 - I_a)}\right) \qquad 2\text{-}12$$

Figure 2-8 *Example of the decay obtained from a flash photolysis experiment*

2.9 Sample preparation

2.9.1 Degassed samples

Solution state samples were degassed where necessary using the freeze-pump-thaw method and 4 of these cycles were employed.

2.9.2 Preparation of chapter 7 complexes

The disodium salts of Eu^{3+}, Tb^{3+}, Dy^{3+} and Yb^{3+} ethoxybenzyl-diethylentriaminepenta-acetic acid were provided by Schering AG; the La^{3+}, Nd^{3+}, Sm^{3+}, Gd^{3+}, and Tb^{3+} complexes were all prepared from the free ligand following the method suggested by Aime *et al.*[12]. Equimolar amounts of the lanthanide(III) salt nitrate/acetate and the monosodium salt of ethoxybenzyl-DTPA were dissolved in H_2O and the pH adjusted to 7.0 with $NaOH_{(aq)}$. Acetone was added to this solution to initiate precipitation of the complex. Acetone was added until precipitation of the solid was complete. The solution

was then evaporated to dryness and dissolved in H_2O. The emission spectrum of the Tb^{3+} complex was compared against the spectrum of the complex provided by Schering AG to ensure the Ln^{3+} ion was fully complexed to the ligand.

2.10 Chemicals used

CHEMICAL NAME	ABBREVIATION	SUPPLIER	GRADE / PURITY
Water	H_2O	—	PURITE
Ethanol	EtOH	Fisher Chemicals	HPLC
Methanol	MeOH	Prolabo	Analar
Isopropanol	Pr^2OH	BDH	Analar
Chloroform	$CHCl_3$	Fisher Chemicals	99.99 %
Dichloromethane	CH_2Cl_2	Fisher Chemicals	99.99 %
Acetonitrile	MeCN	Aldrich	99.3 %
Deuterated water	D_2O	Aldrich	99.9 %
Deuterated methanol	MeOH – d4	Aldrich	99+ %
Toluene	—	BDH	Analar
Cyclohexane	C_6H_6	Fisher Chemicals	99.99 %
Acetone	—	Fisher Chemicals	Analar
Methyl sulfoxide	DMSO	Aldrich	99.8 %
Rhodamine 101	—	—	Suitable as laser dye
Cresyl violet perchlorate	—	Aldrich	Suitable as laser dye
Quinine bisulfate	—	—	Suitable as laser dye
Fluorescein	—	—	Suitable as laser dye
Styryl 9	—	—	Suitable as laser dye
Triethylenetetraaminehexaacetic acid	TTHA	Aldrich	98 %
Diethylenetriaminepentaacetic acid	DTPA	Aldrich	98 %
Ethylenediaminetetraacetic acid	EDTA	Koch-Light Laboratories	Analar
Europium(III) nitrate pentahydrate	$Eu(NO_3)_3.5H_2O$	Aldrich	99.9 %
Europium(III) chloride hexahydrate	$EuCl_3.6H_2O$	Aldrich	99.9 %
Terbium(III) nitrate pentahydrate	$Tb(NO_3)_3.5H_2O$	Aldrich	99.9 %
Terbium(III) chloride hexahydrate	$TbCl_3.6H_2O$	Aldrich	99.9 %
Thulium(III) nitrate pentahydrate	$Tm(NO_3)_3.5H_2O$	Aldrich	99.9 %

Lanthanum(III) acetate hydrate	$La(CH_3CO_2)_3.xH_20$	Aldrich	99.9 %
Neodymium(III) nitrate hexahydrate	$Nd(NO_3)_3.6H_2O$	Aldrich	99.9 %
Samarium(III) nitrate hexahydrate	$Sm(NO_3)_3.6H_2O$	Aldrich	99.9 %
Gadolinium(III) nitrate hexahydrate	$Gd(NO_3)_3.6H_2O$	Aldrich	99.9 %
Complexes used in chapter 4	—	J. A. G. Williams	> 95 %
Complexes used in chapter 5	—	J. A. G. Williams	> 95 %
Micelles used in chapter 6	—	I. Fallis	> 95 %
Complexes used in chapter 7	—	Schering AG	> 95 %
Ethoxybenzyl-diethylenetriaminepentaacetic acid	EOB-DTPA	Schering AG	> 95 %
Complexes used in Appendix A	—	Opsys displays Ltd.	> 95 %
4,4-dimethoxybenzophenone	—	Lancaster	98+ %
Europium tris(6,6,7,7,8,8,8-heptafluoro-2,2-dimethyloctane-3,5-dione)	$Eu(fod)_3$	Aldrich	99 %
Europium 1,4,7,10-tetraazacyclododecane	EuDOTA	D. Parker	> 95 %
Terbium 1,4,7,10-tetraazacyclododecane	TbDOTA	D. Parker	> 95 %
4-acetamidobenzophenone	—	A. Beeby	> 95 %
Benzophenone	—	Aldrich	99+ %
2-naphthylacetic acid	NAA	Aldrich	99 %
Biphenyl	—	Aldrich	99.5 %
Naphthalene	—	Aldrich	99+ %
Hydrochloric acid	HCl	BDH	GPR
Sulfuric acid	H_2SO_4	Fisher Chemicals	95-98 %
Sodium hydroxide	NaOH	Fisher Chemicals	97+ %

Table 2-1 *Table summarising the chemicals used, the source and purity.*

A list of the chemicals used throughout are given in table 2-1.

REFERENCES

[1] Perkin Elmer LS-50 B User's Manual

[2] J. A. Gardecki and M. Maroncelli, Set of secondary emission standards for calibration of the spectral responsivity in emission spectroscopy, *Appl. Spectrosc.*, **1998**, *52*, 1179

[3] W. H. Melhuish, A standard fluorescence spectrum for calibrating spectrofluorophotometers, *J. Phys. Chem.*, **1959**, 762

[4] J. N. Demas, *Excited State Lifetime Measurements*, **1983**, Academic Press, New York.

[5] A. Beeby, S. Faulkner, Luminescence from neodymium(III) in solution, *Chem. Phys. Lett.*, **1997**, *266*, 116

[6] Variable temperature liquid nitrogen cryostat DN 1704, *Operators Handbook*, Oxford instruments

[7] S. l. Murov, I. Carmichael, G. L. Hug, *Handbook of Photochemistry*, **1995**, Marcel Dekker Inc., New York.

[8] T. Karstens, K. Kobe, Rhodamine B and rhodamine 101 as reference substances for fluorescence quantum yield measurements, *J. Phys Chem.*, **1984**, *84*, 1871

[9] D. Magde, J. H. Brannon, T. L. Cremers, J. Olmsted III, Absolute luminescence yield of cresyl violet. A standard for the red, *J. Phys. Chem.*, **1979**, *83*, 696

[10] W. H. Melhuish, Absolute spectrofluorometry, *J. Research, NBS – A: Physics and Chemistry*, **1972**, *76A*, 547

[11] J. Q. Umberger, V. K. LaMer, The kinetics of diffusion controlled molecular and ionic reactions in solution as determined by measurements of the quenching of fluorescence, *J. Am. Chem. Soc.*, **1945**, 1099

[12] S. Aime, F. Benetollo, G. Bombieri, S. Colla, M. Fasano, S. Paoletti, Non-ionic Ln(III) chelates as MRI contrast agents: synthesis, characterisation and ^{1}H NMR relaxometric investigations of bis(benzylamide) diethylenepentaacetic acid Ln(III) and Gd(III) chelates, *Inorg. Chim. Acta*, **1997**, *27*, 63

3.1 Introduction

Interest in the solution state luminescence of lanthanide(III) ions in solution has, understandably, centred around the visible light emitting ions with long lived emission; Sm^{3+}, Eu^{3+}, Tb^{3+}, and Dy^{3+}. Recent work has also taken into account the near infrared emitting ions of Yb^{3+}, Nd^{3+}, and Er^{3+} due to the importance of the optical window in the near-IR for data transmission[1] and the fact that these ions can be sensitised by visible light absorbing chromophores[2].

Although some substantial work has been carried out on Tm^{3+} in the solid state, little is known about the emission properties of Tm^{3+} in solution.

3.1.1 Solid state emission studies of Tm^{3+}

In the solid state Tm^{3+} has been shown to exhibit efficient luminescence and its importance has been highlighted by the possibility of Tm^{3+} ions doped in fluoride glasses and yttrium aluminium garnet (YAG) for use as laser media and fibre amplifiers[3,4] where tunable continuous wave laser emission at room temperature has been demonstrated. Emission from the $^1D_2$ and $^1G_4$ emissive states of Tm^{3+} to the numerous ground states has been shown in various studies[5,6].

It appears from a typical emission spectrum that there are 4 main emission bands of thulium at 450, 650, 780, and 880 nm, although these bands actually correspond to more than one transition.

There is some discrepancy in the literature regarding the assignment of various bands which results from confusion in the position of the $^3F_4$ and $^3H_4$ levels. The 480 nm band is clearly attributed to the $^1G_4 \rightarrow {}^3H_5$ transition but in different studies the band around 650 nm has been assigned to either the $^1G_4 \rightarrow {}^3H_4$ [7] or the $^1G_4 \rightarrow {}^3F_4$ transition[8]. Consequently, there has also been a certain confusion in the assignment of the less intense band at ~ 805 nm, with the transitions being assigned either $^1G_4 \rightarrow {}^3H_5$ [9] or $^3H_4 \rightarrow {}^3H_6$ [10]. Bachir *et al.*[11] have recently brought attention to the discrepancy and have unambiguously attributed the 805 nm band to the $^3H_4 \rightarrow {}^3H_6$ transition following a study with Tm^{3+} ions doped in zinc

oxide. The Tm:ZnO material was mounted as electrodes and the variation of the intensity of emitted light at 480 and 805 nm relative to an applied potential was recorded. The variation observed showed that the two bands could not arise from the same energy levels and that therefore, the 805 nm transition occurs not from the $^1G_4$ but the $^3H_4$ level. This attribution was reinforced by time resolved measurements which showed that the two emission bands had different decay rates, and provided further evidence that the transitions could not be from the same level.

Hong *et al.*[12] exploited the 480 nm bright blue emission from Tm^{3+} to incorporate into an electroluminescent device. Their $Tm(acac)_3phen$ (thulium-tris(acetylacetonato)-(monophenanthroline)) had a triplet energy of 25000 cm^{-1}, so they were able to selectively populate the $^1G_4$ level via an energy transfer mechanism.

3.1.2 Solution state studies on Tm^{3+}

There has been surprisingly little published on the photophysical properties of Tm^{3+} in solution, and most studies have concentrated on the absorption properties[13,8]. It has been shown that certain bands ($^3F_4 \leftarrow {}^3H_6$, $^3H_4 \leftarrow {}^3H_6$, and $^1G_4 \leftarrow {}^3H_6$) show hypersensitive behaviour, and the Judd-Ofelt parameters for Tm^{3+} have been published[8]. There is less information on the emission properties of Tm^{3+} in solution in the literature[14,15,16], with most studies concentrating on the β-diketonate complexes. Even fewer emission spectra have been published, and only one emission spectrum with more than one band was found in the literature, published by Sharma *et al.*[16] who recorded the emission spectrum of Tm^{3+} complexed to dipicolinic acid. Sharma *et al.* also attempted to record the radiative lifetime of their $Tm(DPA)_3$ complex but found that the decays were faster than the time resolution of their instrument ($\leq$ 5 μs). Heller[15] in 1968 published an emission spectrum from the Tm^{3+} ion in a $SeOCl_2$ acid solution of the single $^1G_4 \rightarrow {}^3H_6$ transition. In 1975 Stein and Würzberg[17] reported the emission from a series of lanthanide perchlorates (including Tm^{3+}) in aqueous and deuterated water solutions. They did not report lifetime values or quantum yield data for Tm^{3+} however, suggesting that Tm^{3+} emission is significantly quenched by the lower energy vibrations of molecules in the first solvation layer, in agreement with the results from Sharma *et al.*[16] An interesting study[14] has highlighted a possible detector for trace Tm^{3+} ions in rare earth ion solutions by monitoring the Tm^{3+} emission in the thulium-bis(1'-phenyl-3'-methyl-5'-pyrazol-4'-one)hexanedione-cetyltri-methylammonium bromide (Tm-BPMPHD-CTMAB) complex. In aqueous solution Tm^{3+} forms an ion association with BPMPHD and CTMAB which enhances the thulium

emission 25 fold. Wolbers *et al.*[18] carried out a study on a series of lanthanide(III) ions including thulium with *m*-terphenyl containing ligands in methanol solution, but did not see any sensitised emission from the Tm^{3+} complexes. They attributed the lack of observed emission to the $^1D_2$ emissive level (27800 cm^{-1}) being too high in energy for sensitisation from the *m*-terphenyl triplet state (23500 cm^{-1}).

In the work presented here the excited state kinetics and luminescence spectra of free thulium(III) in a variety of protic solvents and their deuterated analogues are reported. Also investigated is the effect of a range of different chelates on the lifetime of the metal ion.

The Tm^{3+} energy level diagram is represented in fig. 3-1.

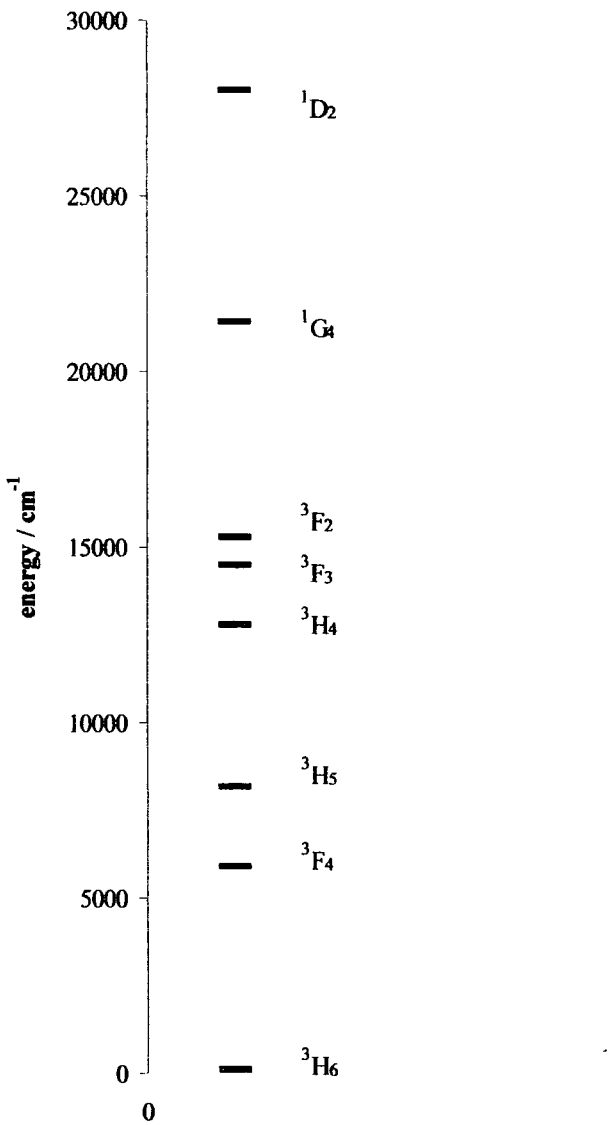

***Figure 3-1** Energy level diagram of the Tm^{3+} ion electronic energy levels*

3.2 Results and discussion

The Tm^{3+} ion was studied in a variety of environments as shown in table 3-1.

Solvent	no chelate	TTHA	DTPA
H_2O	✓	✓	✓
D_2O	✓	✓	✓
2:1 H_2O:D_2O	✓		
MeOH	✓		
MeOH – d4	✓		
DMSO	✓		

***Table 3-1** Tm^{3+} environments studied in this chapter*

TTHA = 1 molar equivalent of triethylenetetraaminehexaacetic acid

DTPA = 1 molar equivalent of diethylenetriaminepentaacetic acid

The molecular structures of TTHA and DTPA are given in fig. 3-1.

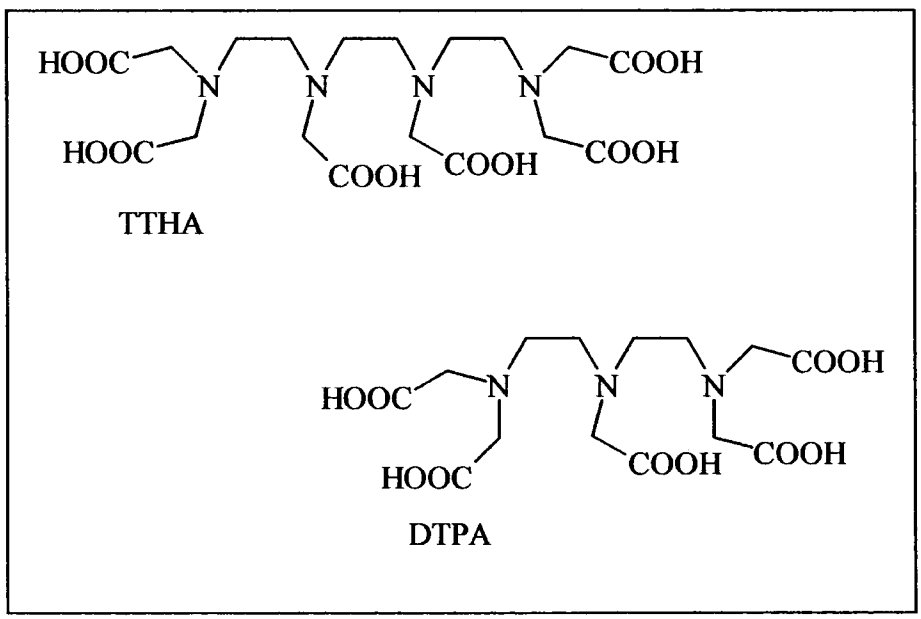

***Figure 3-2** Molecular structures of the chelates used in this chapter*

3.2.1 *Absorption spectra*

The absorption spectrum of Tm^{3+} nitrate in H_2O is shown in fig. 3-3.

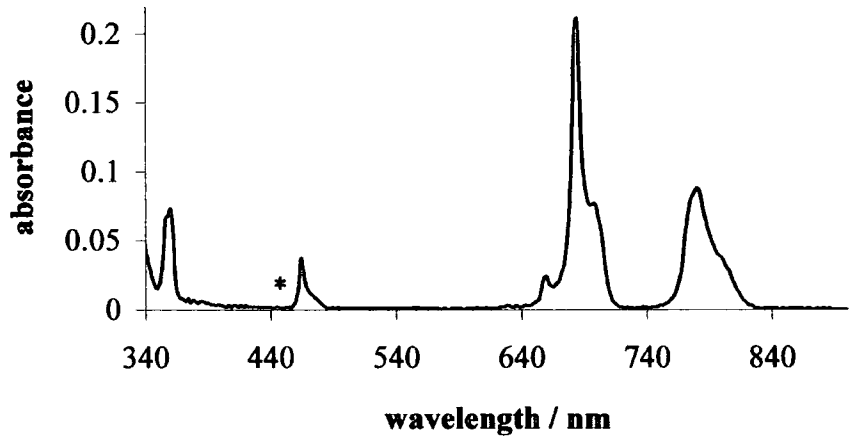

***Figure 3-3** The absorption spectrum of $Tm^{3+}_{(aq)}$ 0.1 mol l^{-1}*

These absorption peaks are of low intensity $\varepsilon < 3$ mol^{-1} dm^3 cm^{-1} and are very typical of those expected of lanthanide ions. Table 3-2 highlights the transitions responsible for the absorption bands. The hypersensitive $^1G_4 \leftarrow {}^3H_6$ transition marked * as described by Gruen *et al.*[19] displays unusual sensitivity to the local environment around the ion, and as with other lanthanide transitions which exhibit hypersensitive behaviour, the $^1G_4 \leftarrow {}^3H_6$ transition obeys the selection rules $|\Delta J| \leq 2$, $|\Delta L| \leq 2$.

Transition	Wavelength / nm
$^1D_2 \leftarrow {}^3H_6$	355
$^1G_4 \leftarrow {}^3H_6$	476*
$^3F_2 \leftarrow {}^3H_6$	649
$^3F_3 \leftarrow {}^3H_6$	689
$^3H_4 \leftarrow {}^3H_6$	781

* = hypersensitive transition

***Table 3-2** Transitions seen in the absorption spectrum*

3.2.2 *Steady state luminescence spectra*

The emission and excitation spectra for all the Tm^{3+} complexes were recorded. An example of a Tm^{3+} emission spectrum is shown in fig. 3-4 where all characteristic bands associated with the ion (at ~ 450, 480, 510, 650, 750, and 780 nm) can be observed. By using an excitation wavelength such that the $^1D_2$ state is populated (360 nm) all emission bands are seen. However, using an excitation wavelength > 360 nm, the emission bands originating from the $^1D_2$ level are excluded.

Recording the excitation spectra of each of these bands also yields interesting differences, for example with λ_{em} = 511 nm a band at 444 nm associated with the $^1D_2 \leftarrow {}^3F_4$ transition is detected. The 444 nm band is absent however, in an excitation spectrum with λ_{em} = 647 nm indicating that the emission from the 511 and 647 nm bands derive from different electronic energy levels.

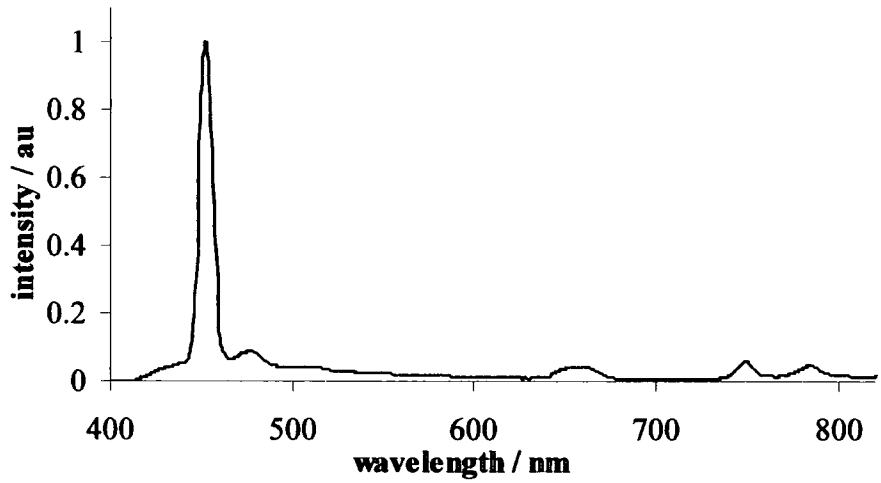

Figure 3-4 *Emission spectrum of 0.2 mol l^{-1} Tm^{3+} in MeOH – d4 λ_{ex} = 360 nm bandpass = 5 nm, emission bandpass = 5 nm*

3.2.3 *Time resolved emission*

3.2.3.1 Assigning the emission transitions

Following direct excitation of the thulium $^1D_2$ state at 355 nm, the kinetic decays from each of the emission bands were recorded.

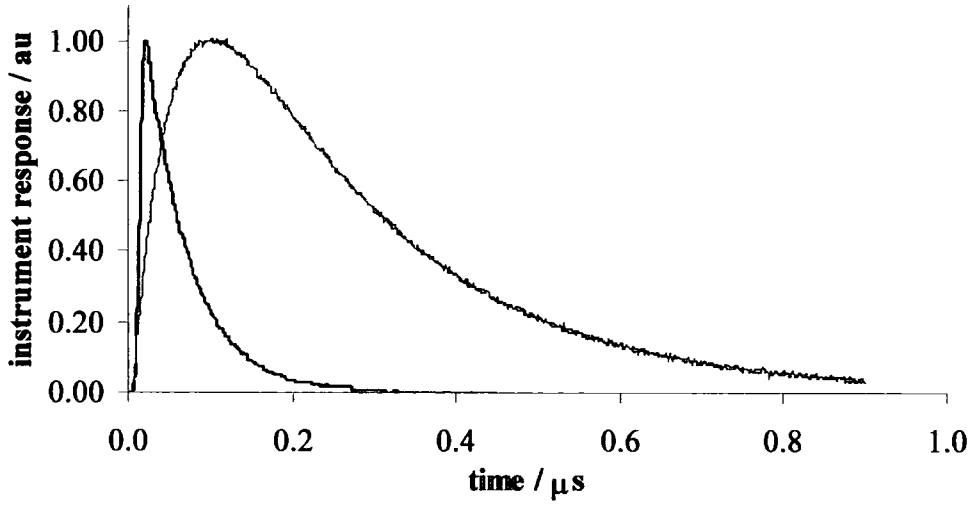

Figure 3-5 *Example of decay profiles from the $^1D_2$ λ_{em} = 451 nm (black) and $^1G_4$ λ_{em} = 479 nm (grey) states of Tm^{3+} in D_2O, λ_{ex} = 355 nm*

Two main decay profiles were observed and are illustrated in fig. 3-5. The decays from the 452, 511, and 659 nm bands fitted to a single exponential function with the same rate constant. The bands at 479 and 647 nm both show a rising edge to the signal followed by a single exponential decay. Both bands showed the same lifetime. The profile from the band at 751 nm displays a fast rise time and a single exponential decay which is different to those associated with the 479 and 647 nm bands. The band at 780 nm was scanned in 2 nm increments from 770 nm to 790 nm and different decay profiles were observed which suggested that the band is composed of emission from more than one state. The kinetic data from the complexes are collected in table 3-3.

wavelength / nm / system	452	479	511	647	659	751	770	790
D_2O	58	253	55	271	58	42	307	279
2:1 D_2O:H_2O	4	26	4					
MeOH	7	12	7	3	7			
MeOH – d4	17	49	17	42	25			
DMSO	58	58	53	66	62			
DTPA – H_2O	8	13	8	19	9			
DTPA – D_2O	104	35	118	38	118			
TTHA – H_2O	13	12	10	12	17			
TTHA – D_2O	93	35	96	38	99			

Table 3-3 *Kinetic decay data from the Tm^{3+} complexes. Values are given in ns; with τ values > 50 ns there is an associated error of ± 10 %, with values < 50 ns, there is an associated error of ± 20 %*

The results show that the bands at 452, 511, 659, and 751 nm all have the same (within experimental error) single exponential decay time. It should be noted that the bands at $\lambda > 600$ nm have weak emission, and the error in fitting the decays from these bands increases as the signal to noise ratio is raised. Comparing the energies from these bands with the electronic energy levels from the energy level diagram (ELD) the f-f transitions leading to these bands can be assigned. It can be seen that these emission bands all originate from the $^1D_2$ state. The transitions being $^1D_2 \rightarrow {}^3H_6$, $^1D_2 \rightarrow {}^3F_4$, $^1D_2 \rightarrow {}^3H_5$, and $^1D_2 \rightarrow {}^3F_3$ respectively. All other transitions display clear associated rise times. In the second series of transitions, which all show the same decay time, and after comparison with the ELD, it can be seen that these transitions originate from the $^1G_4$ level. With the bands at 479 and 647 nm being due to the $^1G_4 \rightarrow {}^3H_6$ and $^1G_4 \rightarrow {}^3F_4$ transitions respectively. The rise time of the $^1G_4$ level matches the decay times from the $^1D_2$ level suggesting a mechanism of $^1D_2 \rightarrow {}^1G_4$ is responsible for the population of the $^1G_4$ level via excitation at $^1D_2$. The profile of the band at 780 nm is however, unlike that from either the $^1D_2$ or the $^1G_4$ states. From the ELD it can be seen that the band at 780 nm corresponds to transitions from both $^1D_2$ and $^1G_4$ states (at 770 and 790 nm) $^1D_2 \rightarrow {}^3F_2$ and $^1G_4 \rightarrow {}^3H_5$

and could also have emission contribution from the $^3H_4 \rightarrow {}^3H_6$ transition as described by Bachir *et al.*[11]. Collecting these data, the energy level diagram of the electronic energy levels can be modified from that produced by Stein and Würzberg[17] and is schematically represented in fig. 3-6 alongside the observed emission transitions.

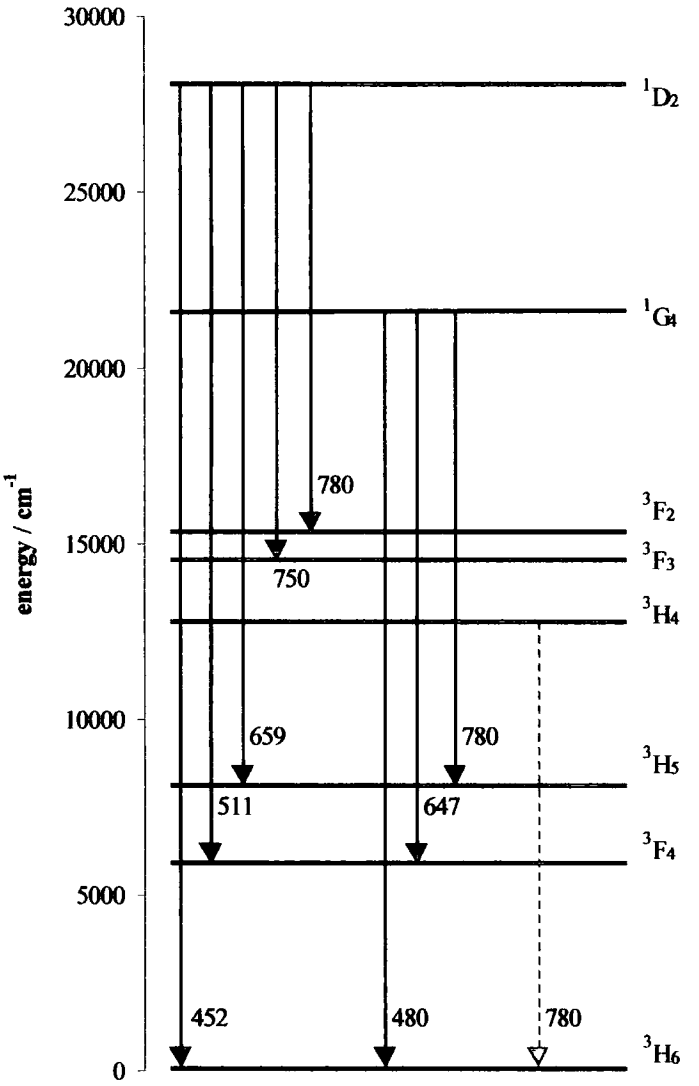

***Figure 3-6** Energy level diagram of the Tm^{3+} ion electronic energy levels showing the emission transitions and corresponding wavelengths*

A summary of the lifetimes of both the $^1D_2$ and $^1G_4$ states for the various chemical environments is shown in table 3-4, and a summary of the emission transitions is given in table 3-5.

System	lifetime of $^1D_2$ state	lifetime of $^1G_4$ state
D_2O	56	266
2:1 D_2O:H_2O	4	26
MeOH	7	12
MeOH – d4	20	46
DMSO	56	62
DTPA – H_2O	8	16
DTPA – D_2O	113	36
TTHA – H_2O	13	12
TTHA – D_2O	96	36

Table 3-4 *Lifetimes of the $^1D_2$ and $^1G_4$ states. Values are given in ns, errors $\tau > 50$ ns ± 10 %, $\tau < 50$ ns ± 20 %*

wavelength / nm	transition
452	$^1D_2 \rightarrow {}^3H_6$
480	$^1G_4 \rightarrow {}^3H_6$
511	$^1D_2 \rightarrow {}^3F_4$
647	$^1G_4 \rightarrow {}^3F_4$
659	$^1D_2 \rightarrow {}^3H_5$
750	$^1D_2 \rightarrow {}^3F_3$
780	$^1D_2 \rightarrow {}^3F_2$ $^1G_4 \rightarrow {}^3H_5$ $^3H_4 \rightarrow {}^3H_6$

Table 3-5 *Transitions seen in the emission spectrum*

3.2.3.2 Quenching

The lifetime of Tm^{3+} in H_2O was shorter than the response time of the detector, but a plot of % D_2O:H_2O vs lifetime yielded an estimate of 40 ps for the lifetime in H_2O solution. This value clearly illustrates the efficient quenching of the excited state by O-H oscillators. This effect is not only seen in the aqua ion, but the lifetime of the chelated Tm^{3+} ion is also significantly enhanced upon deuteration of the solvent. Deuteration increases the emission lifetime by removing the non-radiative decay pathways resulting from the vibration of O-H and C-H bonds. The vibrational stretching frequencies of X-H bonds are higher in energy than X-D bonds so that energy matching of the X-H vibrational levels with the Tm^{3+} excited states affords a much more favourable Franck-Condon overlap integral than the vibrational levels of X-D bonds. This effect has been acknowledged for some time[20].

The lifetimes of the excited states in the chelates generates a surprising result. The lifetime of the $^1D_2$ state of the Tm^{3+} ion in the TTHA complex in D_2O is shorter than the DTPA complex in D_2O whereas in H_2O this is reversed. In addition, the decays of the $^1G_4$ state show identical lifetimes for the two complexes. It had been expected that the lifetime of Tm^{3+} in TTHA would be longer than the lifetime of Tm^{3+} in DTPA since previous studies have found that TTHA protects Ln^{3+} ions more effectively than DTPA with the respective q values being 0 and 1[21]. However, it is suggested that in this case, the solvent interacts with the $^1D_2$ and $^1G_4$ states differently, perhaps due to the solvent vibrational levels being in resonance with either the $^1D_2$ or $^1G_4$ levels.

The lifetime in DMSO solutions is, like D_2O, relatively long lived. DMSO is a strongly coordinating solvent through the oxygen of the sulfoxide bond, and has vibrational levels which do not overlap greatly with the Tm^{3+} excited states. A tendency towards increasing lifetime with increasing coordinating and solvating ability of the solvent is also observed.

3.3 Conclusions

The results presented here describe some photophysical properties of Tm^{3+} in various solvents, and in the presence of some common chelates (TTHA, DTPA) also in a selection of solvents. The absorption, excitation and emission spectra for all systems were recorded. The time resolved luminescence spectra were obtained and the decays analysed allowing the emission transitions to be assigned. The deuteration effect was investigated and enabled an estimate of 40 ps for the lifetime of the Tm^{3+} ion in H_2O to be determined. It was also suggested that in some systems, the solvent interacts with the emissive $^1D_2$ and $^1G_4$ levels in different ways as seen by a shorter than expected radiative decay constant for the TmTTHA in D_2O system.

REFERENCES

[1] M. H. Werts, J. W. Hofstraat, F. A. J. Geurts, J. W. Verhoeven, Fluorescein and eosin as sensitising chromophores in near-infrared luminescent ytterbium(III), neodymium(III) and erbium(III) chelates, *Chem. Phys. Lett.*, **1997**, *276*, 196

[2] M. P. Oude Wolbers, F. C. J. M. van Veggel, F. G. A. Peters, E. S. E. van Beelen, J. W. Hofstraat, F. A. J. Geurts, D. N. Reinhoudt, Sensitised near-infrared emission from Nd^{3+} and Er^{3+} complexes of fluorescein-bearing calix[4]arene cages, *Chem. Eur. J.*, **1998**, *4*, 772

[3] T.Komukai, T. Yamamoto, T. Sugawa, Y. Miyajima, Upconversion pumped thulium-doped fluoride fiber amplifier and laser operating at 1.47 μm, *IEEE J. Quant. Elect.*, **1995**, *31*, 1880

[4] J. B. Gruber, M. D. Seltzer, M. E. Hills, S. B. Stevens, C. A. Morrison, Energy levels and upconversion fluorescence in trivalent thulium-doped yttrium scandium aluminium garnet, *J. Appl. Phys.*, **1993**, *73*, 1929

[5] C. Guery, J. L. Adam, J. Lucas, Optical properties of Tm^{3+} ions in indium-based fluoride glasses, *J. Lumin.*, **1988**, *42*, 181

[6] J. Sanz, R. Cases, R. Alacalá, Optical properties of Tm^{3+} in fluorozirconate glass, *J. Non-Cryst. Solids*, **1987**, *93*, 377

[7] O. A. Serra, E. J. Nasser, P. S. Calefi, I. L. V. Rosa, Luminescence of a new Tm^{3+} β-diketonate compound, *J. Alloys Compds.*, **1998**, *275-277*, 838

[8] S. V. J. Lakshman, C. K. Jayasankar, Optical absorption spectra of the tripositive thulium ion in certain nitrate complexes, *J. Phys. C: Solid State Phys.*, **1984**, *17*, 2967

[9] A. Krier, F. J. Bryant, Cathodoluminescence study of thermal annealing of rare earth-doped zinc sulfide electroluminescent thin films, *J. Phys. D.*, **1984**, *17*, 1093

[10] M. Eyal, R. Reisfeld, A. Schiller, C. Jacobi, C. K. Jørgensen, Energy transfer between manganese(II) and thulium(III) in transition metal fluoride glasses, *Chem. Phys. Lett.*, **1987**, *140*, 595

[11] S. Bachir, J. C. Ronford-Haret, K. Azuma, D. Kouyaté, J. Kossanyi, Direct impact excitation of thlium(III) luminscence in polycrystalline ZnO:Tm^{3+} electrodes in contact with an aqueous electrolyte, and attribution of the luminescence spectrum, *Chem. Phys. Lett.*, **1993**, *213*, 54

[12] Z. Hong, W. Li, D. Zhao, C. Liang, X. Liu, J. Peng, D. Zhao, Spectrally narrow blue light-emitting organic electroluminescent devices utilising thulium complexes, *Synth. Metals*, **1999**, *104*, 165

[13] W. T. Carnall, P. R. Fields, K. Rajnak, Electronic energy levels in the trivalent lanthanide aquo ions. I. Pr^{3+}, Nd^{3+}, Pm^{3+}, Sm^{3+}, Dy^{3+}, Ho^{3+}, Er^{3+}, and Tm^{3+}, *J. Chem. Phys.*, **1968**, *49*, 4424

[14] J. Yang, H. Ge, N. Jie, X. Ren, C. Tong, J. Wang, Study of the fluorescence system thulium-bis(1'-phenyl-3'-methyl-5'-pyrazol-4'-one) hexanedione-cetyltrimethylammonium bromide and its analytical application, *Analyst*, **1995**, *120*, 1705

[15] A. Heller, Liquid lasers – fluorescence, absorption and energy transfer of rare earth ion solutions in selenium oxychloride, *J. Mol. Spect.*, **1968**, *28*, 208

[16] P. K. Sharma, A. R. van Doorn, A. G. J. Staring, Luminescence of a Tm(III) ions in aqueous solution and organic matrices, *J. Lumin.*, **1994**, *62*, 219

[17] G. Stein, E. Würzberg, Energy gap law in the solvent isotope effect on radiationless transitions of rare earth ions, *J. Chem. Phys.*, **1975**, *62*, 208

[18] M. P. Oude Wolbers, F. C. M. van Veggel, B. H. M. Snellink-Ruël, J. W. Hofstraat, F. A. J. Geurts, D. N. Reinhoudt, Photophysical studies of m-terphenyl-sensitised visible and near infrared emission from organic 1:1 lanthanide ion complexes in methnol solutions, *J. Chem. Soc., Perkin Trans. 2*, **1998**, 2141

[19] D. M. Gruen, C. W. De Kock, R. L. McBeth, Electronic spectra of lanthanide compounds in the vapor phase, *Adv. Chem. Ser.*, **1967**, *71*, 102

[20] J. L. Kropp, M. W. Windsor, Enhancement of fluorescence yield of rare earth ions by heavy water, *J. Chem. Phys.*, **1963**, *39*, 2769

[21] R. P. Lauffer, Paramagnetic metal complexes as water proton relaxation agents for NMR imaging: theory and design, *Chem. Rev.*, **1987**, *87*, 901

CHAPTER 4: THE INTRAMOLECULAR SENSITISATION OF LANTHANIDE(III) IONS BY BENZOPHENONE

4.1 Introduction

As a result of their desirable emission properties, the luminescence from Ln^{3+} complexes has found uses in many applications in both the solid and solution states from phosphors in television screens[1] to fluoroimmunoassays[2]. The particular properties of Ln^{3+} ions such as the long lived emission, spectrally narrow emission bands and the low molar extinction coefficients have been discussed earlier. Luminescent lanthanide complexes generally consist of a Ln^{3+} ion in close proximity to an organic chromophore which is used to sensitise the metal ion. The Ln^{3+} ion is also often encapsulated by a chelating group used to protect the ion from the solvent; H_2O for example effectively quenches the emission of Ln^{3+} ions.

It is possible to design the Ln^{3+} ion – chelate – chromophore system to give the Ln^{3+} complex particular properties. In the intramolecular sensitisation process, suitable chromophores with high molar absorption extinction coefficients absorb incoming radiation and then transfer this energy to the Ln^{3+} ion. Energy transfer is thought to occur by a Dexter type mechanism via the chromophore triplet state which must be higher in energy than the Ln^{3+} excited state for sensitisation to occur. Since the Tb^{3+} and Eu^{3+} excited states are at ~ 21000 cm^{-1} and 19000 cm^{-1} respectively and the energy gap between the Ln^{3+}* and the chromophore triplet state required to prevent quenching is ~ 2000 cm^{-1} (see section 1.4.4.2), suitable chromophores usually absorb ultraviolet radiation ($\geq$ 25000 cm^{-1}), although examples in the literature do exist of Eu^{3+} sensitised by visible light absorbing chromophores[3]. This is a driving force behind much research since it means that harmful uv light does not have to be used in biological samples which may themselves possess other uv-chromophores.

Most work on luminescent complexes containing Ln^{3+} ions in solution has concentrated on Eu^{3+} and Tb^{3+} ions with much recent interest focused on the development of suitable complexes for their use in biological samples[4]. The main requirements for a suitable system are: (i) formation of kinetically inert complexes, (ii) Ln^{3+} shielding from quenching O-H oscillators, and (iii) efficient excitation. A successful group of complexes used are based on the macrocycle DOTA[5] (1,4,7,10-tetraazacyclododecane). Various chromophores can be bound onto one or more of the arms for efficient excitation and Ln^{3+} sensitisation. This type of complex is of particular interest for a number of reasons. Firstly, it protects the ion from the solvent very effectively, with only one site being available for coordination by a water molecule in aqueous solution[6,7]. The single H_2O site within the coordination sphere of the Ln^{3+} ion also makes this type of complex useful as shift or contrast agents for NMR and MRI purposes[8]. For MRI, the relaxivity rate of the water proton in GdDOTA increases so that the contrast between it and unbound water is enhanched. Secondly, the complexes formed have high kinetic[9] and thermal stability[10]. Finally, it allows the covalent attachment of tissue/organ specific biomolecules or "targetting vectors" for use in fluoroimmunoassays[11].

Each lanthanide ion emits in a different region of the electromagnetic spectrum e.g. Gd^{3+} emits in the uv, Eu^{3+}, Sm^{3+}, Tb^{3+}, and Dy^{3+} emit in the visible region, and Yb^{3+}, Nd^{3+}, and Er^{3+} emit in the near IR. This means that one organic ligand capable of complexing different Ln^{3+} ions can serve various applications operating at different wavelengths just by changing the complexed Ln^{3+} ion.

Interest in using Ln^{3+} ions which emit in the near IR is growing since it enables excitation to be performed at longer wavelengths[12]. In addition, the near IR region of the spectrum is especially important for optical data transmission, making complexes that emit in this region attractive as laser amplification media[13].

4.1.1 Recent studies on luminescent lanthanide complexes

A complex bearing a naphthyl chromophore reported by Parker and Williams[14] has been shown to give interesting results when in principle acting as a sensitiser to Eu^{3+} and Tb^{3+} ions. In the former case, unusually weak Eu^{3+} emission was observed upon excitation of the naphthyl chromophore. Emission from the naphthyl singlet state was also of weaker intensity than the other ions studied. An electron transfer quenching mechanism involving Eu^{3+} reduction to Eu^{2+} was proposed, explaining both the low emission from the Eu^{3+} ion and from the naphthyl antenna. In the Tb^{3+} complex it was found that the $^5D_4$ triplet state

lies only 9 kJ mol^{-1} lower in energy that the naphthyl triplet state and it was suggested that the low efficiency of Tb^{3+} sensitisation is due to an efficient back energy transfer process. In a later study[15], this was confirmed by a laser flash photolysis experiment. The naphthyl triplet absorption showed an initial rapid decay, with a lifetime matching the rise time associated with the Tb^{3+} signal. Also associated with the decay from the naphthyl triplet absorption was a longer lived decay, which closely matched the rate of Tb^{3+} decay. These observations were interpreted in terms of re-formation of triplet naphthalene by energy transfer from the $^5D_4$ Tb^{3+} state.

Roderígues-Ubis *et al.*[16] have reported an iminodiacetic acid chelate containing an acetophenone unit bound to Eu^{3+} and Tb^{3+} ions. They report extremely high quantum yields of sensitised metal emission (0.2 – 0.25 for Eu^{3+} and 0.95 – 1.00 for Tb^{3+}). They attribute the values achieved to the very effective shielding of the Ln^{3+} ions from the solvent and to the close proximity of the chromophore, since it was demonstrated from absorption measurements that the phenolic oxygen of the acetophenone unit coordinates with the metal. Compared to the reported lifetimes, which are similar to other reported values[17] the quantum yields seem abnormally high.

In a 1:1 complex of $Eu(fod)_3$* and Michler's ketone† Werts *et al.*[3] have demonstrated particularly efficient Eu^{3+} sensitised emission following visible light (450 nm) excitation. Michler's ketone and $Eu(fod)_3$ form a ground state complex by the interaction of the electron rich carbonyl group with the positively charged Eu^{3+} ion. In the process of excitation, electron density is moved to the carbonyl group, a new (charge-transfer) absorption band is formed and due to the small S_1-T_1 energy gap of coordinated Michler's ketone, a bright red glow emerges from the Eu^{3+} ion. This complex is unstable in polar solvents however, as the complex readily hydrolyses.

In order to study the intramolecular energy transfer process from a chromophore to Eu^{3+}, Tb^{3+} and Yb^{3+} ions, the complexes in this chapter make use of benzophenone as a sensitising chromophore to the Ln^{3+} excited states. The complexes were prepared by D. Maffeo and J. A. G. Williams at the University of Durham. The metal ions are chelated by DOTA, and the chromophore is covalently bound to one of the arms of the DOTA ring.

---

* $Eu(fod)_3$ = europium tris(6,6,7,7,8,8,8-heptafluoro-2,2-dimethyloctane-3,5-dione)

† Michler's ketone = 4,4'-bis(*N,N*-dimethylaminobenzophenone)

The lanthanum(III) complexes were also prepared in order to study the triplet state properties of the chromophore. See fig. 4-1 for the complex structures.

The benzophenone chromophore has previously been shown by McCarthy and Winefordner to sensitise Eu^{3+} and Tb^{3+} ions[18]. However in their work the sensitisation process was via an intermolecular energy transfer process as both the Ln^{3+} and benzophenone were free in acetonitrile solution.

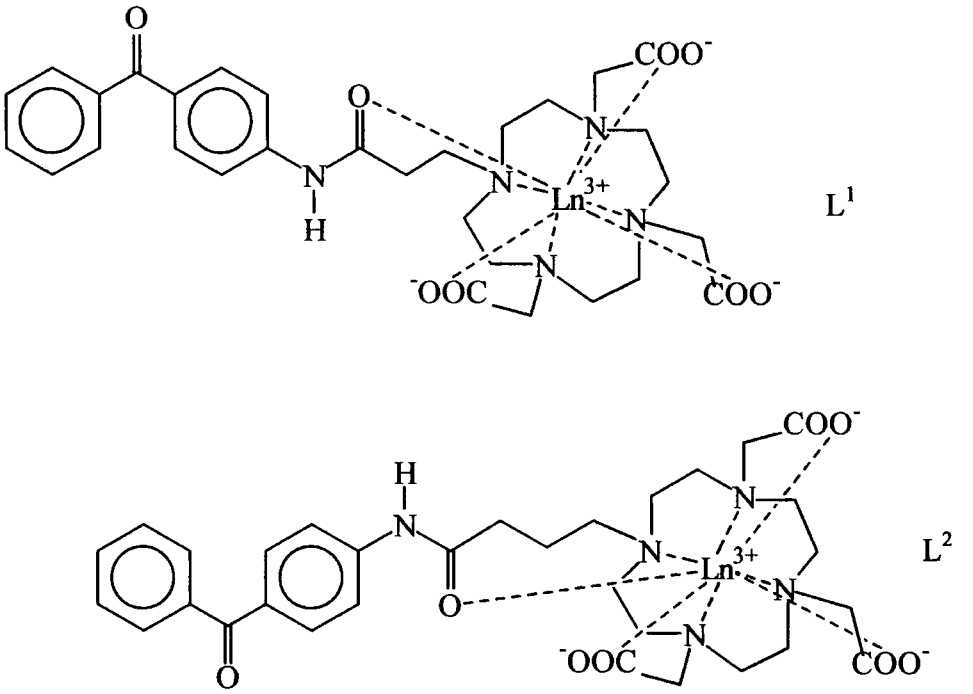

Figure 4-1 *Molecular structures of the lanthanide complexes studied in this chapter*

The fact that the lowest excited state of the antenna chomophore should have a sufficiently high energy restricts the number of suitable chromophores which can be applied as sensitisers for particular ions[19]. Ideally chromophores with absorption bands extending into the visible region of the spectrum would be used. However, if the triplet state is only slightly higher in energy (≤ 1500 cm^{-1}) than the luminescent state of the ion, back energy transfer can occur. Sato and Wada[20] found that the optimum energy for a sensitiser is ~ 2000 cm^{-1} above the excited state of the Ln^{3+} ion.

According to the mechanism of energy transfer, the quantum yield of lanthanide emission that is excited via the antenna chromophore Φ_{tot}, can be given by:

$$\Phi_{tot} = \Phi_T . \eta_{ET} . \eta_{Ln} \qquad 4\text{-}1$$

Φ_T = triplet yield of chromophore

η_{ET} = efficiency of energy transfer

η_{Ln} = efficiency of lanthanide emission

From equation 4-1 it can be seen that any chromophore with a triplet yield of one would maximise the emission quantum yield. However, perhaps surprisingly, very few studies have employed chromophores with unity triplet yields[16]. Benzophenone (BP)[21], like many aromatic ketones has a triplet yield of 1, so that no fluorescence is seen from this molecule. The carbonyl group of aromatic ketones imparts n,π* character to the molecule which enhances the spin-orbit coupling of the system. This results in molecules of this type having high triplet yields. In a degassed solution of benzophenone, even at room temperature, the characteristic phosphorescence emission spectrum can be observed.

4.2 Results and discussion

4.2.1 Absorption and excitation spectra

The absorption spectra of all the complexes studied show a broad band in the uv region of the spectrum with $\lambda_{max} \sim 300$ nm. This band is attributed to the $\pi^* \leftarrow \pi$ transition of the BP. From the absorption spectrum, the energy of the S_1 state was determined to be 320 kJ mol^{-1} ± 5 kJ mol^{-1}. The excitation spectrum from the Ln^{3+} emission bands closely resembles the absorption spectrum and can be seen in fig. 4-2.

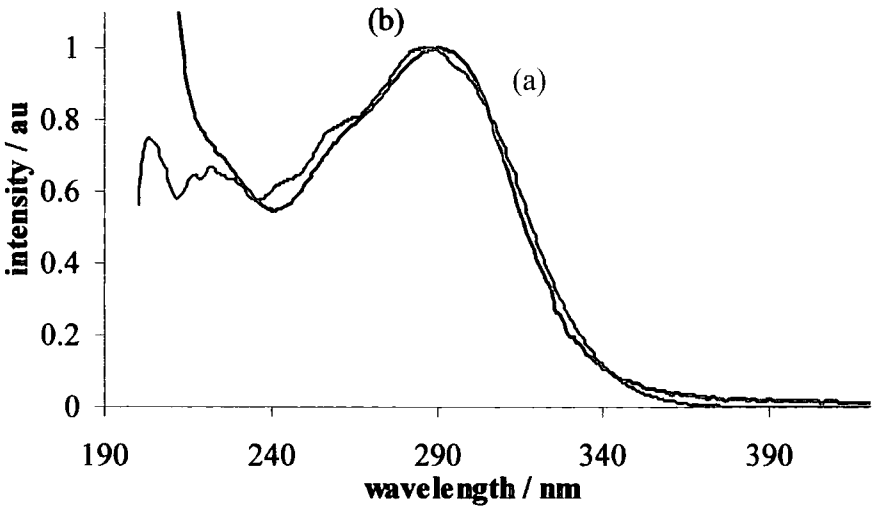

Figure 4-2 *Normalised excitation (λ_{em} = 617 nm bandpass = 5 nm, excitation bandpass = 5 nm) (a) and absorption (b) spectra of EuL^2 in H_2O*

The similar profiles of the absorption and excitation spectra prove that the Ln^{3+} ions are excited via the BP group and therefore energy transfer occurs.

4.2.2 The lanthanum complexes

The La^{3+} ion is electrochemically inactive and does not have any excited state energy levels which are lower in energy than either the S_1 or T_1 states of the BP. The core electronic structure of La^{3+} comprises of entirely filled shells with the f- orbital unoccupied. No electronic f-f or other transitions < 30000 cm^{-1} are therefore expected because the process of promoting an electron out of a filled shell requires much higher energies. Energy transfer in the La complexes therefore does not occur, and any emission observed from this complex is from the BP moiety. Indeed, upon cooling the LaL^1 and LaL^2 complexes in ethanol:methanol solutions to 77 K, the characteristic phosphorescence due to the $T_1 \rightarrow S_0$ transitions in BP was observed in a spectrum very similar to that seen for the model BP compound, 4-acetamidobenzophenone. See fig. 4-3.

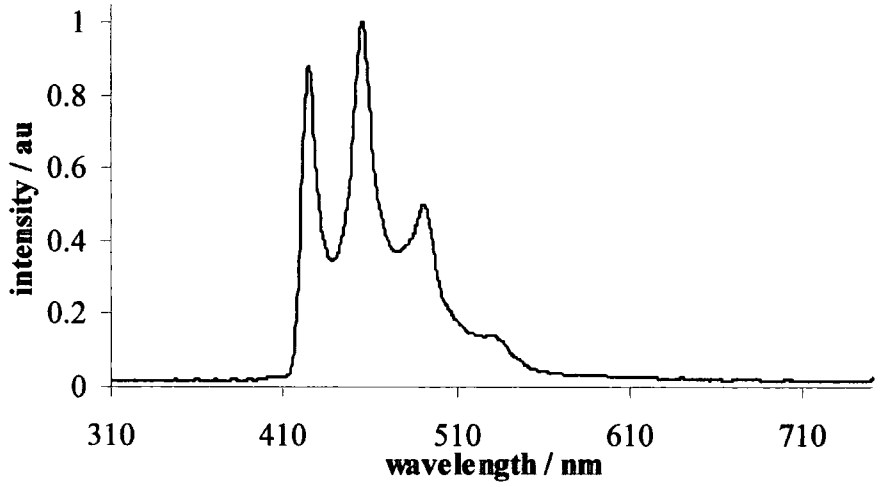

Figure 4-3 *Total emission spectrum of LaL^1 in a 4:1 EtOH:MeOH glass at 77 K λ_{ex} = 300 nm bandpass = 2.5 nm, emission bandpass = 2.5 nm*

All emission seen in the total emission spectrum is phosphorescence, it cannot be observed in aerated solution at RT, and from this spectrum, the triplet energy, E_T, was determined to be 282 kJ mol^{-1} ± 5 kJ mol^{-1}. This energy is sufficiently high to enable the sensitisation of both Eu^{3+} and Tb^{3+} ions, with a low probability of back energy transfer occurring at room temperature.

The lifetime of the BP phosphorescence was also recorded at 77 K and found to be ~ 20 ms. This lifetime is similar to that of the antenna in the absence of an attached ligand, and gives $k_T = 5 \times 10^5\ s^{-1}$ (k_T = decay constant of the chromophore triplet state). This data compares favourably to the model compound of 4-acetamidobenzophenone, E_T = 282 kJ mol^{-1} ± 5 kJ mol^{-1}, τ = 24 ms, ($k_T = 4.2 \times 10^5\ s^{-1}$) and means that the triplet state properties are not significantly affected by the presence of a heavy metal, as expected for compounds with n,π* triplet states. n,π* triplet states already possess a large degree of spin-orbit coupling so that any external effect induced by the proximity of a heavy nucleus is negligible[22].

4.2.3 Sensitisation of Ln^{3+} ions

4.2.3.1 Steady state emission

TERBIUM

Upon excitation at 300 nm in aqueous solution, the emission spectra of both the TbL^1 and the TbL^2 complexes showed the typical green narrow band emission corresponding to the Tb^{3+} metal centred f-f transitions ($^5D_4 \rightarrow {}^7F_J$). The strongest emission is centred at 545 nm and corresponds to the hypersensitive $^5D_4 \rightarrow {}^7F_5$ transition. The Tb^{3+} spectrum shows some fine structure, but unlike the diagnostic Eu^{3+} spectrum, it does not provide a basis for a reliable probe of the symmetry, the J values involved in the transitions are high so that the crystal field splits the levels into many sublevels $(2J + 1)^1$. The intensity of the emission was unaffected by degassing the solutions. The effect of oxygen on the sensitised emission intensity gives an indication of the energy transfer rate, since the competing oxygen quenching rate is equal to the product of the diffusion controlled quenching constant and the oxygen concentration ($k_{diff}[O_2]$). However, since degassing the solutions did not influence the luminescence intensity, this means that energy transfer is a fast process[23] ($k_{ET} > 10^7\ s^{-1}$). As expected, deuteration of the solvent increases the emission intensity, due to the O-D oscillators being much less efficient quenchers of the Ln^{3+} excited states than O-H oscillators[24].

EUROPIUM

The emission spectrum of the EuL^1 and EuL^2 complexes in H_2O show the typical narrow bands corresponding to the Eu^{3+} centred $^5D_0 \rightarrow {}^7F_J$ transitions (see fig. 4-4) with the strongest emission located around 612 nm originating from the hypersensitive $^5D_0 \rightarrow {}^7F_2$ transition. As with the terbium complexes, the intensity of emission is unaffected by degassing the solution, so that energy transfer from the BP triplet state is expected to be a fast and one way process.

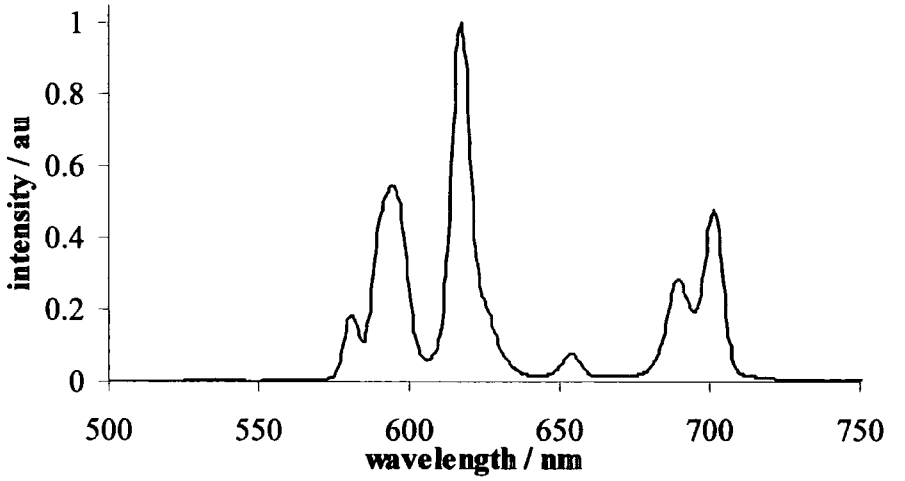

Figure 4-4 *Steady state emission spectrum of* EuL^2 *in* H_2O. λ_{ex} *= 291 nm bandpass = 5 nm, emission bandpass = 5 nm*

The relative intensities and splitting in the Eu^{3+} emission bands are influenced by the symmetry of the first coordination sphere.

The $^5D_0 \rightarrow {}^7F_1$ transition, which is a magnetic dipole (MD) transition, is largely independent of the local chemical environment in the coordination sphere around the ion. The emission band centred around 612 nm, the $^5D_0 \rightarrow {}^7F_2$ transition ($\Delta J = 2$), is an electric dipole (ED) transition, and since it obeys the selection rules $|\Delta J| \leq 2$, $|\Delta L| \leq 2$, $\Delta S = 0$ is extremely sensitive to the symmetry of the environment and is termed hypersensitive. It has been established that the intensity ratio of the $^5D_0 \rightarrow {}^7F_2$ transition and the $^5D_0 \rightarrow {}^7F_1$ transition is a measure for the symmetry of the coordination sphere[25]. In a centrosymmetric environment, the magnetic dipole $\Delta J = 1$ band is the most intense since the ED transitions require mixing of f-d wavefunctions to occur. This process is dependent on the symmetry around the ion, and in centrosymmetric environments such mixing does not take place. Distortion of the symmetry around the ion causes an enhancement of the ED transitions, in particular the hypersensitive $\Delta J = 2$ transition. Complexes with an asymmetric coordination sphere such as lanthanide tris(*β*-diketonate) complexes[26] have $\Delta J = 2/\Delta J = 1$ intensity ratios generally ranging from 8 to 40, whereas low intensity ratios such as that of 0.67 has been reported for the centrosymmetric Eu-tris(oxydiacetate) complex[25]. In the present cases, the EuL^1 complex has a $\Delta J = 2/\Delta J = 1$ ratio of 1, and the

EuL^2 has a $\Delta J = 2/\Delta J = 1$ ratio of 1.5. For both complexes therefore, the environment around the ion is relatively symmetric, although the values suggest that there is an increase in the asymmetry around the Eu^{3+} ion with the addition of an extra CH_2 group into the arm of the ligand. This effect will be discussed in further detail in section 4.2.5.

The Eu^{3+} spectra both at room temperature and at 77 K do not show any splitting of the $^5D_0 \rightarrow {}^7F_0$ emission band within the spectral resolution (FWHM = 3 nm). The Eu^{3+} $^7F_0$ state is non-degenerate and cannot be split by the ligand field; therefore, the single peak at 580 nm is indicative of there being only one (time averaged) luminescent Eu^{3+} species in solution.

YTTERBIUM

The emission spectra show a (relatively) broad emission band at 980 nm corresponding to the emission from the single excited state, $^2F_{5/2}$ in the $^2F_{5/2} \rightarrow {}^2F_{7/2}$ transition see fig. 4-5. The Yb^{3+} complex showed increased emission when the solution was degassed, implying that the energy transfer process occurs at a slower rate for this complex and that the triplet state is populated for a significant time period before energy transfer occurs. The effect of deuteration, as expected from the smaller energy gap between the excited and ground state of Yb^{3+}, is more significant for this complex, with an approximate 15 fold increase in emission intensity in D_2O compared with an identically absorbing solution in H_2O.

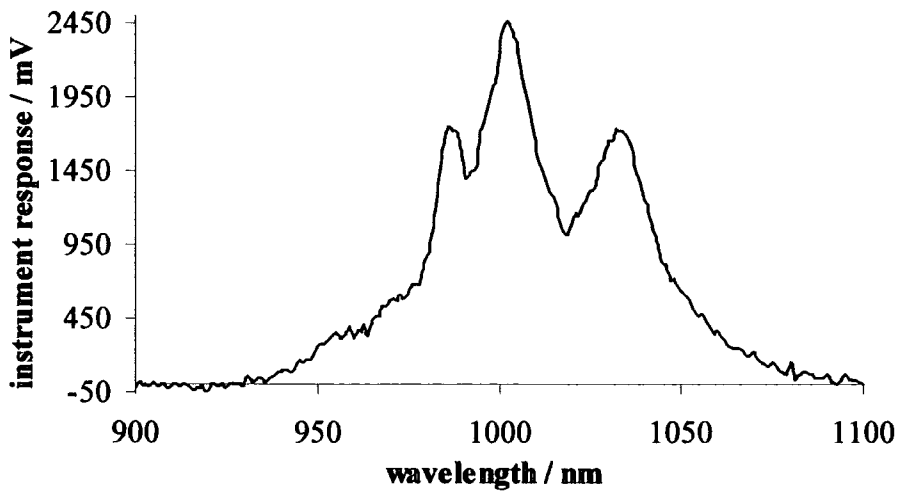

Figure 4-5 *Emission spectrum of* YbL^1 *in degassed* H_2O. $\lambda_{ex} = 307.5$ *nm bandpass = 13 nm, emission bandpass = 5 nm*

The fact that the Yb^{3+} ion is sensitised despite there being no spectral overlap (J) between the emission from the BP triplet state (410 – 610 nm) and the absorption spectrum of the Yb^{3+} ion[27] (850 – 1050 nm) confirms that in this complex the mechanism of energy transfer is not that described by Förster, which relies heavily on J. More probable is energy transfer by a Dexter mechanism, which although this also includes a J term, its significance is reduced. The actual mechanism of energy transfer in the YbL1 complex is thought to involve the vibrational levels of the solvent and will be discussed in further detail in section 4.2.4.2.

At 77 K both the Eu^{3+} and Tb^{3+} complexes show negligible emission < 5 % from the BP group, this implies that all the energy from the BP group is transferred to the Ln^{3+} ion.

4.2.3.2 Emission quantum yields

The quantum yields of emission were determined for the Eu^{3+} and Tb^{3+} complexes in aerated H_2O and D_2O solution, and are shown in table 4-1. The quantum yields for the Yb^{3+} complex were not determined due not in the least to the lack of suitable emission quantum yield standards in the near-IR region. It is expected that the quantum yield for the YbL^1 complex would be low as this ion is more sensitive to non radiative deactivation processes than Eu^{3+} and Tb^{3+}, and previous estimates of Yb complexes all show quantum yields which are low[28].

solvent	EuL^1	EuL^2	TbL^1	TbL^2
H_2O	0.093	0.097	0.27	0.41
D_2O	0.38	0.35	0.41	0.63

***Table 4-1** Emission quantum yield data for LnL^1 and LnL^2 complexes*

It was determined in Dexter's theory[29] of energy transfer that the rate of the process decreases exponentially with distance between the donor and acceptor species, and that in Förster's theory, the rate of the energy transfer process will decrease following a $^1/r^6$ function. This would suggest that the rate of Eu^{3+} and Tb^{3+} ion sensitisation would be slower for the complex with an extra CH_2 group in the arm of the ligand, if indeed this extra group pushes the BP chromophore further away from the Ln^{3+} ion. However, a decrease in the efficiency of energy transfer is not seen in these complexes. The quantum

yield of emission for the EuL^1 and EuL^2 complexes appears to be unaffected by the addition of an extra CH_2 group into the system, and the Tb^{3+} complex actually shows a significant increase in the emission quantum yield for the complex with an additional CH_2 group. Again, this will be discussed further in section 4.2.5.

The quantum yield values themselves indicate efficient sensitisation for the Eu^{3+} and Tb^{3+} complexes in aqueous solution. With previous complexes of this type showing values in the region of ~ 10^{-3} – 0.014 and 10^{-3} – 0.28 for Eu^{3+} and Tb^{3+} ions respectively[30,17].

4.2.4 Time resolved emission

4.2.4.1 The europium and terbium complexes

The complexes all showed single exponential decays with values similar to those of related complexes of this type[6]. Single exponential decays are representative of a single emitting species in solution. The lifetime values increase significantly in D_2O, caused by the well known sensitivity of the Ln^{3+} ions to O-H oscillators. The actual values are shown in table 4-2.

solvent	EuL^1	EuL^2	TbL^1	TbL^2
τ / ms H_2O	0.61	0.60	1.74	1.58
τ / ms D_2O	2.26	2.03	1.14	2.48
q	1.25	1.20	1.27	0.97

Table 4-2 *Lifetime data (values ± 5 %) for LnL^1 and LnL^2 (Eu^{3+} and Tb^{3+}) complexes. The calculated q-values (± 0.5) are also shown and are uncorrected for the weaker effect of outer-sphere water molecules*

The q value representing the number of coordinated solvent molecules was calculated for each complex using the method described by Horrocks[31] from the corresponding lifetimes in H_2O and D_2O. The value was found to be ~ 1.25 ± 0.5, for all complexes with the exception of the TbL^2 complex which appears to be in a more tightly bound environment (q = 0.97 ± 0.5). This effect has previously been seen for analogous Eu^{3+} and Tb^{3+} complexes[23], where it was suggested that the smaller q value for the Tb^{3+} complex might be the result of the smaller ionic radius of the Tb^{3+} ion (0.923 Å compared to 0.950 Å for

Eu^{3+}). This results in a more compact complex that leaves less space in the first coordination sphere of the lanthanide ion for solvent coordination. An alternative explanation has also been given in the literature[30] for similar DOTA complexes involving the Eu^{3+} and Tb^{3+} lanthanide ions; it was suggested that this type of behaviour is consistent with an additional deactivation mechanism for the excited europium $^5D_0$ state through coupling to amide N-H vibrational levels, resulting in a higher q-value than for the terbium complex. It is anomalous however, for the terbium ions in the 2 complexes to have different q-values. Nonetheless, for both Eu^{3+} and Tb^{3+} complexes, it should be noted that the accuracy of the Horrocks equation is low for small numbers of coordinating water molecules as is indicated by the error of ± 0.5. Values of ~ 1 are typical of macrocyclic complexes of this type[8].

The excited state kinetics were investigated in further detail in order to obtain more information on the energy transfer process occurring.

TERBIUM

The terbium emission was monitored at 545 nm following BP excitation at 266 nm. The Tb^{3+} emission showed the absence of a rise time which is, seemingly, faster than the response time of the detector system (< 50 ns). See fig. 4-6. This indicates that the $^5D_4$ emissive state is formed within this time, i. e. $k_{ET} > 2 \times 10^7\ s^{-1}$, and the emission from this state followed a single exponential decay.

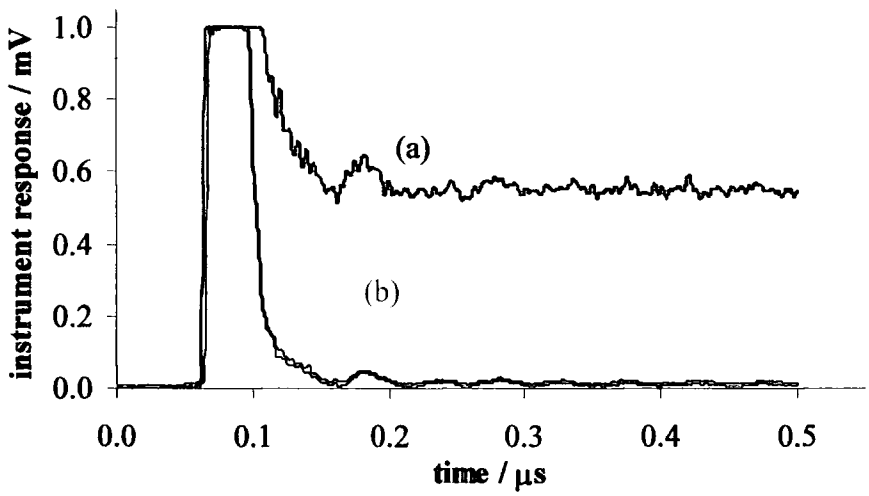

Figure 4-6 *Time resolved emission spectrum of TbL^1 in H_2O - kinetic profile of the signal recorded on a short time scale (a) signal (b) instrument response function*

The sharp spike at the start of the signal is due to scattered light in the system and was ignored in the fitting process.

EUROPIUM

The europium complexes show a more complex kinetic profile. Monitoring the $^5D_0 \rightarrow {}^7F_1$ transition at 595 nm reveals two components to the rising edge of the signal as can be seen in the inset of fig. 4-7.

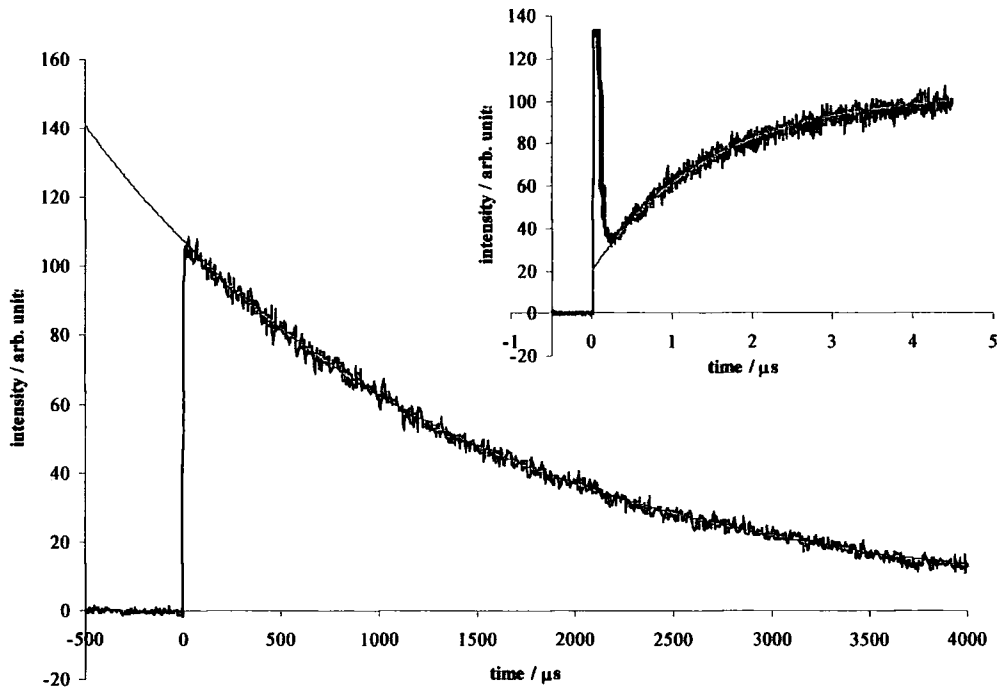

Figure 4-7 *Time resolved emission spectrum of EuL[1] in H_2O – kinetic profile of decay (main) and grow-in of signal (inset); black line = actual data, grey line = fitted curve*

The first contributes ~ 20 % of the signal, and like the Tb^{3+} signal is formed within the response time of the detector i.e. $k_{ET} > 2 \times 10^7\ s^{-1}$. The second, showed a lifetime of 1.45 µs ± 0.1 µs.

Monitoring the $^5D_1 \rightarrow {}^7F_1$ emission band at 583 nm, shows a short lived emission which has an identical lifetime as the main contributing feature of the $^5D_0$ rise time, that is, 1.45 µs ± 0.1 µs. The rise time of the $^5D_1$ emission band was also faster than the reponse time of the detector.

In summary, there are 2 contributing processes which lead to the population of the emissive $^5D_0$ state. One of these processes has the same decay constant as the lifetime of the $^5D_1$ state, suggesting that the main contributing route for the population of the $^5D_0$ state

is via vibrational relaxation from the $^5D_1$ state. So that the processes which lead to Eu^{3+}* states can be described thus:

$$BP^* + Eu^{3+}(^7F_0) \rightarrow BP + Eu^{3+}(^5D_0)$$
$$BP^* + Eu^{3+}(^7F_0) \rightarrow BP + Eu^{3+}(^5D_1)$$
$$Eu^{3+}(^5D_1) \rightarrow Eu^{3+}(^5D_0)$$

BP* = benzophenone in its triplet excited state

Both the $^5D_1$ and $^5D_0$ states of Eu^{3+} can be expected to be sensitised by BP as both levels lie below the triplet state of the BP group.

It should be noted that although the $^5D_1$ emission was monitored, the contribution of emission from this level to the total emission observed in the Eu^{3+} complexes is negligible, < 1 %, the $^5D_0$ level being the main emissive state.

An alternative explanation for the rapid initial rise to the signal of the $^5D_0$ emission is that the "hidden", overlapping $^5D_1 \rightarrow {}^7F_4$ emission is responsible. Overlapping emission from the short lived $^5D_1$ state would lead to a kinetic profile similar to that shown in figure 4-7. The ambiguity between this process and the grow-in mechanism described previously could be clarified by investigating the emission profile from the $^5D_0$ state where there is no possible underlying emission from the $^5D_1$ level, for example by monitoring the emission from the $^5D_0 \rightarrow {}^7F_4$ transition at ~ 700 nm. If the emission profile is changed from that shown above, then the rapid initial rise to the signal in figure 4-7 would be due to the "hidden", overlapping $^5D_1 \rightarrow {}^7F_4$ emission. If the signal is unchanged, then direct population of the $^5D_0$ state from the BP triplet level as described above would be the process occurring.

The energy transfer processes occurring in the Eu^{3+} and Tb^{3+} complexes can be represented in a simple photophysical model represented schematically, as shown in fig. 4-8.

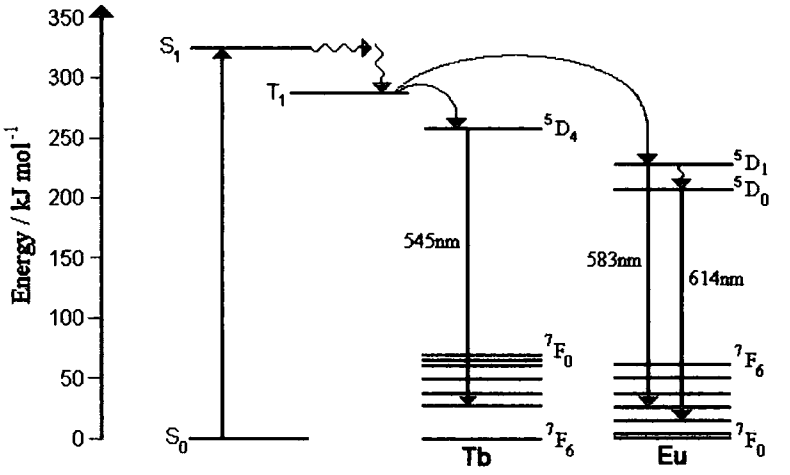

Figure 4-8 *Schematic representation of the energy transfer processes involved in EuL^n and TbL^n complexes.*

The time resolved data also highlights an interesting difference between the complexes. The lifetimes of the two europium complexes are the same in a given solvent within experimental error, but the terbium complex displays significantly longer lived emission in the case of the complex with the extra CH_2 group in the arm of the ligand.

4.2.4.2 YbL^1 Excited state kinetics

All YbL^1 decays showed functions of:

$$I(t) = -A_1.\exp\left(\frac{-t}{\tau_1}\right) + A_2.\exp\left(\frac{-t}{\tau_2}\right) \qquad 4\text{-}2$$

A summary of the data obtained from the kinetics of the ytterbium complex are shown in table 4-3.

	H_2O aerated	H_2O degassed	D_2O aerated	D_2O degassed
τ_1 / μs (grow-in)	0.52	0.57	0.94	1.80
τ_2 / μs (decay)	1.23	1.88	7.65	8.90

Table 4-3 *Lifetime data (± 10 %) for YbL*[1]

From the lifetime data it can be seen that the Yb^{3+} complex is significantly shorter lived than the Eu^{3+} and Tb^{3+} analogues, and is of the order of microseconds as opposed to milliseconds. This is attributed to the much greater sensitivity of the Yb^{3+} ion to quenching from the high frequency solvent and ligand vibrational levels than the Eu^{3+} and Tb^{3+} ions. Less efficient energy transfer could also contribute to the reduced lifetime of the emissive state, since there is an increase in emission intensity and of the lifetime with degassing.

In all systems (H_2O, D_2O, aerated and degassed) there is a rise time and a single exponential decay. In the case of Yb^{3+}, energy transfer occurs more slowly (since there is a large difference between the BP triplet and the Yb^{3+}* states). A similar observation was made by Crosby and Kasha[32], who suggested that the mechanism of energy transfer involves interaction between the high vibrational levels of the solvent coupled with the $^2F_{5/2}$ excited state of the ytterbium ion and the pure π,π* electronic states of the chromophore. Since X-H oscillators have a higher vibrational frequency than X-D oscillators, the rate of energy transfer from the T_1 state in H_2O is faster than the rate in D_2O, and this leads to a slower rise time to the Yb^{3+}* signal in deuterated solvents[33]. O_2 is also known to deactivate triplet states therefore the rate of energy transfer goes down and the rise time increases upon degassing the solution.

$$T_1 + Yb^{3+} \xrightarrow{k_{ET}\ \text{slow}} S_0 + Yb^{3+*} \xrightarrow{k_{lum}\ \text{fast}} S_0 + Yb^{3+} + h\nu$$
$$\downarrow k_Q[O_2]$$

The single exponential decays are of the order of 10^7 s^{-1}.

4.2.5 The effect of an extra CH_2 group

4.2.5.1 Hypersensitivity

The transitions of the Ln^{3+} ions are parity forbidden; that they are in fact observed means that they must derive intensity (or become allowed) via a separate mechanism. In fact,

there are two main schemes, magnetic dipole (MD) and electric dipole (ED). The transitions involved in producing the emission spectrum of Eu^{3+} are composed of either MD (the $\Delta J = 1$ band) or ED intensity (the bands of $\Delta J = 2$, 4, and 6), whereas all the transitions of the Tb^{3+} emission spectrum are composed of both MD and ED intensity. It is established that ED transitions are sensitive to the local environment around the ion, unlike MD transitions, and that some ED transitions display unusual sensitivity to the environment and are termed hypersensitive. These transitions follow the selection rules Δl, $\Delta S = 0$ and $|\Delta J|$, $|\Delta L| \leq 2$. The $^5D_0 \rightarrow {}^7F_2$ band of Eu^{3+} is a well known example of a hypersensitive emission transition, but the $^5D_4 \rightarrow {}^7F_5$ transition of Tb^{3+} is also hypersensitive, though to a lesser degree than the $\Delta J = 2$ band of Eu^{3+}. The sensitivity to the environment displayed by these transitions is that in symmetric environments the hypersensitive transitions have an intensity comparable to that of the aquo ion. In asymmetric environments however, they can display as much as a 200 fold increase in the oscillator strength (intensity) compared to other transitions in the emission spectrum[34].

4.2.5.2 Results

TbL^2 shows more efficient sensitisation than TbL^1. This is despite the antenna group being further separated from the metal ion by an extra CH_2 group and the addition of extra C-H oscillators into the system. An increase in emission is against Dexter's theory of energy transfer:

$$k_{ET} \sim \exp -\frac{2r}{L} \qquad 4\text{-}3$$

r = distance between the D and A.

L = D-A separation relative to their van der Waals radii

The observations of an increase in lifetime and quantum yield in the TbL^2 complex compared to the TbL^1 complex and no apparent decrease in lifetime or quantum yield in EuL^2 compared to EuL^1, conflict with the theory of Dexter, emphasising the need for an additional explanation.

The normalised emission spectra for the Tb^{3+} and Eu^{3+} complexes shown in figs. 4-9 and 4-10 respectively verify that the oscillator strengths of the hypersensitive transitions for

both Eu^{3+} and Tb^{3+} have an increased intensity in the L^2 complexes compared to the L^1 complexes.

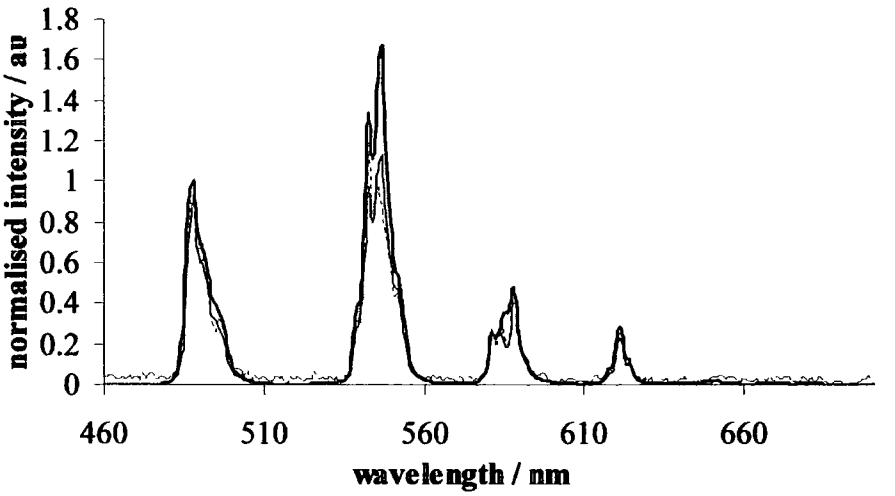

Figure 4-9 *Normalised steady state emission spectra of TbL^n complexes in H_2O; black line = TbL^2; grey line = TbL^1; dotted line = TbDOTA (for comparison) λ_{ex} = 230 nm bandpass = 1 nm, emission bandpass = 1 nm*

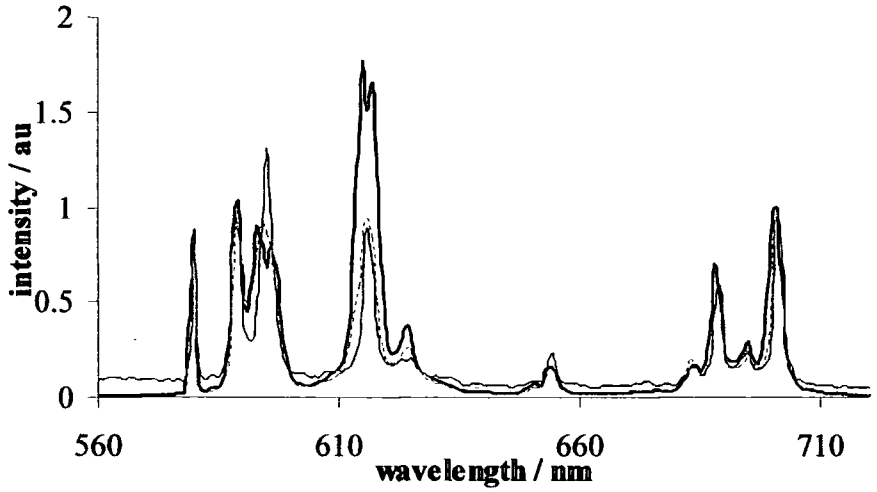

Figure 4-10 *Normalised steady state emission spectra of EuL^n complexes in H_2O; black line = EuL^2; grey line = EuL^1; dotted line = EuDOTA (for comparison) λ_{ex} = 396 nm bandpass = 1 nm, emission bandpass = 1 nm*

Crystal structures of the complexes could not be obtained although it is clear that an increase in the hypersensitive transitions must result from an increase in the asymmetry around the ion. Therefore, it is suggested that the carbonyl group in the arm of the ligand (which is known to bind to the Ln^{3+} ion from the q values) has to alter its position in the case of the LnL^2 complex in order to coordinate with the metal ion. The 'twisting' of the arm of the ligand increases the asymmetry around the ion, increasing the oscillator strength of the hypersensitive transitions. The increase in the oscillator strength hence increases the integrated area under the emission spectra and yields an increase in the emission quantum yield of the Tb^{3+} complex in spite of the larger distance between the benzophenone group and the Tb^{3+} ion. In the case of the Eu^{3+} complex, the increase in oscillator strength of the $\Delta J = 2$ band counteracts any decrease in intensity seen by the extra distance between the Ln^{3+} ion and the BP group, and the addition of the extra CH_2 quencher. The quantum yield thus appears to remain constant.

4.2.6 Estimating the efficiency of the energy transfer process

A photophysical model for the processes occurring following excitation of the BP group has been represented in fig. 4-8. Each of the steps in the energy transfer process has a rate constant, where the efficiency of each process is equal to the ratio of the rate of that particular process and the sum of the rates of all competing processes (including the process itself).

In order to establish the efficiency of energy transfer, η_{ET} from equation 4-1 ($\Phi_{tot} = \Phi_T.\eta_{ET}.\eta_{Ln}$), the efficiency of lanthanide emission, η_{Ln} has to be determined. The overall quantum yield of emission Φ_{tot} is easily measured from the emission quantum yield measurements. Φ_T for benzophenone[22] is known to be equal to 1, but, both η_{ET} and η_{Ln} are more difficult parameters to determine.

It is likely that as in other studies of energy transfer in lanthanide complexes[35], the triplet state of the chromophore is an intermediate in the process; indeed the oxygen sensitivity (in the case of YbL[1]) suggests that this is in fact the case. It has been predicted from low temperature measurements, which show < 5 % emission from the BP moiety, that the large majority of the energy absorbed by the benzophenone group will be transferred to the Ln^{3+} ion. It is possible that some of the energy transferred to the Ln^{3+} ions is direct to the ground state.

The η_{Ln} is determined by the way in which the radiative processes k_R, can compete with non-radiative processes, k_{NR} as given by equation 4-4. These non-radiative processes usually consist of the transfer of energy from lanthanide ions to nearby vibrational oscillators.

$$\eta_{Ln} = \frac{k_R}{k_R + k_{NR}} = \frac{\tau_{obs}}{\tau_0} \qquad 4\text{-}4$$

τ_{obs} = observed lifetime

τ_0 = pure radiative lifetime

If both the pure radiative decay rate constant ($k_R = 1/\tau_0$) and the observed lifetime are known, the luminescence efficiency from the lanthanide can therefore be calculated.

The pure radiative lifetimes for luminescent Ln^{3+} complexes are long (in the order of milliseconds[27]) and despite often being assumed as constant they do actually vary with the chemical environment around the ion[36]. However, for Eu^{3+} at least, the pure radiative lifetime can be determined more accurately from the corrected emission spectrum.

The $^5D_0 \rightarrow {}^7F_1$ transition of Eu^{3+} is entirely MD in nature, which results in it being unaffected by the ions surroundings. Because the oscillator strength of this transition is constant, the emission from this band can be used as a reference, with the intensity of the other transition bands compared to it.

A number of examples exist in the literature where the pure radiative lifetime of Eu^{3+} is determined from the emission spectrum[37,38,39]. So that following this method, the efficiency of europium(III) emission can be calculated using the observed emission lifetime[40], see equation 4-4.

The spontaneous emission probability, A for the $^5D_0 \rightarrow {}^7F_1$ transition can be calculated[38]:

$$A\left({}^5D_0 \rightarrow {}^7F_1\right) = 50\,s^{-1}$$

The spontaneous emission probability of a transition relates the pure radiative rate constant to the branching ratio of the transition by equation 4-5:

$$\beta({}^5D_0 \rightarrow {}^7F_J) = \left(\frac{A({}^5D_0 \rightarrow {}^7F_J)}{k_R}\right) \qquad 4\text{-}5$$

The branching ratio, β, is the relative contribution for each $^5D_0 \rightarrow {}^7F_J$ transition in the emission spectrum and is found by integrating over the entire transition. See fig. 4-11 for an example of integrated areas.

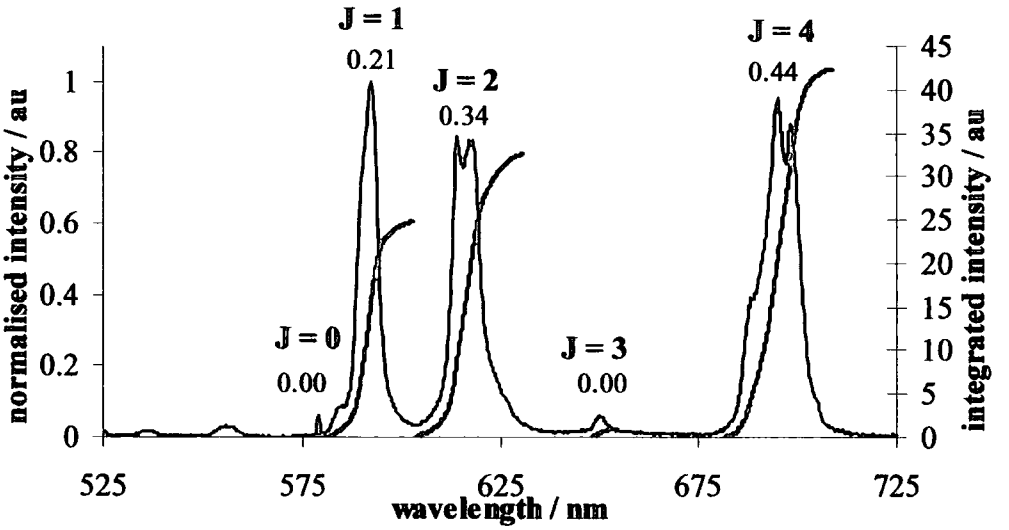

Figure 4-11 *Black = fully corrected emission spectrum of Eu^{3+} nitrate in H_2O, grey = integrated areas of transitions. λ_{ex} = 396 nm bandpass = 2 nm, emission bandpass = 0.5 nm*

Thus, using the spontaneous emission probability for the $\Delta J = 1$ transition and its relative contribution to the total emission spectrum, the pure radiative lifetime can be calculated.

$$\frac{1}{\tau_0} = A(^5D_0 \rightarrow {}^7F_1).\frac{\bar{\nu}(^5D_0 \rightarrow {}^7F_1)}{\beta(^5D_0 \rightarrow {}^7F_1)}.\Sigma\frac{\beta(^5D_0 \rightarrow {}^7F_J)}{\bar{\nu}(^5D_0 \rightarrow {}^7F_J)}.n^3 \qquad 4\text{-}6$$

This simplifies to equation 4-7 when the constants (frequencies of transitions and spontaneous emission probability) are added.

$$\frac{1}{\tau_0} = 13.64\ s^{-1}\ .\ n^3\ .\left(\frac{I_{tot}}{I_{(^5D_0 \rightarrow {}^7F_1)}}\right) \qquad 4\text{-}7$$

I_{tot} = total of all integrated areas (1)

$I_{^5D_0 \rightarrow {}^7F_1}$ = integrated area of the $^5D_0 \rightarrow {}^7F_1$ transition relative to I_{tot}

Once τ_0 has been calculated, the efficiency of Eu^{3+} emission can be determined using equation 4-3. This method for the calculation of emission quantum yields works well for

Eu^{3+} because it has an internal reference transition which is pure MD in nature. Other Ln^{3+} ions do not have similar transitions; for example all of the observed emission bands of Tb^{3+} are composed of both MD and ED intensity[27].

This method works well for the calculation of η_{Eu} in $Eu^{3+}(aq)$, with a value of 0.017 being obtained (c.f. 0.015 measured and 0.019 literature[41]).

For sensitised emission a summary of the calculation results is given in table 4-4.

	EuL^1		EuL^2	
	H_2O	D_2O	H_2O	D_2O
I_{J1}	0.21	0.21	0.16	0.17
k_R / s^{-1}	157	156	202	195
τ_0 / ms	6.38	6.41	4.95	5.14
Φ_{tot}	0.097	0.38	0.095	0.35
τ_{obs} / ms	0.61	2.26	0.61	2.03
η_{Ln}	0.096	0.351	0.123	0.395
η_{ET}	1.01	1.08	0.77	0.89
k_{NR} / s^{-1}	1483	286	1437	298

Table 4-4 *Summary of the data for EuL^n used in the calculation of the efficiency of energy transfer. Errors in calculations, ± 10 %*

I_{J1} = branching ratio of the $^5D_0 \rightarrow {}^7F_1$ transition

k_R = radiative rate constant

τ_0 = pure radiative lifetime

Φ_{tot} = overall emission quantum yield

τ_{obs} = observed lifetime

η_{Ln} = efficiency of lanthanide emission step

η_{ET} = efficiency of energy transfer step

k_{NR} = nonradiative rate constant

For the EuL^1 complex it is calculated that all the energy absorbed by the BP group is transferred to the Eu^{3+} ion, but that not all of the energy transferred is seen as Eu^{3+} emission. It is possible that some of the energy is transferred directly to the non emissive states ground states, also that non-radiative decay from the $Eu^{3+}*$ states could also occur (even in D_2O solution through the X-H bonds of the ligand).

From table 4-4 it can also be seen that deuteration of the solvent has little effect on the relative intensity of the bands (it is the overall intensity of all bands in the spectrum that is increased).

The addition of an extra CH_2 group into the arm of the ligand does however change the *relative* intensity of the bands, which is due to the increased oscillator strength of the hypersensitive ($\Delta J = 2$) transition in the L^2 complex and affects the efficiency of Eu^{3+} emission, the radiative rate constant and the pure radiative lifetime accordingly. Since the lifetimes for the analogous complexes are fairly constant, this means that the efficiency of energy transfer must be different for the two complexes. Indeed, the L^2 complex shows less efficient energy transfer than the L^1 complex.

The calculated k_{NR} values for the two complexes in the corresponding solvents are not significantly different indicating that the extra C-H oscillators introduced into the EuL^2 complex do not play a significant role in quenching the Eu^{3+} $^5D_0$ state.

The efficiency of energy transfer for the Tb^{3+} complexes were not calculated since the emission bands of Tb^{3+} consist of both MD and ED intensity, and no reference transitions with constant oscillator strengths exist. It can be shown however, that the relative increase in the TbL^2 hypersensitive emission band compared to the TbL^1 emission spectrum has a similar effect as that seen in the Eu complexes. Thus, the efficiency of energy transfer is lowered in the more asymmetric complex, in accordance with Dexter's theory of energy transfer.

4.2.6.1 Aside

An alternative method for the determination of η_{Ln} has recently been discussed by Xiao and Selvin[42]. The observed lifetime of a Ln^{3+} ion in a luminescent complex is determined (τ_{Ln}) and its emission spectrum recorded.

A fluorophore with a known quantum yield, Φ_{fluor} is added to the solution. The fluorophore is chosen so that it acts as an energy acceptor from the lanthanide ion, and should not absorb in the same region as the complex. The efficiency of energy transfer E_{ET}

between the Ln^{3+} ion and the fluorophore is then calculated from the lifetime and emission intensity measurements.

$$E_{ET} = 1 - \left(\frac{\tau_{fluor}}{\tau_{Ln}} \right) \qquad 4\text{-}7$$

τ_{fluor} = lifetime of fluorophore in presence of Ln^{3+} complex.

E_{ET} can also be determined using the intensity of fluorescent emission, I_{fluor} in the presence of the Ln^{3+} complex and by comparing it to the residual Ln^{3+} emission in the presence of fluorescence, $I_{Ln\ fluor}$.

$$E_{ET} = \frac{\left(\frac{I_{fluor}}{\Phi_{fluor}} \right)}{\left(\frac{I_{Ln\ fluor}}{\eta_{Ln} + \frac{I_{fluor}}{\Phi_{fluor}}} \right)} \qquad 4\text{-}8$$

By combining equations 4-8 and 4-9, η_{Ln} can be readily calculated using equation 4-9.

$$\eta_{Ln} = \Phi_{fluor} I_{Ln\ fluor} \frac{(\tau_{Ln} - \tau_{fluor})}{(I_{fluor} \tau_{fluor})} \qquad 4\text{-}9$$

k_R and k_{NR} are determined in the usual way, (by rearrangement of equation 4-3).

4.3 Conclusions

The organic chromophore benzophenone (BP) has been shown to efficiently sensitise both the $^5D_0$ and $^5D_1$ states of Eu^{3+} and the $^5D_4$ state of Tb^{3+}. The excited state kinetics were investigated in detail, and the mechanism of energy transfer determined. It has been demonstrated that the $^5D_0$ state of europium is populated by both the BP triplet state directly and also following vibrational relaxation from the $^5D_1$ state.

The near-IR emitting Yb^{3+} ion was also shown to be sensitised by benzophenone, although energy transfer to this ion is less efficient as judged by its sensitivity to the presence of O_2.

The addition of an extra CH_2 group into the arm of the ligand has been investigated, and it was determined that the extra CH_2 group introduces asymmetry into the environment

around the Ln^{3+} ions as judged by the increase in the oscillator strength of the hypersensitive emission transitions in both the Eu^{3+} and Tb^{3+} complexes.

Finally, the efficiency of energy transfer in the two Eu^{3+} complexes was estimated using a method relating the constant oscillator strength of the $\Delta J = 1$ transition to the pure radiative lifetime. The efficiency of energy transfer was found to be equal to one in the case of EuL^1, and to be slightly less efficient in the case of the EuL^2 complex, again as a result of the increase in the oscillator strength of the hypersensitive transition.

REFERENCES

[1] G. Blasse, B. C. Grabmaier, *Luminescent Materials*, **1994**, Springer-Verlag, New York

[2] I. Hemmilä, V.-M. Mukkala, H. Takalo, Development of luminescent lanthanide chelate labels for diagnostic assays, *J. Alloys Compds.*, **1997**, *249*, 158

[3] M. H. V. Werts, M. A. Duin, J. W. Hofstraat, J. W. Verhoeven, Bathochromacity of Micher's ketone upon coordination with lanthanide(III) β-diketonates enables efficient sensitisation of Eu^{3+} for luminescence under visible light excitation, *Chem. Commun.*, **1999**, 799

[4] M. Elbanowski, B. Mąkowska, The lanthanides as luminescent probes in investigations of biochemical systems, *J. Photochem. Photobiol. A: Chem.*, **1996**, *99*, 85

[5] D. Parker, J. A. G. Williams, Getting excited about lanthanide complexation chemistry, *J. Chem. Soc., Dalton Trans.*, **1996**, 3613

[6] A. Beeby, I. M. Clarkson, R. S. Dickins, S. Faulkner, D. Parker, L. Royle, A. S. de Sousa, J. A. G. Williams, M. Woods, Non-radiative deactivation of the excited states of europium, terbium and ytterbium complexes by proximate energy matched O-H, N-H and C-H oscillators: an improved luminescence method for establishing solution hydration states, *J. Chem. Soc., Perkin Trans. 2*, **1999**, 493

[7] S. Amin, D. A. Voss, Jr, W. DeW. Horrocks, Jr, C. H. Lake, M. R. Churchill, J. R. Morrow, Laser induced luminescence studies and crystal structure of the europium(III) complex of 1,4,7,10-tetrakis(carbamoylmethyl)-1,4,,10-tetraazacyclododecane. The link between phosphate diester binding and catalysis by lanthanide(III) macrocyclic complexes, *Inorg. Chem.*, **1995**, *34*, 3294

[8] R. B. Lauffer, Paramagnetic metal complexes as water proton relaxation agents for NMR imaging: theory and design, *Chem. Rev.*, **1987**, *87*, 901

[9] C. J. Broan, J. P. L. Cox, A. S. Craig, R. Kataky, D. Parker, A. Harrison, A. M. Randall, G. Ferguson, Structure and solution stability of indium and gallium complexes of 1,4,7-triazacyclononanetriacetate and of yttrium complexes of 1,4,7,10-tetraazacyclododecane tetraacetate and related ligands: kinetically stable complexes for use in imaging and radioimmunotherapy. X-Ray molecular structure of the indium and gallium complexes of 1,4,7-triacetic acid, *J. Chem. Soc., Perkin Trans. 2*, **1991**, 87

[10] S. Amin, J. R. Morrow, C. H. Lake, M. R. Churchill, Lanthanide(III) teraamide macrocyclic complexes as synthetic ribonucleases: structure and catalytic properties of $[La(tcmc)(CF_3SO_3)(EtOH)](CF_3SO_3)_2$, *Angew. Chem. Int. Ed. Engl.*, **1994**, *33*, 773

[11] S. Aime, M. Botta, E. Garino, S. G. Crich, G. Giovenzana, R. Pagliarin, G. Palmisano, M. Sisti, Non-covalent conjugates between cationic polyamino acids and Gd^{3+} chelates: A route for seeking accumulation of MRI contrast agents at tumor targeting sites, *Chem. Eur. J.*, **2000**, *6*, 2609

[12] M. H. V. Werts, J. W. Hofstraat, F. A. J. Geurts, J. W. Verhoeven, Fluorescein and eosin as sensitising chromophores in near-infrared luminescent ytterbium(III), neodymium(III) and erbium(III) chelates, *Chem. Phys. Lett.*, **1997**, *276*, 196

[13] M. P. Oude Wolbers, F. C. J. M. van Veggel, F. G. A. Peters, E. S. E. van Beelen, J. W. Hofstraat, F. A. J. Geurts, D. N. Reinhoudt, Sensitised near infrared emission from Nd^{3+} and Er^{3+} complexes of fluorescein bearing calix[4]arene cages, *Chem. Eur. J.*, **1998**, *4*, 772

[14] D. Parker, J. A. G. Williams, Luminescence behaviour of cadmium, lead, zinc, copper, nickel, and lanthanide complexes of octadentate macrocyclic ligands bearing naphthyl chromophores, *J. Chem. Soc., Perkin Trans. 2*, **1995**, 1305

[15] A. Beeby, D. Parker, J. A. G. Williams, Photochemical investgations of functionalised 1,4,7,10-tetraazacyclododecane ligands incorporating naphthyl chromophores, *J. Chem. Soc., Perkin Trans. 2*, **1996**, 1565

[16] J. C. Roderíguz-Ubis, M. T. Alonso, O. Juanes, R. Sedano, E. Brunet, The discovery of a single ligand based on acetophenone bearing excellent quantum yields for the excitation of Eu^{3+} and Tb^{3+}, *J. Lumin.*, **1998**, *79*, 121

[17] M. Murru, D. Parker, G. Williams, A. Beeby, Luminescence behaviour of stable europium and terbium complexes of tetraaza phosphinates: efficient through-space energy transfer from phenyl to terbium, *J. Chem. Soc., Chem. Commun.*, **1993**, 1116

[18] W. J. McCarthy, J. D. Winefordner, Intermolecular energy transfer as a means of chemical analysis. Sensitisation of rare earth emission in dilute solution by aromatic carbonyl compounds, *Anal. Chem.*, **1966**, *38*, 848

[19] M. Latva, H. Takalo, V. M. Mukkala, C. Matachescu, J. C. Rodríguez-Ubis, J. Kankare, Correlation between the lowest triplet state energy level of the ligand and lanthanide(III) luminescence quantum yield, *J. Lumin.*, **1997**, *75*, 149

[20] S. Sato, M. Wada, *Bull. Chem. Soc. Jpn.*, **1970**, *43*, 1955

[21] F. Wilkinson, *Organic Molecular Photophysics*, **1975**, Wiley, New York

[22] N. J. Turro, *Modern Molecular Photochemistry*, **1991**, Mill Valley, California

[23] M. P. Oude Wolbers, F. C. J. M. van Veggel, B. H. M. Snellink-Ruël, J. W. Hofstraat, F. A. Guerts, D. N. Reinhoudt, Photophysical studies of m-terphenylsensitised visible and near infrared emission from organic 1:1 lanthanide ion complexes in methanol solutions, *J. Chem. Soc., Perkin Trans. 2*, **1998**, 2141

[24] J. L. Kropp, M. W. Windsor, Luminescence and energy transfer in solutions of rare-earth complexes. I. Enhancement of fluorescence of deuterium substitution, *J. Chem. Phys.*, **1965**, *42*, 1599

[25] A. F. Kirby, D. Foster, F. S. Richardson, Comparison of $^7F_J \leftarrow {}^5D_0$ emission spectra for Eu(III) in crystalline environments of octahedral, near-octahedral and trigonal symmetry, *Chem. Phys. Lett.*, **1983**, *95*, 507

[26] A. K. Trikha, L. B. Zinner, K. Zinner, P. C. Isolani, Emission spectra of europium(III) β-diketonate complexes with N-bases, *Polyhedron*, **1996**, *1*, 1651

[27] Geschneider and Eyring, *Handbook on the Physics and Chemistry of the Rare Earths*, **1979** Chapter 24, W. T. Carnall, North-Holland Publishing Company, Amsterdam

[28] S. I. Klink, G. A. Hebbink, L. Grave, F. C. J. M. van Veggel, D. N. Reinhoudt, L. H. Sloof, A. Polman, J. W. Hofstraat, Sensitised near-infrared luminescence from polydentate triphenylene-functionalised Nd^{3+},Yb^{3+} and Er^{3+} complexes, *J. Appl. Phys.*, **1999**, *86*, 1181

[29] D. L. Dexter, A theory of sensitised luminescence in solids, *J. Chem. Phys.*, **1953**, *21*, 836

[30] D. Parker, J. A. G. Williams, Modest effectiveness of carbostyril 124 as a sensitising chromophore in europium and terbium amide complexes based on 1,4,7,10-tetraazacyclododecane, *J. Chem. Soc., Perkin Trans. 2*, **1996**, 1581

[31] W. DeW. Horrocks Jr, D. R. Sudnick, Lanthanide ion probes of structure in biology. Laser induced luminescence decay constants provide a direct measure of the number of metal-coordinated water molecules, *J. Am. Chem. Soc.*, **1979**, *101*, 334

[32] G. A. Crosby, M. Kasha, Intramolecular energy transfer in ytterbium organic chelates, *Spectrochim. Acta*, **1958**, *10*, 377

[33] A. Beeby, S. Faulkner, J. A. G. Williams, Near-IR luminescence and energy transfer in lanthanide complexes, part 2: pH dependence of the energy transfer mechanism in a phenanthridine appended ytterbium complex, Submitted to *J. Chem. Soc., Dalton Trans.*, (Aug **2001**)

[34] R. D. Peacock, The intensities of lanthanide f↔f transitions, *Struct. Bonding*, **1975**, *22*, 82

[35] G. Crosby, R. Whan, R. Alire, Intramolecular energy transfer in rare earth chelates. Role of the triplet state, *J. Chem. Phys.*, **1961**, *34*, 743

[36] E. B. Van der Tol, H. J. van Ramesdonk, J. W. Verhoeven, F. J. Steemers, E. G. Kerver, W. Verboom, D. N. Reinhoudt, Tetraazatriphenylenes as extremely efficient antenna chromophores for luminescent lanthanide ions, *Chem. Eur. J.*, **1998**, *4*, 2315

[37] L. D. Carlos, Y. Messaddeq, H. F. Brito, R. A. Sá Ferreira, V. de Zea Bermudez, S. J. L. Ribeiro, Full color phosphors from europium(III) based organosilicates, *Adv. Mater.*, **2000**, *12*, 594

[38] G. F. de Sá, O. L. Malta, C. de Mello Donegá, A. M. Simas, R. L. Longo, P. A. Santa-Cruz, E. F. da Silva Jr, Spectroscopic properties and design of highly luminescent lanthanide coordination complexes, *Coord. Chem. Rev.*, **2000**, *196*, 165

[39] M. F. Hazenkamp, G. Blasse, Rare-earth ions adsorbed onto porous glass. Luminescence as a characterising tool, *Chem. Mater.*, **1990**, *2*, 105

[40] A. Gilbert, J. Baggott, *Essentials of Molecular Photochemistry*, **1991**, Blackwell, Oxford

[41] G. Stein, E. Würzberg, Energy gap law in the solvent isotope effect on radiationless transitions of rare earth ions, *J. Chem. Phys.*, **1975**, *62*, 208

[42] M. Xiao, P. R. Selvin, Quantum yields of luminescent lanthanide chelates and far-red dyes measured by resonance energy transfer, *J. Am. Chem. Soc.*, **2001**, *123*, 7067

CHAPTER 5: INTERACTIONS EFFECTING THE EFFICIENCY OF ENERGY TRANSFER TO EUROPIUM(III) IONS BY ACETOPHENONE CONTAINING LIGANDS

5.1 Introduction

The sensitisation of lanthanide luminescence by organic chromophores is already applied as labels for marking molecules in fluoroimmunoassays and in fluorescence microscopy[1,2]. The major advantage over organic molecules is the long luminescent lifetimes, ms for Eu^{3+} and Tb^{3+} ions[3] cf. ns-ps for organic molecules. This allows time-gated detection to be used to selectively distinguish the Ln^{3+} emission from the autofluorescence of the biological media. Time-gated luminescence can allow detection of low level signals and has lead to the introduction of assays where the luminescence replaces more harmful procedures using radioactive probes. Other potential uses such as luminescent sensors and light amplification are ensuring that the area of luminescent lanthanide complexes remains an active field of research[4,5].

As discussed in chapter 4, the use of an organic chromophore to populate the Ln^{3+} excited state by energy transfer overcomes the problem of the inherently low molar absorption extinction coefficients of these ions ($\varepsilon < 10\ mol^{-1}\ dm^3\ cm^{-1}$) and this is a method that is now well established[6,7]. The energy transfer process is recognised to occur via the triplet state of the organic chromophore[8,9] following initial excitation to its singlet excited state. It is therefore preferable for the chromophores used to have high intersystem crossing yields.

The overall quantum yield of luminescence Φ_{tot}, from the complex can be given by the product of the triplet yield of the chromophore (Φ_T) and the efficiencies of energy transfer (η_{ET}) and metal centred luminescence (η_{Ln})[10].

$$\Phi_{tot} = \Phi_T . \eta_{ET} . \eta_{Ln} \qquad 5\text{-}1$$

Aromatic ketones with n,π* triplet states have large triplet quantum yields and should therefore be particularly suitable as sensitisers, as demonstrated in the previous chapter. One requirement of the sensitiser however is that it has a sufficiently high triplet energy. The emissive levels of the Eu^{3+} and Tb^{3+} ions are at ~ 19000 cm^{-1} and 21000 cm^{-1} respectively, and since the triplet energy should be at least 1500 cm^{-1} higher in energy such that thermally activated back energy transfer is avoided[8] chromophores with triplet energies of $\geq$ 22500 cm^{-1} are typically used. With high triplet yields, chromophores tend to have singlet state energies in the uv region (~ 25000 cm^{-1}) which is disadvantageous for the applicability of visible light emitting Ln^{3+} complexes for fluoroimmunoassays since harmful uv radiation must be used in biological environments. It has recently been demonstrated however, that efficient sensitisation of Eu^{3+} luminescence can be achieved using blue light excitation. A 1:1 mix of $Eu(fod)_3$* and Michler's ketone† in benzene solution results in a complex with a bathochromically shifted absorption band which extends into the visible region of the spectrum (> 400 nm) [11]. The auxiliary ligand of Michler's ketone has a very small $S_1 \rightarrow T_1$ energy gap, and in a so called push-pull complex from Michler's ketone to $Eu(fod)_3$, the benzophenone efficiently sensitises the Eu^{3+} ion with Φ_{tot} = 0.20. One disadvantage of this complex is that it is unstable in polar solvents, making it unsuitable for many applications. The acridone chromophore, which also has a small singlet-triplet energy gap has also recently been shown to allow longer wavelength sensitisation of europium(III)[12]. This complex is based on a DOTA ring and so offers increased stability over the Michler's ketone:$Eu(fod)_3$ complex and quantum yields in both H_2O and D_2O were determined (with values of 0.014 and 0.035 respectively). Current investigations on luminescent lanthanide complexes are involved in areas to improve stability of long wavelength sensitised emission and on improving the efficiency of energy transfer.

In the previous chapter benzophenone was found to sensitise Eu^{3+} and Tb^{3+} ions in a water soluble complex with the achievement of high emission quantum yields. In this chapter, *para*-substituted acetophenone containing ligands are also shown to sensitise Eu^{3+} ions. A series of complexes synthesised by D. Maffeo and J. A. G. Williams at the University of Durham were expected to show increasing charge donation character. It will be shown that

* $Eu(fod)_3$ = europium tris(6,6,7,7,8,8,8-heptafluoro-2,2-dimethyloctane-3,5-dione)

† Michler's ketone = 4,4'-bis-(*N,N*-dimethylamino)-benzophenone

the efficiency of europium(III) sensitisation is highly dependent upon the substituent in the *para* position of the acetophenone chromophore, and that in the case of a dimethylamino substituted complex, the Eu^{3+} emission is also extremely sensitive to solvent.

5.2 Results and discussion

5.2.1 Molecular structures

A DOTA (1,4,7,10-tetraazacyclododecane) macrocyclic chelate with carboxylate donors on 3 of the 4 arms and an acetophenone containing chromophore bound to the fourth is studied in a series with bound gadolinium(III) and europium(III) ions. The acetophenone containing chromophore is substituted in the *para* position with either a dimethylamino NMe_2 group, a methoxy MeO group or unsubstituted with X = H. See fig. 5-1 for the molecular structures of the complexes studied in this chapter.

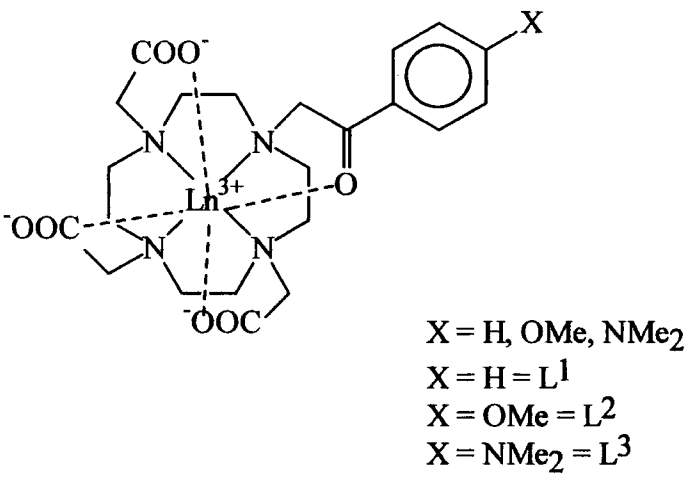

***Figure 5-1** Molecular structures of the complexes studied in this chapter*

Energy transfer from the acetophenone chromophore to the Eu^{3+} ion was investigated by means of Eu^{3+} sensitised emission.

The Gd^{3+} complexes were also studied as they provide an appropriate means of probing the triplet state properties of the chromophore. Gd^{3+} does not have any available excited state energy levels below the chromophore triplet (or singlet) state[13] for energy transfer so that any emission observed will be from the chromophore component, and the ion has a similar size and binding properties[14] to Eu^{3+} providing a suitable model complex.

5.2.2 *Absorption and excitation spectra*

In a preliminary experiment, a 1:1 mix of 4,4'-dimethoxybenzophenone:$Eu(fod)_3$ was prepared in toluene solution. The solution did not show a bathochromically shifted absorption band as seen with the Michler's ketone:$Eu(fod)_3$ complex, suggesting that there is a less significant charge transfer interaction upon excitation between the auxiliary ligand and the Eu^{3+} ion. The emission spectrum of a 1 x 10^{-3} mol l^{-1} solution of $Eu(fod)_3$ in toluene was recorded and plotted against a 1 x 10^{-3} mol l^{-1} 4,4'-dimethoxy-benzophenone:$Eu(fod)_3$ mix emission spectrum, recorded under identical conditions, with λ_{ex} = 365 nm. The emission spectra showed clear sensitisation, although both $Eu(fod)_3$ and the 1:1 complex absorbed radiation at the excitation wavelength ($Abs_{max} < 0.2$), the europium spectrum of the 1:1 complex was over double the intensity seen from the $Eu(fod)_3$ spectrum, in addition the normalised spectra (at $\Delta J = 1$) show that the hypersensitive $\Delta J = 2$ band is increased in intensity in the 1:1 complex mix compared with the free $Eu(fod)_3$ complex. With the methoxy substituted benzophenone it is still thought therefore that the carbonyl oxygen interacts with the Eu^{3+} ion, but that the amount of electron density moving from the chromophore to the Eu^{3+} ion is reduced. This indicates that the benzophenone must occupy a site within the coordination sphere of the $Eu(fod)_3$ as seen in the Michler's ketone:$Eu(fod)_3$ complex despite the absence of a clear charge transfer band in the absorption spectrum.

5.2.2.1 LnL^1

The GdL^1 and EuL^1 complexes show a broad absorption band centred at 265 nm in H_2O, which is not notably different to either the free ligand or the acetophenone molecule itself. This implies that there is no appreciable charge transfer between the chromophore and the Ln^{3+} ion, as expected since the phenyl ring is unlikely to act as a significant electron donor. However, as with the 4,4'dimethoxybenzophenone:$Eu(fod)_3$ example, the lack of a charge transfer band does not mean that the carbonyl group of the acetophenone is not bound to the Ln^{3+} ion, but that the extent of the negative charge on the oxygen is reduced. The excitation spectrum of EuL^1 (and GdL^1 studied at 77 K) closely resembles the absorption spectrum (see fig. 5-2) and proves that the Eu^{3+} ion is sensitised by the chromophore, and that in the case of GdL^1, the phosphorescence seen is due to the chromophore.

The S_1 energy level was estimated to be at 33000 cm^{-1} ± 500 cm^{-1} from the uv-vis absorption spectrum and the band corresponds to the $\pi^* \leftarrow \pi$ transition.

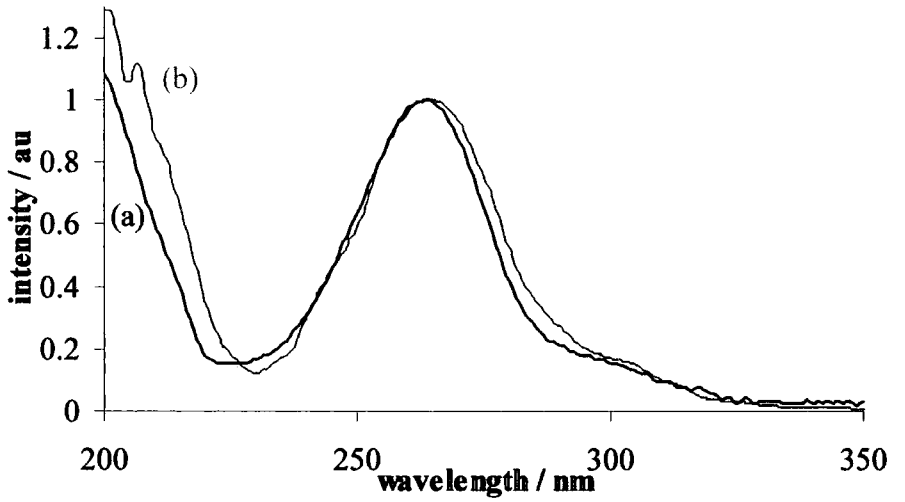

***Figure 5-2** Normalised (a) absorption (b) excitation (λ_{em} = 593 nm bandpass = 5 nm, excitation bandpass = 5 nm) spectra of EuL^1 in H_2O*

5.2.2.2 LnL^2

The absorption band of the *para*-methoxy substituted complex is red shifted in comparison to the LnL^1 complex to 305 nm, due to an increase in the electron donation from the methoxy group to the carbonyl of the acetophenone. Despite the red shift observed in this complex compared to the unsubstituted complex, there was again little change in the absorption maximum compared to the free ligand. This correlates with the result seen in the 4,4'-dimethoxybenzophenone:$Eu(fod)_3$ complex, implying that the methoxy group is not a sufficiently effective electron donor to impart a substantial amount of negative charge character to the oxygen of the ketone. The excitation spectrum again closely matches the absorption spectrum proving that the occurrence of Eu^{3+} emission is through the acetophenone moiety.

The S_1 energy level was estimated to be at 29000 cm^{-1} ± 500 cm^{-1}.

5.2.2.3 LnL^3

The π, π* singlet excited states of the LnL^3 complexes are substantially lower in energy than the L^1 and L^2 complexes, with λ_{max} = 375 nm in the uv/vis absorption spectrum of LnL^3 in H_2O and the band extending into the visible region (> 400 nm). In addition, this band is significantly red shifted compared with the free ligand (λ_{max} = 339 nm) by more than 30 nm see fig. 5-3, suggesting that the carbonyl oxygen on the acetophenone has now

acquired negative charge through a redistribution of electron density in the complex. This occurs upon excitation, as an effective negative charge moves from the lone pair of the nitrogen on the dimethylamino group to the carbonyl on the acetophenone. A coordination bond to the Eu^{3+} ion is formed and gives the red shifted (from the free ligand) charge transfer band. A comparable bathochromic shift (of 23 – 29 nm) is also observed in organic solvents.

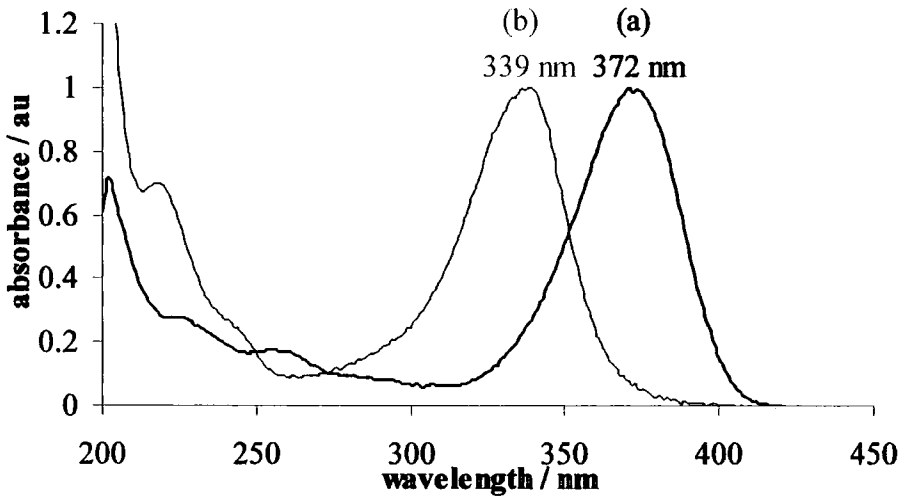

Figure 5-3 Normalised absorption spectra (a) LnL^3 and (b) free ligand (L^3), in EtOH

The redistribution of the electron density in the LnL^3 complexes gives a quinoidal structure to the excited complex; this is illustrated in fig. 5-4.

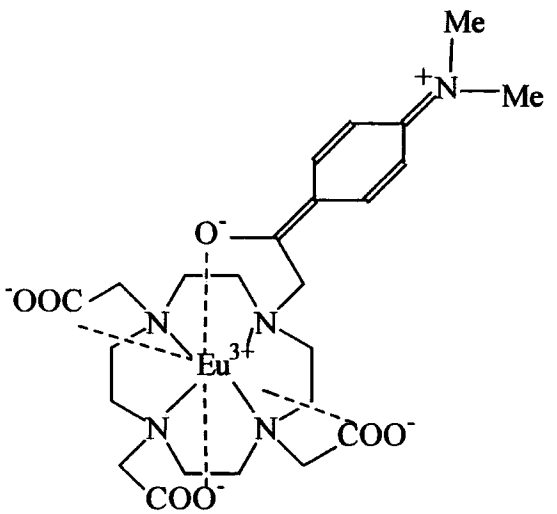

Figure 5-4 Quinoidal structure of LnL^3

The S_1 energy level is estimated to be at 25000 cm^{-1}, ± 500 cm^{-1}.

5.2.3 Antenna properties

5.2.3.1 The triplet states

The Gd^{3+} complexes allow the determination of the triplet state properties of the chromophore in an LnL^n environment since energy transfer to a Gd^{3+} excited state is not possible. This is due to its excited state (^6P) being higher in energy than the T_1 state of the acetophenone free molecule. Energy transfer from the singlet state is unlikely due to competing processes such as the more favourable $S_1 \rightarrow T_1$ intersystem crossing.

The measurements on the GdL^n complexes were recorded at 77 K as the chromophore triplet state, as with other organic triplet states, is readily deactivated at room temperature by collisions with other species and by dissolved O_2.

The steady state emission spectra of GdL^n show no luminescence at RT, but display intense phosphorescence with some vibrational structure upon cooling due to the $n \leftarrow \pi^*$ transition from the triplet state of the chromophore.

Table 5-1 shows the triplet state energies of the complexes in EPA and H_2O glasses.

Solvent	GdL^1	GdL^2	GdL^3
E_T / cm^{-1} EPA	25600	24500	21000
E_T / cm^{-1} H_2O	25300	24500	20000

Table 5-1 *GdL^n triplet energy data (± 500 cm^{-1})*

The triplet energies of the L^n complexes decrease as the electron donating ability of the chromophore increases, in union with the lowering in energy of the singlet state. The dimethylamino substituted L^3 complex has the greatest effect on the triplet state of the chromophore, being over 5000 cm^{-1} lower in energy than the unsubstituted L^1 acetophenone complex.

The energies of all L^n complex triplet states are of sufficient energy to allow sensitisation of both the Eu^{3+} $^5D_0$ and $^5D_1$ states (E = 17300 and 19000 cm^{-1} respectively).

The lifetimes of the chromophore emission from the Gd^{3+} complexes were also recorded at 77 K and the results are displayed in table 5-2.

solvent	GdL^1	GdL^2	GdL^3
τ / ms EPA	10.4	7.9	15.9
τ / ms H_2O	2.3	72.5	< 0.5

Table 5-2 *GdL^n lifetime data (± 10 %) of the triplet states*

The lifetimes do not appear to correlate with the charge transfer ability of the chromophore, and may be quite independent of it. This result seems particularly true for the GdL^n complexes in H_2O where the lifetime of the triplet state in the GdL^2 complex appears to be unusually long. However, it should be noted that the GdL^3 complex is practically non-emissive in H_2O, displaying an anomalously short lifetime. Also, H_2O is not an ideal solvent for low temperature measurements, as it does not form a clear glass. Although this is not expected to affect the observed lifetime of the complex, the amount of radiation absorbed and emitted from the sample will certainly be influenced in a manner which is difficult to control.

5.2.3.2 $S_1 - T_1$ energy gap

The $S_1 - T_1$ energy gap of the chromophores decreases across the series in conjunction with the lowering in energy of the individual states (the values are shown in table 5-3).

LnL^1	LnL^2	LnL^3
7600	4500	3500

Table 5-3 *$S_1 - T_1$ energy gap data. Values are given in cm^{-1} (± 500 cm^{-1})*

The $S_1 - T_1$ energy gap in the LnL^3 complex is comparable to that observed in the Michler's ketone:$Eu(fod)_3$ complex[7], both lying at ~ 3500 cm^{-1}.

5.2.4 Steady state emission EuL^n

5.2.4.1 Emission spectra

The intensities of all complexes studied were unaffected by degassing the solutions, indicating that the energy transfer process is a fast and one way process.

5.2.4.1.1 EuL^1

The unsubstituted L^1 acetophenone Eu^{3+} complexes show metal centred sensitised emission in aqueous solution, an example of the emission spectrum being shown in fig. 5-5.

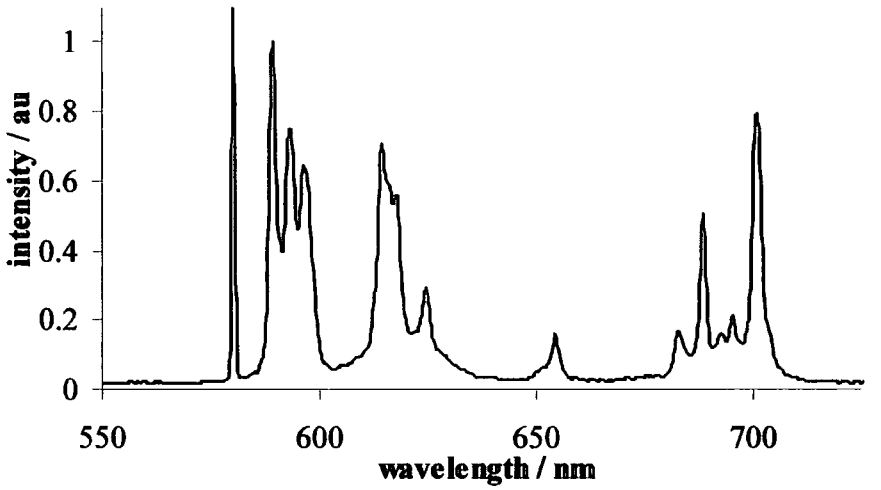

***Figure 5-5** Steady state emission spectrum of EuL^1 in H_2O $\lambda_{ex} = 264$ nm bandpass = 0.5 nm, emission bandpass = 0.5 nm*

The emission spectrum highlights a number of interesting points, firstly, the hypersensitive $\Delta J = 2$ band of Eu^{3+} at 612 nm is lower in intensity than the magnetic dipole $\Delta J = 1$ band at 593 nm indicating that the electric field experienced by the Eu^{3+} ion is of relatively low symmetry. The $\Delta J = 2/ \Delta J = 1$ ratio which can be used as an indication of the symmetry around the ion[15] (< 1 indicating highly symmetric sites, and in more unsymmetric sites e.g. β-diketonates[16] values typically are in the range 10-40) for this EuL^1 complex is 0.7, highly indicative of a centrosymmetric Eu^{3+} environment.

The emission spectrum is also rather similar in profile to that of EuDOTA (not shown), suggesting that the chromophore does not play a significant role in affecting the coordination field surrounding the ion.

The emission spectrum also shows a moderately intense $^5D_0 \rightarrow {}^7F_0$ transition and does not show any splitting. A relatively strong $\Delta J = 0$ transition indicates that the Eu^{3+} ion experiences a (relatively) strong ligand field component[17] for Ln^{3+} ions. The unsplit $\Delta J = 0$ transition indicates that there is a single (time averaged) Eu^{3+} environment.

5.2.4.1.2 EuL^2

Intense metal centred emission was observed in aqueous solution. The spectral profile of the L^2 complex is not significantly different in profile to that of the L^1 complex, an exception being that the hypersensitive $\Delta J = 2$ transition is now more intense than the magnetic dipole $\Delta J = 1$ transition, the $\Delta J = 2/ \Delta J = 1$ ratio being considerably higher at 1.3. This suggests that the electric field experienced by the Eu^{3+} ion is slightly distorted, nevertheless the $\Delta J = 2/ \Delta J = 1$ value still remains indicative of a centrosymmetric environment. The higher $\Delta J = 2/\Delta J = 1$ ratio stimulated by the *para*-methoxy group results from added electron donation from the methoxy to the carbonyl of the ketone, which in turn donates to the Eu^{3+} ion, influencing the electric field surrounding the ion.

5.2.4.1.3 EuL^3

The most significant feature of the luminescence in the EuL^3 complex is the complete lack of emission in aqueous solutions. If this were simply enhanced sensitivity to quenching of emission by O-H oscillators then deuteration of the solvent would be expected to have an observed effect on the intensity, however, there is also a complete lack of emission in D_2O solutions. In non-aqueous solutions however, it was found that sensitisation was in fact occurring and was resulting in metal centred Eu^{3+} emission observed with high intensity. It is unlikely that back energy transfer is occurring in H_2O and is responsible for the lack of emission seen in this complex. Firstly, degassing the solution does not affect the negligible signal, and secondly, the triplet state at 21500 cm^{-1} is sufficiently energetic for this process to be unfavourable[8].

Also highly noteworthy is that the Eu^{3+} emission profile in non-aqueous solutions in now dominated by hypersensitive $\Delta J = 2$ transition and is much more intense than $\Delta J = 1$. The $\Delta J = 2/ \Delta J = 1$ ratio in MeCN = 6.2, a value more like that seen in Eu^{3+} β–diketonates, see fig. 5-6.

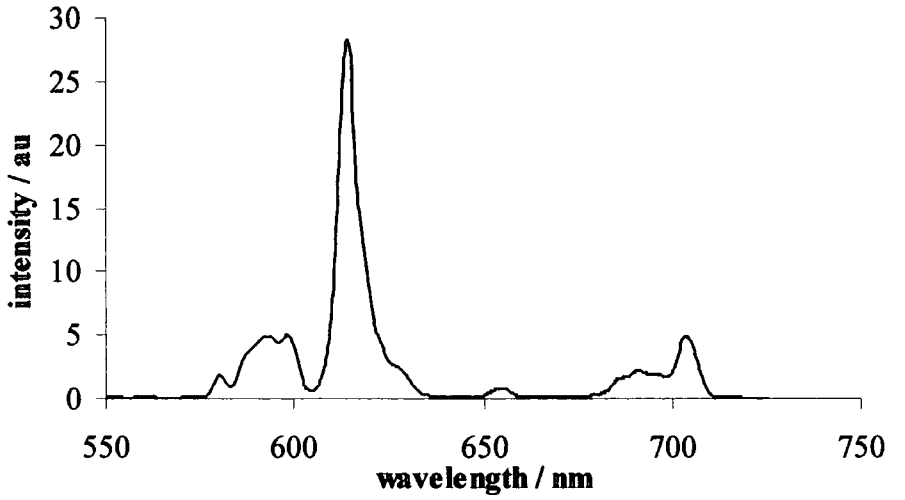

Figure 5-6 *Steady state emission spectrum of* EuL^3 *in acetonitrile,* $\lambda_{ex} = 401$ *nm bandpass = 2.5 nm, emission bandpass = 2.5 nm*

This substantial change in the emission spectrum is associated with the introduction of a considerable alteration in the symmetry of the electric field surrounding the ion. Induced by the large degree of electron donation seen from the dimethylamino substituent on the chromophore to the Eu^{3+} ion, this can also be substantiated by the presence of the quinoidal charge-transfer band seen in the absorption spectrum. The now negatively charged ketone binds to the Eu^{3+} ion and imparts significant asymmetry into the coordination environment, increasing the oscillator strength of the hypersensitive $\Delta J = 2$ transition via an increase in Ω_2.

The emission intensity of this complex is highly solvent dependent (see fig. 5-7). However, the intensity varied erratically and showed no correlation to either the dielectric constant, nor to other solvent parameters such as that of Reichardt[18].

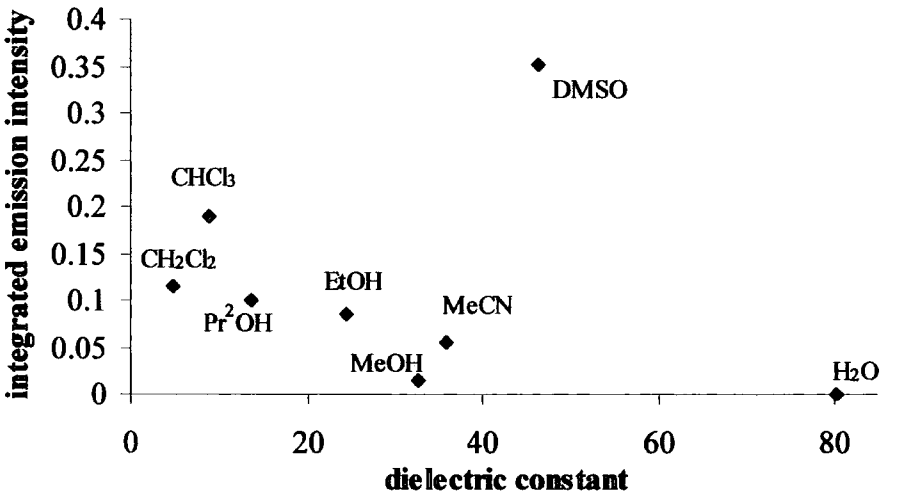

***Figure 5-7** Solvent dependence of emission intensity with dielectric constant for EuL^3, solutions have identical absorbances at λ_{ex}*

The tendency of the emission from this complex to be very sensitive to solvent is not readily explained and may be a combination of effects; as well as solvent polarity, the binding ability of the solvent may also play a role in the efficiency of Eu^{3+} emission. There is also evidence to suggest that the triplet state of the chromophore varies slightly with solvent, although, again with no particular pattern.

The structure of the $\Delta J = 1$ transition band structure also changes with solvent, examples being shown in fig. 5-8.

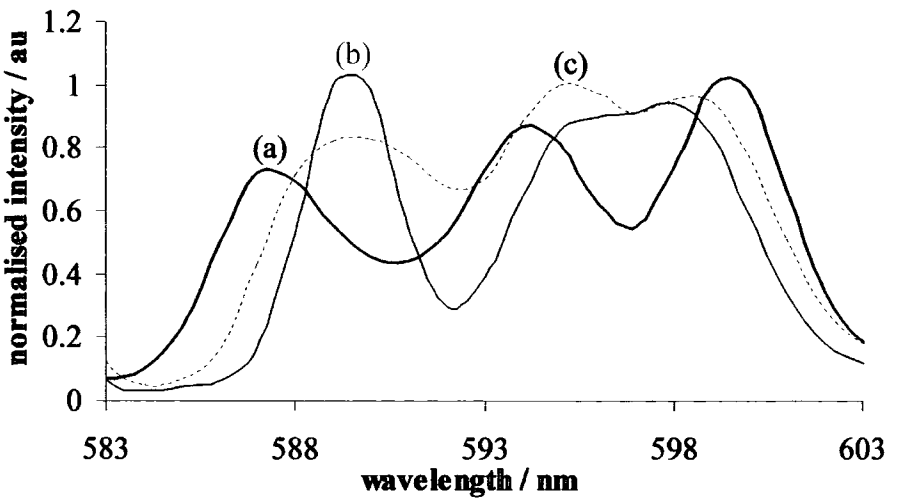

Figure 5-8 *$\Delta J = 1$ Eu^{3+} emission band variation of structure with solvent (a) black line = acetonitrile, (b) grey line = ethanol (c) dotted line = chloroform; $\lambda_{ex} = 375$ nm bandpass = 2 nm, emission bandpass = 2 nm*

The $\Delta J = 1$ transition is magnetic dipole in nature, the oscillator strength of which is independent of the environment, however, as observed here, the structure can certainly change with the chemical environment around the ion. For all solvents, a crystal field splitting with three bands is observed. The presence of three crystal field levels indicates a total removal of crystal field degeneracy[18,19], and this is an indication that the symmetry at the Eu^{3+} site is low, (also seen by the single $\Delta J = 0$ band).

The differences in the splitting patterns associated with the $\Delta J = 1$ transition in different solvents is due to changes in the axial symmetry around the Eu^{3+} ion. The amount of splitting of the $\Delta J = 1$ transition can be seen as a rough measure of the magnitude of the reduction in axial symmetry[20]. Thus, from fig. 5-8, it can be seen that in acetonitrile solution the axial symmetry around the Eu^{3+} site shows the greatest degree of deviation, and that in ethanol the Eu^{3+} site is most symmetric with regards to the perpendicular axis.

5.2.4.2 Emission quantum yields, Φ_{tot}

The quantum yields of emission for the EuL^n complexes in a variety of different solvents were determined and are shown in table 5-4.

	EuL^1	EuL^2	EuL^3
H_2O	0.006	0.098	-
D_2O	0.021	0.34	-
DMSO	0.026	0.257	0.351
MeOH	0.011	-	0.014

Table 5-4 *EuL^n quantum yield data. Note: inherent error associated with Φ measurements is ± 10 %*

The quantum yields for the unsubstituted EuL^1 complex in H_2O and D_2O are slightly lower than those for the methoxy substituted EuL^2 complex in H_2O and D_2O. This difference between the two complexes results from the slight increase in the electron donating ability of the chromophore. The increase in the oscillator strength of the hypersensitive $\Delta J = 2$ transition gives rise to an increase in the rate of radiative decay, k_R, and therefore quantum yield.

Comparing the quantum yields of the EuL^n complexes in the strongly coordinating solvent of DMSO shows the expected trend in metal centred luminescence with the sensitisation increasing with the electron donating ability of the *para* substituent on the acetophenone group. The quantum yield of the EuL^3 complex in DMSO is extremely high for a Eu^{3+} complex in solution, and reveals that the Eu^{3+} ion is very efficiently sensitised by the ligand, and that the rate of radiative decay is enhanced.

After the 13.5 fold increase in the quantum yield of EuL^3 in DMSO compared with the EuL^1 complex it is significant that there is only a 1.3 fold increase in emission intensity of the same complexes in MeOH. This is striking evidence of the (relative) stability of emission from EuL^1 compared with the extraordinary sensitivity of the emission in the EuL^3 complex to the solvent.

5.2.5 Time resolved data

The lifetime data for the EuL^1 and EuL^2 complexes in H_2O and D_2O solvents are displayed in table 5-5.

	EuL^1	EuL^2
τ / ms H_2O	0.62	0.63
τ / ms D_2O	2.26	2.18
q	1.24	1.2

Table 5-5 *EuL^1 and EuL^2 lifetime data in H_2O and D_2O. The q values (± 0.5) are also shown and are uncorrected for the weaker effect of outer sphere water molecules*

The time resolved data for the L^1 and L^2 complexes present single exponential decays signifying the presence of single Eu^{3+} sites. The increase in the observed lifetime upon deuteration of the solvent is due to the well known sensitivity of the Eu^{3+} ion to non radiative deactivation by O-H oscillators. It is interesting however, that although the emission quantum yields of the EuL^1 and EuL^2 complexes in the analogous solvents are different, the lifetimes are unaffected by the *para* substituent. This can be compared with the result seen in the Gd^{3+} complexes, where although the energy of the singlet and triplet states changes with substitution on the acetophenone group, the rate of deactivation is not significantly altered by the substituent.

How the efficiency of energy transfer is affected by the observed lifetimes and the emission spectra will be demonstrated in section 5.2.6.

The q values calculated for these complexes were determined to be 1.24 and 1.20 for EuL^1 and EuL^2 respectively. These values indicate that there is approximately one bound water molecule, and not two. This adds evidence to the hypothesis supporting the ketone coordination to the Ln^{3+} ions in all the complexes despite the absence of a bathochromic shift in the absorption spectra. With Ln^{3+} ions preferring coordination numbers of 9, as seen in similar DOTA substituted complexes, 7 coordination sites are occupied by the ligating atoms on the DOTA ring and the carboxylate arms, the ketone provides an eighth donor atom, and the final site is available for the binding of a solvent molecule.

The ratio of the lifetimes in H_2O and D_2O was equal (within experimental error) to the ratio of the luminescence quantum yields in H_2O and D_2O for both the respective EuL^1 and EuL^2 complexes indicating that k_R is constant.

	τ_1 / ms	A_1	τ_2 / ms	A_2
MeCN	0.554	0.173	0.188	0.826
MeOH	0.123	-	-	-
EtOH	0.349	-	-	-
Pr^2OH	0.688	-	-	-
DMSO	1.290	-	-	-
CH_2Cl_2	0.326	0.468	0.934	0.532
$CHCl_3$	0.871	0.682	0.315	0.318

Table 5-6 *EuL^3 lifetime data, τ value error ± 5 %*

For the EuL^3 complex (data shown in table 5-6), it appears that in coordinating solvents (DMSO, Pr^2OH, EtOH, and MeOH) the lifetime decays follow single exponential profiles representing a single Eu^{3+} site, but that in non-coordinating solvents (CH_2Cl_2, $CHCl_3$, and MeCN) the decay profiles indicate the presence of two or more species and follow double exponential profiles. It is thought that there is a slow water exchange process occurring with the complex and trace amounts of water found in the solvent. Batsanov *et al.*[21] investigated the water exchange rate in Yb and Eu(III) tetraamide complexes where the ligand offers 8 coordination sites and the final site may either be occupied/unoccupied by a single H_2O molecule in a slow water exchange equilibrium. The shorter lived species (H_2O coordinated) may be observed simultaneously to the longer lived (8 coordinate) species at temperatures below 280 K (lowering the temperature lowers the rate of H_2O exchange) with the observation of a biexponential decay. At higher temperatures, the rate of exchange increases and a monoexponential decay is recorded.

5.2.6 Estimating the efficiency of energy transfer

It was demonstrated in the previous chapter that it is possible to estimate the efficiency of the Eu^{3+} emission step in the energy transfer process. This parameter can be determined from the relative band intensities of a fully corrected emission spectrum and the observed radiative lifetime. Estimating the efficiency of energy transfer, which can also then be determined using equation 5-1, depends upon the assumption that the triplet yield of the

chromophore, Φ_T is unity, an assumption which is appropriate for sensitisers with n, π^* triplet states.

Briefly, if the pure radiative lifetime, τ_0 is known, the efficiency of Eu^{3+} emission (η_{Eu}) can be calculated:

$$\eta_{Eu} = \frac{\tau_{obs}}{\tau_0} \qquad 5\text{-}2$$

τ_{obs} = observed emission lifetime / ms

Since the $\Delta J = 1$ transition is composed of entirely magnetic dipole intensity, and therefore has a constant oscillator strength, the spontaneous emission probability for this transition is known, allowing the pure radiative rate constant to be determined. See section 4.2.6 for details on the calculation. A summary of the results calculated for the EuL^n complexes is given in table 5-7.

	EuL^1					
	H_2O	D_2O	MeOH	EtOH	Pr^2OH	DMSO
I_{J1}	0.238	0.25	0.2	0.197	0.201	0.173
k_R	135.7	129.2	159.9	174.7	177.4	255.4
τ_0	7.37	7.74	6.25	5.72	5.64	3.92
Φ_{tot}	0.058	0.214	0.011	0.014	0.018	0.026
τ_{obs}	0.616	2.257	0.914	0.994	0.825	1.808
η_{Ln}	0.08	0.291	0.146	0.174	0.146	0.461
$\Phi_T \cdot \eta_{ET}$	0.75	0.74	0.08	0.08	0.12	0.006
k_{NR}	1479.8	313.3	935.3	829.3	1037.7	298.6

	EuL^2			EuL^3			
	H_2O	D_2O	DMSO	MeOH	EtOH	Pr^2OH	DMSO
I_{J1}	0.215	0.214	0.163	0.138	0.147	0.152	0.123
k_R / s^{-1}	150.3	151	271.1	232	234	235	359
τ_0 / ms	6.65	6.62	3.69	4.31	4.27	4.26	2.79
Φ_{tot}	0.093	0.343	0.257	0.014	0.086	0.1	0.351
τ_{obs} / ms	0.625	2.183	1.608	0.123	0.349	0.688	1.29
η_{Ln}	0.094	0.33	0.436	0.029	0.082	0.162	0.462
$\Phi_T \cdot \eta_{ET}$	0.99	1.04	0.59	0.48	1.049	0.617	0.96
k_{NR} / s^{-1}	1449.7	307.1	350.1	1219	2631	7896	418

***Table 5-7** Summary of the data for EuL^n used in the calculation of the efficiency of energy transfer. Calculated values have ± 10 % associated error*

I_{J1} = relative intensity of the $\Delta J = 1$ transition

k_R = pure radiative rate constant

k_{NR} = nonradiative rate constant

The efficiency calculation results show that the relative intensity of the $\Delta J = 1$ transition to the other transitions in a given complex is lower in DMSO than in any of the other solvents. This is due to the increase in the oscillator strength of the hypersensitive $\Delta J = 2$ transition when the strongly coordinating DMSO is bound to the metal ion. It can also be seen that the pure radiative lifetime is not a constant value for any of the complexes in the various solvents; this reflects the susceptibility of the $\Delta J = 2$ transition of the Eu^{3+} ion to the slight changes in the chemical environment around the ion.

Although Φ_{tot} changes with solvent for the L^1 and L^2 complexes, this can be rationalised by the quenching commonly observed in Ln^{3+} ions by X-H oscillators. The emission quantum yield is dependent on the number of high frequency oscillators in the vicinity of the Eu^{3+} ion. This is not the case with the EuL^3 complex, in which the degree of the variation does not correspond well to the expected variation in intensity from simply X-H quenching. Also, the $\Delta J = 2$ transition varies in intensity dramatically as the solvent is changed.

For the EuL^n complexes, k_{NR} is calculated on the assumption that $\Phi_T.\eta_{ET}$ (the overall efficiency of energy transfer) is constant. This may not necessarily be true, particularly for the EuL^3 complex, in which the properties of the triplet state also appear to show some dependence on the environment.

It appears that the main limiting factor on the efficiency of lanthanide emission is not the efficiency of energy transfer, but the quenching of the Eu^{3+} excited states. It is possible that the energy is being transferred direct to the ground states of Eu^{3+}, in which case it would be necessary to induce a further increase in the Ω_2 value. This would have the effect of increasing both the rate of Eu^{3+} emission and increasing the total area under the Eu^{3+} emission spectrum. It is clear that there is significant quenching by X-H oscillators; in order to further improve the efficiency of Eu^{3+} emission it would be necessary to make some structural changes to the molecule. For example using phosphinate instead of carboxylate donors on the DOTA ring has been shown to reduce q values to 0, by sterically hindering the coordination of H_2O molecules[22]. Additionally, deuteration of the ligand has also been shown to further increase Ln^{3+} emission by removing the deactivation pathways provided by the coupling to C-H and N-H vibration levels[23]

5.2.7 TbL^1

The terbium complex of the unsubstituted acetophenone, TbL^1 was also prepared and its photophysics investigated. As with the EuL^1 complex, the absorption spectrum has $\lambda_{max} = 285$ nm, and the excitation spectrum closely resembles this. The complex showed green metal centred luminescence in aqueous solution and the intensity of the emission was not affected by degassing the solutions. An example of the emission spectrum is shown in fig. 5-9.

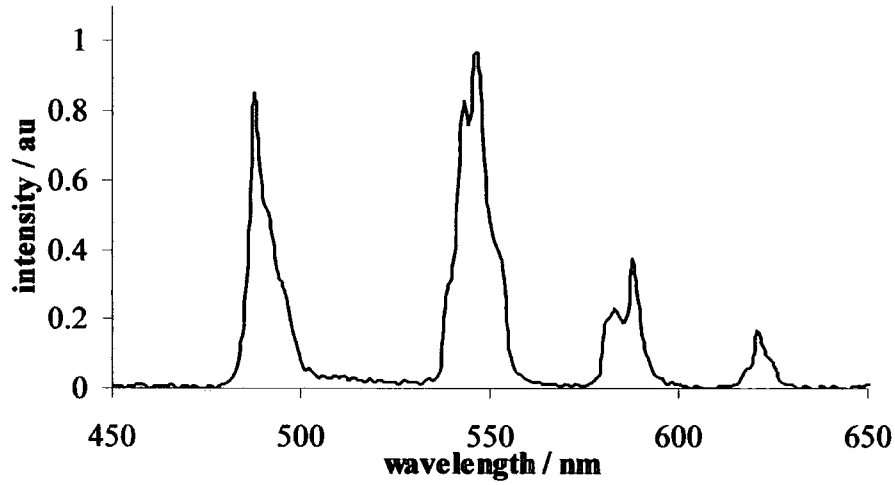

Figure 5-9 *Steady state emission spectrum of TbL^1 in H_2O, $\lambda_{ex} = 263$ nm bandpass = 2.5 nm, emission bandpass = 1 nm*

The luminescence quantum yield and lifetime data for TbL^1 are given in table 5-8.

Φ_{tot} H_2O	0.12
Φ_{tot} D_2O	0.23
τ / ms H_2O	1.6
τ / ms D_2O	2.6
q	0.98

Table 5-8 *Quantum yield (± 10 %) and lifetime (± 5 %) data summary for TbL^1*

From the lifetime data a q value of 0.98 was determined, indicating that the Tb^{3+} ion is in a slightly more tightly bound environment than the Eu^{3+} ion, which has a calculated q value of 1.24. This effect has previously been seen for analogous Eu^{3+} and Tb^{3+} complexes[24], and in fact for the LnL^2 complexes studied in the previous chapter. It was suggested that the smaller q value for the Tb^{3+} complex might be the result of the smaller ionic radius of the Tb^{3+} ion (0.923 Å compared to 0.950 Å for Eu^{3+}, due to the lanthanide ion contraction). This results in a more compact complex that leaves less space in the first coordination sphere of the lanthanide ion for solvent coordination. However, a different explanation may also be responsible for the higher observed hydration state of the Eu^{3+} complex. In an analogous DOTA complex with bound Eu^{3+} and Tb^{3+} ions and carbostyril 124 as a sensitising chromophore, Parker and Williams[25] found q-values of 1.02 and 1.28 for the Tb^{3+} and Eu^{3+} complexes respectively. It was argued that this type of behaviour is consistent with an N-H/N-D exchange process, with the existence of an additional deactivation mechanism for the excited Eu^{3+} $^5D_0$ state through coupling to amide N-H vibrational levels, resulting in a higher q-value than expected for the Eu^{3+} complex.

The quantum yield results represent effective energy transfer to the Tb^{3+} ion, although as with the Eu^{3+} complex the extent of emission is not so effective as that seen with the benzophenone sensitised Ln^{3+} ions seen in the previous chapter. This is perhaps a result of the singlet and triplet states being higher in energy in the acetophenone complexes, so that there is a less favourable energy matching between the Ln^{3+} excited state and the chromophore triplet state[8].

5.3 Conclusions

It has been shown that the europium(III) ion can be intramolecularly sensitised by acetophenone containing ligands and that the efficiency of sensitisation is strongly dependent upon the *para* substituent of the chromophore, with a tendency to increased efficiency with increasing electron donating ability of the substituent. The triplet properties of the chromophores were determined from the gadolinium(III) containing complexes, and it was found that the triplet state lowers in energy with the increased electron donating ability of the chromophore. This follows the same trend as the singlet state, with an increase in the observed λ_{max} with increasing push-pull character of the complex and the $S_1 - T_1$ energy gap also lowers across the series. The observed and pure radiative lifetimes, and the emission quantum yields have been determined in various solvents. The calculated q values indicate the presence of a single water molecule in the

binding site of the unsubstituted and methoxy substituted complexes. The dimethylamino substituted complex, which represents the largest degree of electron donation from the chromophore to the Ln^{3+} ion, displays extreme sensitivity to the solvent. The complex is unemissive in H_2O and D_2O solutions hence a q value for this complex could not be determined. The complex displays intense emission in chlorinated solvents and in DMSO, although the emission intensity does not correlate well with either the dielectric constant or other solvent parameters such as that of Reichardt, it is possible that the emission is dependent on more than one factor. In chelating solvents it was found that the lifetime of the dimethylamino substituted complex was a single exponential decay and that in nonligating solvents, the lifetime followed a double exponential profile. It is suggested that the 'non-chelating' solvents can be in either an on or an off position, that is, either within or beyond the first coordination sphere of the Eu^{3+} ion. The increase in the efficiency of sensitisation of the complexes across the series can be judged by the $\Delta J = 2/\Delta J = 1$ ratio, which is also found to increase due to distortion of the electric field around the ion.

The photophysical properties of the unsubstituted Tb^{3+} complex were also determined.

REFERENCES

[1] M. Elbanowski, B. Makowska, The lanthanides as luminescent probes in investigations of biochemical systems, *J. Photochem. Photobiol. B: Chem.*, **1996**, *99*, 85

[2] A. Beeby, S. W. Botchway, I. M. Clarkson, S. Faulkner, A. W. Parker, D. Parker, J. A. G. Williams, Intermolecular energy transfer mechanisms between ligands in ternary rare earth complexes with aromatic carboxylic acids and 1,10-phenanthroline, *J. Photochem. Photobiol. B: Biol.*, **2000**, *57*, 83

[3] Geschneider and Eyring, *Handbook on the Physics and Chemistry of the Rare Earths*, **1979**, Ch. 24, W. T. Carnall, North-Holland Publishing Company, Amsterdam

[4] D. Parker, P. K. Senanayake, J. A. G. Williams, Luminescent sensors for pH, pO_2, halide and hydroxide ions using phenanthridine as a photosensitiser in macrocyclic europium and terbium complexes, *J. Chem. Soc., Perkin Trans. 2*, **1998**, 2129

[5] Q. J. Zhang, P. Wang, X. F. Sun, Y. Zhou, P. Dai, P. Yang, M. Hai, J. P. Xie, Amplified spontaneous emission of an Nd^{3+}-doped poly(methylmethacrylate) optical fiber at ambient temperature, *Appl. Phys. Lett.*, **1998**, *72*, 407

[6] B. Alpha, R. Ballardini, V. Balzarni, J.-M. Lehn, S. Perathoner and N. Sabbatini, Antenna effect in luminescent lanthanide cryptates: A photophysical study, *Photochem. Photobiol.*, **1990**, *52*, 299

[7] M. H. V. Werts, J. W. Hofstraat, F. A. J. Geurts, J. W. Verhoeven, Fluorescein and eosin as sensitising chromophores in near-infrared luminescent ytterbium(III), neodymium(III) and erbium(III) chelates, *Chem. Phys. Lett.*, **1997**, *276*, 196

[8] M. Latva, H. Takalo, V.-M. Mukkala, C. Matachescu, J. C. Rodríguez-Ubis, J. Kankare, Correlation between the lowest triplet state energy level of the ligand and lanthanide(III) luminescence quantum yield, *J. Lumin*, **1997**, *75*, 149

[9] G. Crosby, R. Whan, R. Alire, Intermolecular energy transfer in rare earth chelates. Role of the triplet state, *J. Chem. Phys.* **1961**, *34*, 743

[10] M. H. V. Werts, Luminescent lanthanide complexes, *Ph.D. Thesis*, **2000**, University of Amsterdam

[11] M. H. V. Werts, M. A. Duin, J. W. Hofsraat, J. W. Verhoeven, Bathochromacity of Michler's ketone upon coordination with lanthanide(III) β-diketonates enables efficient sensitisation of Eu^{3+} for luminescence under visible light excitation, *Chem. Commun.*, **1999**, 799

[12] A. Dadabhoy, S. Faulkner, P. G. Sammes, Small singlet-triplet energy gap of acridone enables longer wavelength sensitisation of europium(III) luminescence, *J. Chem. Soc., Perkin Trans. 2*, **2000**, 2359

[13] C. V. P. de Melo, G. Vicentini, P. C. Isolani, J. Zukerman-Schpector, E. E. Castanello, Spectroscopic studies of lanthanide picrate complexes with N,N-dimethylacetamide. Structure of the La compound, *J. Alloys Compd.*, **1998**, *277*, 242

[14] Cotton and Wilkinson, *Advanced Inorganic Chemistry*, **1988**, John Wiley and Sons Inc., New York

[15] A. F. Kirby, D. Foster, F. S. Richardson, Comparison of $^7F_J \leftarrow {}^5D_0$ emission spectra for Eu(III) in crystalline environments of octahedral, near-octahedral and trigonal symmetry, *Chem. Phys. Lett.*, **1983**, *95*, 507

[16] A. K. Trikha, L. B. Zinner, K. Zinner, P. C. Isolani, Emission spectra of europium(III) β-diketonate complexes with N-bases, *Polyhedron*, **1996**, *1*, 1651

[17] G. Blasse, A Bril, On the Eu^{3+} fluorescence in mixed metal oxides II. The $^5D_0 \rightarrow {}^7F_0$ emission, *Philips Res. Rep.*, **1966**, *21*, 368

[18] C. Reichardt, Solvents and solvent effects in organic chemistry, **1988**

[19] R. Van Deun, K. Binnemans, C. Gorller-Walrand, J. L. Adam, Optical properties of Eu^{3+}-doped fluorophosphate glasses, *J. Phys.: Condens. Matter*, **1998**, *10*, 7231

[20] K. Binnemans, C. Görller-Walrand, A simple model for crystal field splittings of the $^7F_1$ and $^5D_1$ energy levels of Eu^{3+}, *Chem. Phys. Lett.*, **1995**, *245*, 75

[21] J. E. Muñoz Santiuste, B. Macalik, J. García Solé, Optical detection of Eu^{3+} sites in $LiNbO_3$:Eu^{3+} and $LiNbO_3$:MgO:Eu^{3+}, *Phys. Rev. B.*, **1993**, *47*, 88

[22] A. S. Batsanov, A. Beeby, J. I. Bruce, J. A. K. Howard, A. M. Kenwright, D. Parker, Direct NMR and luminescence observation of water exchange at cationic ytterbium and europium centres, *Chem. Commun.*, **1999**, 1011

[23] S. Aime, M. Botta, D. Parker, J. A. G. Williams, Extent of hydration of octadentate lanthanide complexes incorporating phosphinate donors: solution relaxometry and luminescence studies, *J. Chem. Soc., Dalton Trans.*, **1996**, 17

[24] A. Beeby, I. M. Clarkson, R. S. Dickins, S. Faulkner, D. Parker, L. Royle, A. S. de Sousa, J. A. G. Williams, M. Woods, Non-radiative deactivation of the excited states of europium, terbium and ytterbium complexes by proximate energy matched O-H, N-H and C-H oscillators: an improved luminescence method for establishing solution hydration states, *J. Chem. Soc., Perkin Trans. 2*, **1999**, 493

[25] M. P. Oude Wolbers, F. C. J. M. van Veggel, B. H. M. Snellink-Rüel, J. W. Hofstraat, F. A. Guerts, D. N. Reinhoudt, Photophysical studies of m-terphenyl-sensitised visible and near infrared emission from organic 1:1 lanthanide ion complexes in methanol solutions, *J. Chem. Soc., Perkin Trans. 2*, **1998**, 2141

[26] D. Parker, J. A. G. Williams, Modest effectiveness of carbostyril 124 as a sensiting chromophore in europium and terbium amide complexes based on 1,4,7,10-tetraazacyclododecane, *J. Chem. Soc., Perkin Trans. 2*, **1996**, 1581

CHAPTER 6: AQUEOUS MICELLES CONTAINING BOUND LANTHANIDE(III) IONS: A STUDY OF INTERMOLECULAR ENERGY TRANSFER AND THE EFFECT OF CARBON CHAIN LENGTH

6.1 Introduction

Luminescent lanthanide complexes have been extensively studied since Weissman[1] first demonstrated sensitised europium(III) emission in the 1940s. Sensitised emission allows the desirable emission properties of Ln^{3+} ions to be utilised despite the problems associated with the binding of quenching solvent molecules and the inherently low molar absorption coefficients. By building appropriate systems around the Ln^{3+} ion, namely the introduction of protecting chelate groups with the incorporation of suitable sensitisers, the production of efficient luminescent lanthanide complexes continues to be an active area of research[2].

In the process of energy transfer, the antenna chromophore is excited to its singlet state from where intersystem crossing occurs to yield the antenna in its triplet excited state. It is from this transient state that sensitisation of Ln^{3+} ions occurs by the transfer of energy from the $T_1 \rightarrow Ln^{3+}*$ states in a highly distance dependent electron exchange process[3].

One of the most interesting applications of luminescent lanthanide complexes is as luminescent labels in clinical analysis where they can be used as an alternative to radioactive probes. By 'gating out' the short-lived auto-fluorescence from the biological media, the long-lived lanthanide luminescence can by detected. The similarities between the Ln^{3+} ions and Ca^{2+} for example make the lanthanides particularly suitable as luminescent probes for Ca^{2+} ions since they fit well in the Ca^{2+} binding sites. Lanthanides react with biologically active compounds replacing the Ca^{2+} ions and can serve as probes providing information on these materials and the biochemical processes occurring in them[4].

Organisation of reactants into suitable compartments is an inherent property of biological systems. Boundaries of the compartments are defined by the cell membrane. To better understand the processes occurring *in situ*, micelles are often used as an appropriate model[5].

6.1.1 Micelles

Micelles are aggregates of amphiphilic molecules formed in solution due to hydrophobic repulsive interactions of the nonpolar portions of the molecules and the electrostatic repulsions of the polar portions. The monomer has two regions of widely different polarity. The nonpolar hydrophobic 'tail' is usually a hydrocarbon chain, and the polar, hydrophilic 'head group' is either ionic or neutral. At concentrations above the critical micellar concentration (CMC) in aqueous solution, surfactant monomer units can form spherical, vesicular, lamellar, cylindrical or ellipsoidal micelles where the head groups face the bulk solvent and the nonpolar tails point towards the core of the micelle where they are better protected from the polar water molecules. The CMC is the minimum concentration of monomer necessary for micellisation to occur; below the CMC the monomer units are randomly distributed in solution. Due to the two distinct ends of a monomer surfactant molecule, there are two main types of micelles that can form, normal micelles with the hydrophobic tail towards the micellar core (aqueous micelles, as described above), or reverse micelles with the hydrophilic head group pointed towards the core. These are represented schematically in fig. 6-1.

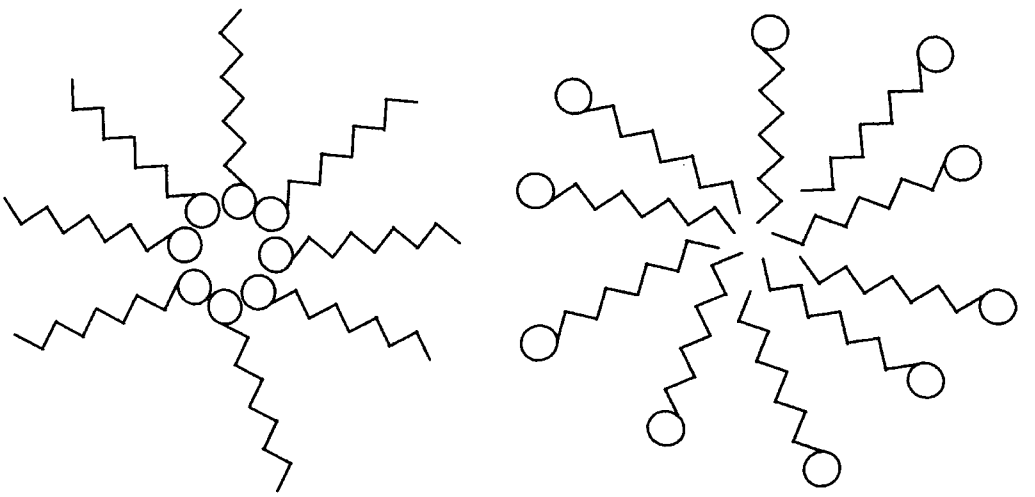

(a) OIL (b) WATER

Figure 6-1 *Cross sections of reverse (a) and normal (b) spherical micelles*

Micelles provide a unique environment in which to study the sensitisation of lanthanide emission, because they allow the compartmentalisation of the antenna and Ln^{3+} ion with the antenna groups either located in the core of the micelle or in the bulk solution

depending on the polarity of the chromophore and the micelle core. Flint *et al.*[6,7,8] has published a number of papers on intermolecular energy transfer between lanthanide complex ions in aqueous micellar solution and have shown that the decay kinetics of electronically excited lanthanide(III) ions free in aqueous solutions are markedly changed when those Ln^{3+} ions are associated with an anionic micellar surface. Three important interactions were highlighted: (a) the distortion of the complex ion by the positive charges on the micellar surface and the adjacent negatively charged anions, giving the change in the radiative relaxation rate, (b) the exclusion of water molecules from the outer coordination sphere of the complex ion and the resultant change in the non-radiative relaxation rate, and (c) energy transfer to nearby lanthanide ions on the micellar surface from hydrophobic chromophores solubilised in the core of the micelle.

Escabi-Perez *et al.*[9] investigated energy transfer from triplet naphthalene to Tb^{3+} solubilised in an aqueous anionic micellar solution (sodium dodecyl sulfate, SDS). It was shown that triplet naphthalene, located in the core of the micelle sensitises the lanthanide ion which is attracted to the surface of the micelle by the SO_3^- groups of the monomer units. It was found that sensitisation of Tb^{3+} ions by naphthalene (Np) can only occur above the CMC and if the chromophore can migrate to the micelle surface during the lifetime of its excited state. In the absence of micelles, energy transfer was prevented, attributed to triplet-triplet annihilation of the sensitiser. In a similar study, Almgren *et al.*[10] extended the number of chromophores used to include biphenyl and phenanthrene, and demonstrated sensitised emission to both Eu^{3+} and Tb^{3+} ions. By using aerosol OT, or NaAOT, (bis-(2-ethylhexyl)sulfosuccinate), a reverse micelle, Mwalupindi *et al.*[11] demonstrated energy transfer from 2-naphthylacetic acid in the bulk solvent to the lanthanide ions of Tb^{3+} and Eu^{3+} in the polar core of the micelle.

The main focus of the study presented here is the investigation of energy transfer from hydrophobic chromophores solubilised in the core of normal aqueous micelles to *bound* Tb^{3+} and Eu^{3+} ions at the micelle surface. Factors that may influence the energy transfer efficiency such as the length of the monomer carbon chain and the presence of dissolved molecular oxygen are also examined. Studies of energy transfer from a donor to an acceptor localised in different parts of a micelle, can provide significant information about the structure and the mechanism of energy transfer[12].

6.2 Results and discussion

The molecular structures of the surfactant and control monomer units studied in this chapter are illustrated in fig. 6-2. They were prepared by I. A. Fallis at Cardiff University.

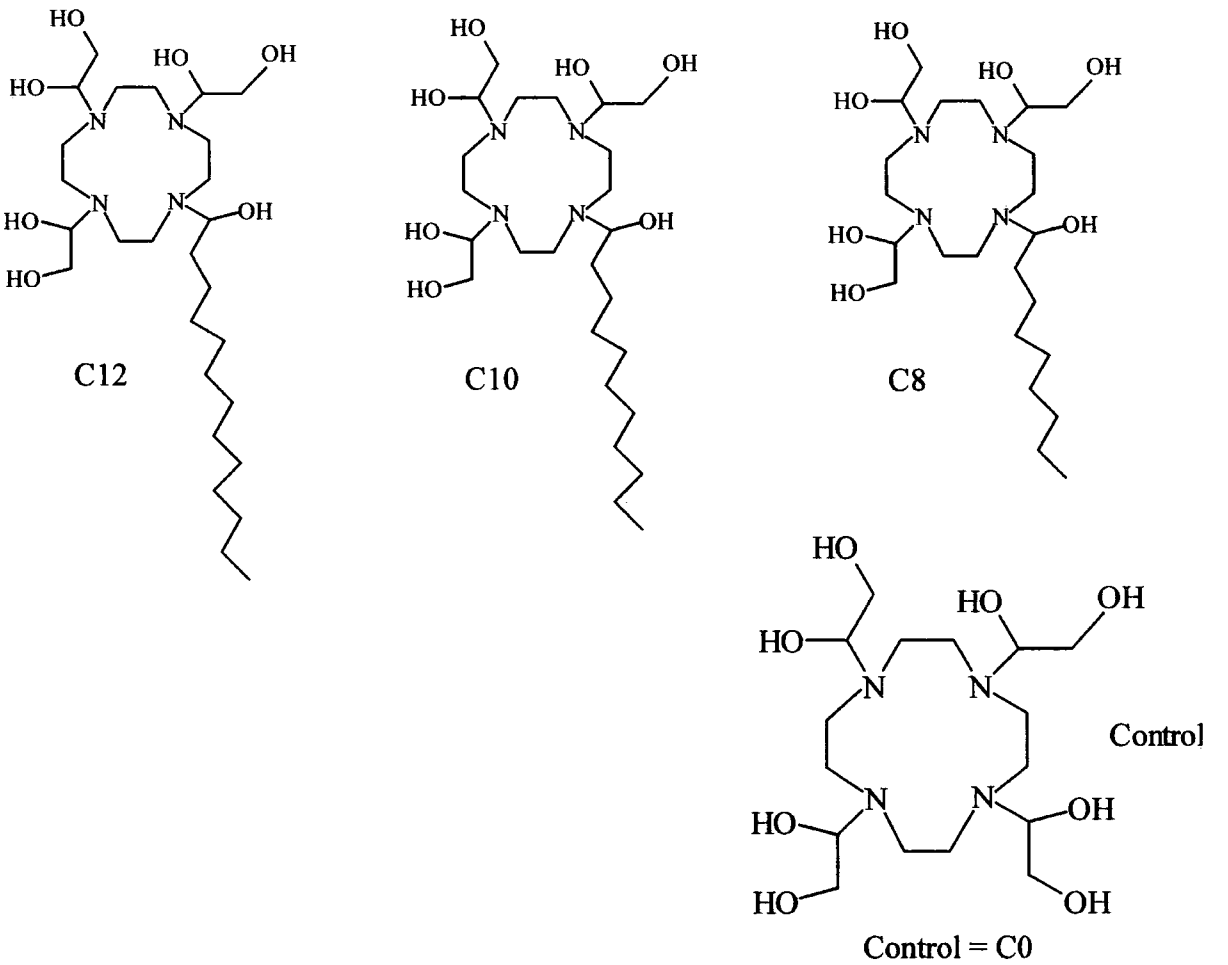

***Figure 6-2** Molecular structures of the surfactant monomer units studied in this chapter*

All solutions were prepared in aqueous solution and sonicated in an ultrasonic bath for at least 15 minutes.

6.2.1 CMC determination

The critical micelle concentrations (CMCs) for the surfactants were determined by examining the spectral changes in the absorption spectrum of the dye acridine orange (AO). The absorbance of AO changes at the CMC as normal surfactant is added to the solution. Below the CMC, the dye molecules exist as groups of aggregates free in solution, above the CMC, the dye enters the hydrophobic core of the micelle and as the

concentration of free dye decreases, a new band associated with the micelle bound dye appears.

The absorption spectra of solutions of 6 x 10^{-5} mol l^{-1} AO with varying surfactant concentrations in the range 1 x 10^{-4} mol l^{-1} to 1 x 10^{-1} mol l^{-1} were recorded. From a plot of change in AO absorbance vs. surfactant concentration, the CMC was determined as the point at which the two linear portions of each curve bisected the x axis.

Fig. 6-3 shows the change in the absorbance of the AO at 479 nm with increasing C12 concentration.

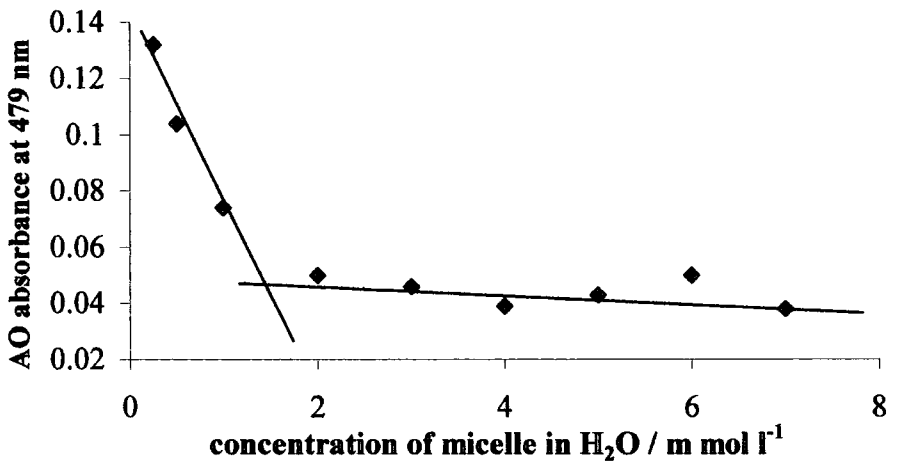

***Figure 6-3** Change in absorbance of AO dye at 479 nm with increasing concentration of C12 surfactant*

CMC / mol l^{-1}		
C12	**C10**	**C8**
1.5 x 10^{-3}	5 x 10^{-3}	11 x 10^{-3}

***Table 6-1** Summary of the CMC values obtained for the surfactants used in this chapter*

It is seen that as the length of the carbon chain increases, the CMC decreases. This is because as the carbon chain length increases, the hydrophobicity of the chain also increases and therefore the CMC reduces.

6.2.2 Ln^{3+} coordination environment

In a preliminary experiment, the q values of the bound Tb^{3+} in C12 surfactant and of bound Eu^{3+} in the control chelate were determined following direct metal excitation. 1:1 $TbCl_3$:C12 and 1:1 $EuCl_3$:Control were mixed in H_2O and D_2O and the lifetimes, given in table 6-2 allowed the determination of the number of bound water molecules, q following the method of Horrocks and Sudnick[13].

	Tb:C12	Eu:C0
τ / ms H_2O	0.752	0.321
τ / ms D_2O	1.368	1.12
q	2.5	2.3

Table 6-2 *Lifetime data (± 10 %) of Tb:C12 and Eu:C0 in H_2O and D_2O, the q-values (± 0.5) (uncorrected for outer sphere effects) are also included*

The single exponential decays imply that there is a single time-averaged Ln^{3+} site.

The q value obtained indicates that the O-H substituted arms of the macrocycle do not bind the metal as well as the carboxylate arms of DOTA and that there are on average 2.4 coordinated water molecules in the first coordination sphere of the Ln^{3+} ion. Also, the similarity of the q-values for both the C12 surfactant and the control chelate indicate that the Ln^{3+} coordination environment is unaffected by the alkyl chain on the ligand and that the control is a good model for the sensitised emission studies. (Similar q-values for Tb:C0 and Eu:C12 were obtained).

6.2.3 Possible sensitisers

The chromophores which were tested to sensitise Tb^{3+} were benzophenone, naphthalene, biphenyl and 2-naphthylacetic acid. It was found that below the CMC none of the chromophores used sensitised the emission of Tb^{3+} and that as with the Escabi-Perez *et al.* study[9], a likely reason for this is the triplet-triplet annihilation of the chromophore in solution. Above the CMC, the chromophore 2-napthylacetic acid (NAA) alone was found to clearly sensitise the Tb^{3+} and Eu^{3+} ions.

It is thought that the charged acetate group on the NAA attracts the chromophore slightly closer to the polar surface of the micelle than the other more hydrophobic chromophores

studied, increasing the efficiency of energy transfer through a reduction in the distance between the donor and acceptor[3]. It has previously been suggested[14] that in reverse micelles the acetic acid group on the NAA chromophore binds to Ln^{3+} ions in the core of the micelle. Benzophenone, naphthalene, and biphenyl are seemingly located at the centre of the micellar core and may be too far removed from the Ln^{3+} ion to effect sensitisation.

6.2.3.1 Effect of carbon chain length

A study of the degree of sensitisation with decreasing carbon chain length of the surfactant was undertaken and it was found that as the carbon chain length decreases (and the CMC increases), the degree of sensitisation decreases. This can be justified by the concentration of chromophore solubilised in the core of the micelle. The amount of material solubilised in micelles generally increases with the size of the micelle[15]. The lower the CMC, the longer the carbon chain length, and the larger the micelle. Thus with large micelles, more of the hydrophobic chromophore can enter the micelle in a position to sensitise the Ln^{3+} ion. See fig. 6-4.

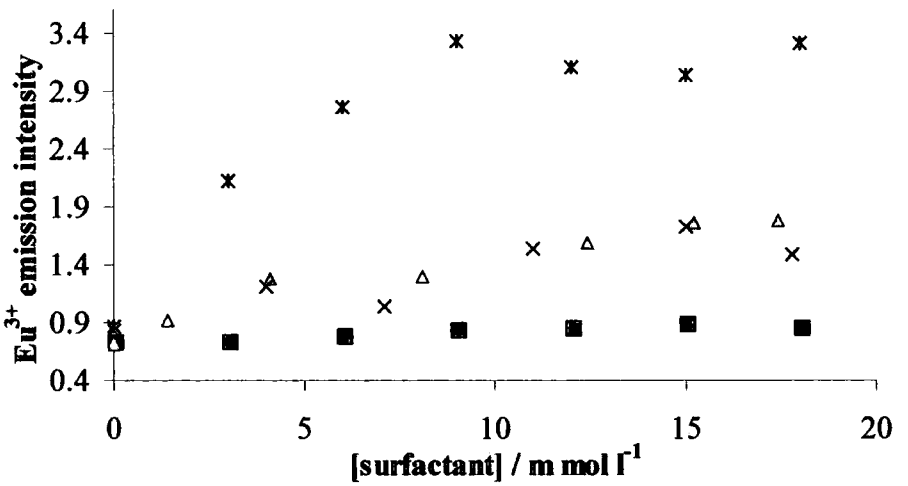

Figure 6-4 *Intensity of Eu^{3+} sensitised emission by NAA with increasing surfactant concentration. [$EuCl_3$] = 2 x 10^{-2} mol l^{-1} [NAA] = 6 x 10^{-5} mol l^{-1}. Black filled squares = C0, black stars = C12, grey filled triangles = C10, black crosses = C8*

6.2.3.2 The effect of O_2

Since the energy transfer process takes place through the 2-naphthylacetic acid triplet state, O_2 may compete with the Ln^{3+} ions as an acceptor of the excitation energy. In that case, less Ln^{3+} emission will be observed. Degassing the solutions of both Eu^{3+} and Tb^{3+}

sensitised emission brings about an increase in the relative intensity of emission. Since the effect of oxygen on the sensitised luminescence intensity gives an indication of the energy transfer rate[16] it is possible to infer from the sensitivity of the lanthanide emission that the rate of energy transfer is slow.

From this brief study it is inferred that the 2-naphthylacetic acid is a good sensitiser to use for these complexes. Within the limited range of materials available it is clear that the increased chain length gives rise to the more emissive micelles.

6.2.4 C12 studies with 2-naphthylacetic acid

6.2.4.1 Sensitised Tb^{3+} emission

6.2.4.1.1 uv-vis spectra

The absorption spectra of 5 x 10^{-3} mol l^{-1} C12 in H_2O (grey) and 6 x 10^{-5} mol l^{-1} NAA in H_2O (black) are shown in fig. 6-5. The band at ~ 270 nm is seen to be due to NAA, and is not significantly different to the absorption spectrum of the free NAA molecule in H_2O with λ_{max} ~ 270 nm.

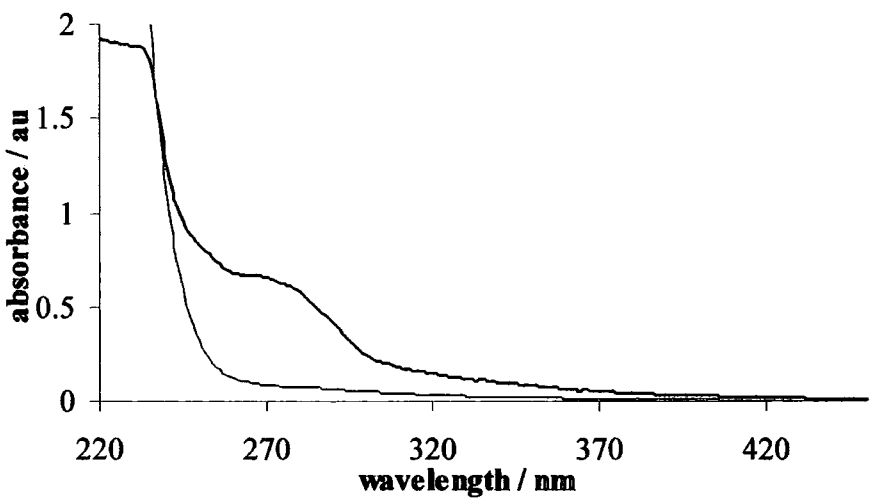

***Figure 6-5** Absorption spectra, black = 5 x 10^{-3} mol l^{-1} C12 + 6 x 10^{-5} mol l^{-1} NAA in H_2O, grey = 5 x 10^{-3} mol l^{-1} C12 in H_2O*

6.2.4.1.2 luminescence spectra

As can be seen in fig. 6-6 both the NAA and Tb^{3+} emit in solution upon excitation at the NAA absorption band (280 nm). However, as the concentration of micelle in solution increases there are two significant changes in the emission spectra namely, that the intensity of the broad emission centred at 340 nm decreases, and the intensity of the Tb^{3+} emission increases.

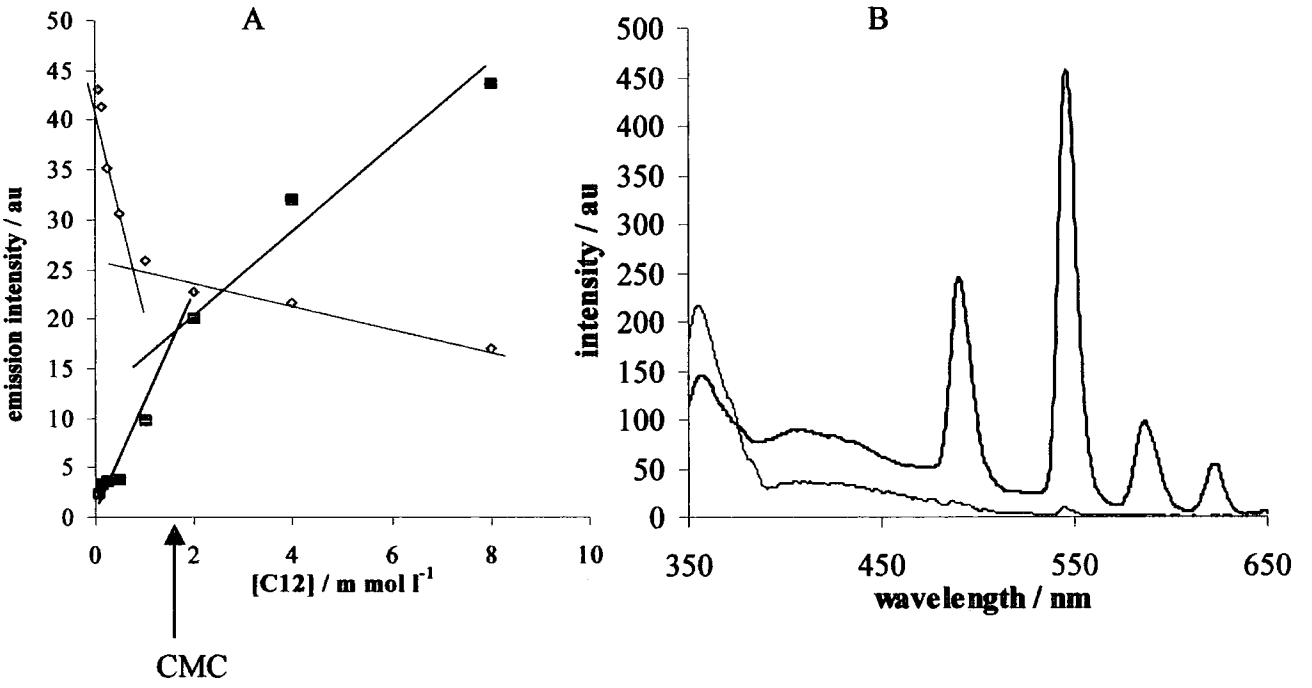

Figure 6-6 *λ_{ex} = 229 nm, bandpass = 2.5 nm, emission bandpass = 2.5 nm (A) Black = intensity of NAA fluorescence, grey = intensity of Tb^{3+} sensitised emission, with increasing C12 concentration (B) Steady state emission spectra, black = above the CMC (4 x 10^{-3} mol l^{-1}), grey = below the CMC (5 x 10^{-4} mol l^{-1}),*

Although the absence of a sharp change in the emission intensity at the CMC, ~ 1.5 m mol l^{-1}, it appears that this region is a turning point in the emission properties of the system.

The features of the emission spectra indicate that Tb^{3+} is indeed sensitised by NAA in aqueous micellar solution, and this is confirmed by the excitation spectra of the NAA and Tb^{3+}, which both show the same band at ~ 270 nm, confirming that the emission has the same NAA source.

6.2.4.2 Sensitised Eu^{3+} emission

The Eu^{3+} ion also shows significant sensitisation upon excitation at the NAA absorption band (at ~ 270 nm) above the CMC of a C12 solution.

In an aqueous solution of NAA and $EuCl_3$, both NAA and Eu^{3+} emission is observed (λ_{ex} = 282 nm). When C12 surfactant is added to the solution, to a concentration above the CMC, the fluorescence emission of NAA is dramatically quenched (by 77 %), and the emission intensity of Eu^{3+} increases substantially (by 11 %). The spectra are shown in fig. 6-7.

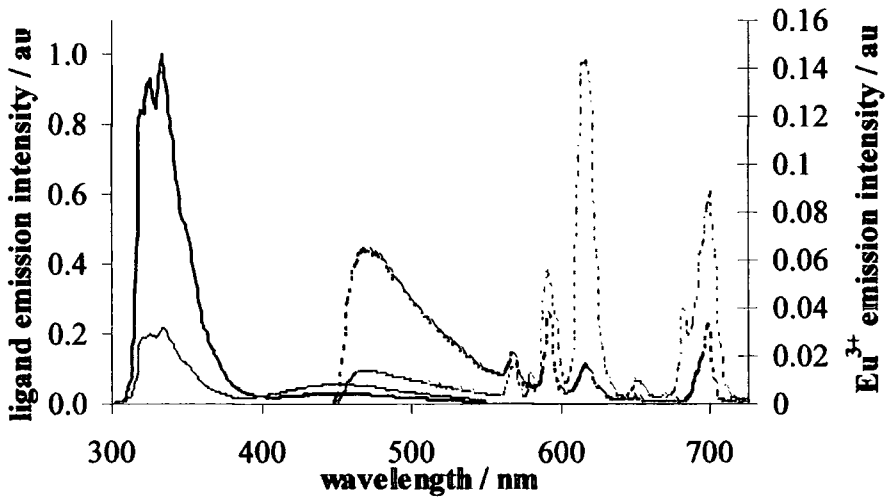

***Figure 6-7** Emission spectra of 4 x 10^{-3} mol l^{-1} Eu^{3+} + 6 x 10^{-5} mol l^{-1} NAA in the presence (black) and absence (grey) of 4 x 10^{-3} mol l^{-1} C12 in H_2O; λ_{ex} = 282 nm, bandpass = 2.5 nm, emission bandpass = 2.5 nm*

In addition, it can be deduced that the environment around the Eu^{3+} ion changes when the surfactant is added to the solution. The Eu^{3+} emission spectrum of 4 x 10^{-3} mol l^{-1} Eu^{3+} + 6 x 10^{-3} mol l^{-1} NAA in H_2O shows a $\Delta J = 2/\Delta J = 1$ ratio of 0.5, but when the micelle is added to the solution to a concentration above the CMC, and in a 1:1 ratio to $EuCl_3$, (4 x 10^{-3} mol l^{-1} Eu^{3+} + 6 x 10^{-3} mol l^{-1} NAA + 4 x 10^{-3} mol l^{-1} C12) the $\Delta J = 2/\Delta J = 1$ ratio increases to 2.5. The $\Delta J = 2$ transition at 615 nm is hypersensitive and responds to changes in the local environment around the ion. The fact that the $\Delta J = 2/\Delta J = 1$ ratio increases upon addition of C12 indicates that the Eu^{3+} is now in a bound environment. In addition, the intensity of all the Eu^{3+} bands increases upon addition of C12 signifying that energy

transfer from NAA to Eu^{3+} is more efficient in micellar solution, from the $\Delta J = 4$ transition this increase is approximately 3 fold.

Comparison of the emission spectra (not shown) following direct metal excitation at 396 nm of the Eu^{3+} : NAA : C12 and Eu^{3+} : C0 species indicates little difference in the spectral profiles. One difference between the two spectra is the $\Delta J = 2/\Delta J = 1$ band ratios. The Eu^{3+} : NAA : C12 ratio is ~ 2.5, and the Eu^{3+} : C0 is ~ 2, suggesting that the former system provides the most asymmetric Eu^{3+} site.

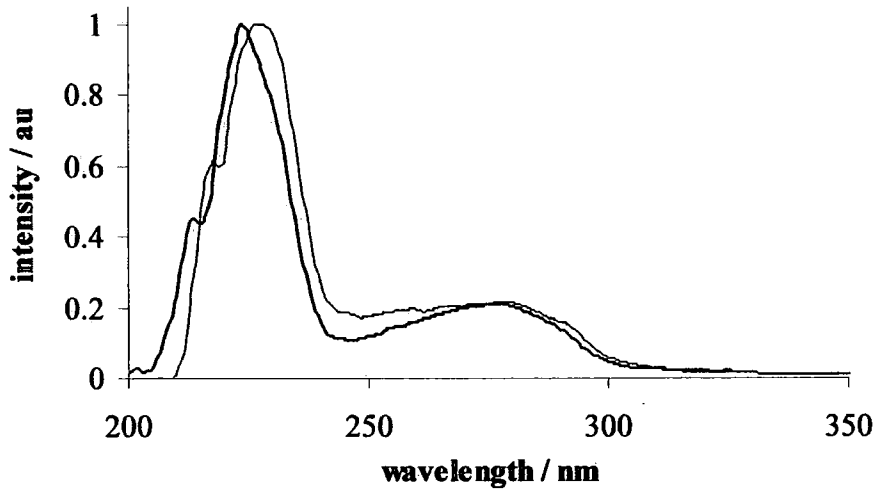

Figure 6-8 *Normalised excitation spectra, black = from NAA emission (λem = 340 nm) grey = from Eu^{3+} emission (λem = 615 nm); emission bandpass = 5 nm, excitation bandpass = 5 nm*

The excitation spectra shown in fig. 6-8 of the Eu^{3+} emission in the presence of C12 show the broad band at 280 nm due to NAA and prove that the emission is due to energy transfer.

6.3 Conclusions

Energy transfer to bound Tb^{3+} and Eu^{3+} ions at the surface of aqueous micelles has been demonstrated using the 2-naphthylacetic acid (NAA) chromophore. It is found that the surfactant monomer units bind the Ln^{3+} ions such that average q-values of 2.4 are obtained. It was observed that the intensity of Ln^{3+} emission is dependent upon the carbon chain length of the surfactant unit. Increasing the carbon chain length increases the size of the micelle, which therefore increases the concentration of chromophore located in the core of the micelle, in a position to sensitise the Eu^{3+} and Tb^{3+} ions. Aggregation numbers

in aqueous solution increase with an increase in the length of the hydrophobic group, and any factor that causes an increase in either the diameter of the micelle or its aggregation number produces an increase in the solubilisation capacity of the micelle[15].

Above the surfactant CMC there is a dramatic increase in the intensity of the lanthanide(III) emission indicating that the NAA chromophore is solubilised in the core of the micelle, this was confirmed by a study using the monomer unit without a carbon chain, i.e. a system with bound Ln^{3+} ions in the absence of micellisation. In the unorganised solution it is presumed that energy transfer does not occur: the rate of quenching by O_2 or T-T annihilation is greater than the rate of ET.

Both above and below the CMC, NAA fluoresces upon excitation, however, above the CMC the intensity of this emission dramatically decreases in the presence of Eu^{3+} and Tb^{3+} ions as the energy is transferred to the proximate Ln^{3+} ions.

It was found that benzophenone, biphenyl and naphthalene do not sensitise Ln^{3+} emission, which is believed to be due to their being spatially too distant from the Ln^{3+} ion. The acetic acid group on the NAA chromophore allows the closer approach of the antenna to the surface of the micelle by an electrostatic attraction to the bulk water.

REFERENCES

[1] S. I. Weissman, Intramolecular energy transfer. The fluorescence of complexes of europium, *J. Chem. Phys.*, **1942**, *10*, 214

[2] G. F. de Sá, O. L. Malta, C. de Mello Donegá, A. M. Simas, R. L. Longo, P. A. Santa Cruz, E. F. da Silva Jr, Spectroscopic properties and design of highly luminescent lanthanide coordination complexes, *Coord. Chem. Rev.*, **2000**, *196*, 165

[3] D. L. Dexter, A theory of sensitised luminescence in solids, *J. Chem. Phys.*, **1953**, *21*, 836

[4] M. Elbanowski, B. Makowska, The lanthanides as luminescence probes in investigations of biochemical systems, *J. Photochem. Photobiol. A:Chem.*, **1996**, *99*, 85

[5] M. Tabak, I. E. Borisevitch, Interaction of dipyridamole with micelles of lysophosphatidylcholine and with bovine serum albumin – fluorescence studies, *Biochim. Biophys. Acta*, **1992**, *1116*, 241

[6] W. Dong, C. D. Flint, Intermolecular energy transfer between lanthanide complex ions in micellar solution, *J. Chem. Soc., Faraday Trans.*, **1992**, *88*, 3435

[7] W. Dong, C. D. Flint, Association of the tris(dipicolinato) europium(III) anion with cetyltrimethyl-ammonim chloride, *J. Chem. Soc., Faraday Trans.*, **1992**, *88*, 705

[8] J. R. Darwent, W. Dong, C. D. Flint, Intermolecular energy transfer between phenanthrene and lanthanide ions in aqueous micellar systems, *J. Chem. Soc., Faraday Trans.*, **1983**, *89*, 873

[9] J. R. Escabi-Perez, F. Nome, J. H. Fendler, Energy transfer in micellar systems. Steady state and time resolved luminescence of aqueous micelle solubilised naphthalene and terbium chloride, *J. Am. Chem. Soc.*, **1997**, *99*, 7749

[10] M. Almgren, F. Grieser, J. K. Thomas, Energy transfer from triplet aromatic hydrocarbons to Tb^{3+} and Eu^{3+} in aqueous micellar solution, *J. Am. Chem. Soc.*, **1979**, *101*, 2021

[11] A. G. Mwalupindi, L. A. Blyshak, T. T. Ndou, I. M. Warner, Sensitised room-temperature luminescence in reverse micelles using lanthanide counterions as acceptors, *Anal. Chem.*, **1991**, *63*, 1326

[12] E. L. Wehry, *Modern Fluorescence Spectroscopy*, **1976**, Plenum Press, New York.

[13] W. de. W. Horrocks Jr, G. F. Sudnick, Lanthanide ion probes of structure in biology. Laser induced luminescence decay constants provide a direct measure of the number of metal coordinated water molecules, *J. Am. Chem. Soc.*, **1979**, *101*, 334

[14] S. FitzGerald, Investigation into the development of near infra-red liquid phase laser gain media, *MSc Project Report*, **1999**, University of Durham

[15] M. J. Rosen, *Surfactants and Interfacial Phenomena*, **1989**, Wiley, New York

[16] S. I. Klink, L. Grave, D. N. Reinhoudt, F. C. J. M. van Veggel, M. H. V. Werts, F. A. J. Geurts, J. W. Hofstraat, A systematic study of the photophysical processes in polydentate triphenylene functionalised Eu^{3+}, Tb^{3+}, Nd^{3+} Yb^{3+}, and Er^{3+} complexes, *J. Phys. Chem. A*, **2000**, *104*, 5457

CHAPTER 7: ENERGY AND ELECTRON TRANSFER PROCESSES IN LANTHANIDE(III) COMPLEXES

7.1 Introduction

The lanthanide ions provide an interesting field of study, not least due to their unique emission properties. The emission from the lanthanides covers the spectral range from the uv (Gd^{3+}) through the visible, (Tb^{3+}, Sm^{3+}, Dy^{3+} and Eu^{3+}) and into the near infrared (Yb^{3+}, Nd^{3+}, and Er^{3+}). The emission from these ions resulting from f-f transitions is much longer lived than for organic molecules owing to the transitions being forbidden by the parity selection rule (Eu^{3+} and Tb^{3+} lifetimes are of the order of ms cf. ns for organic molecules). While the forbidden nature of these transitions benefits the emission properties, the intensity of the absorption bands suffers as a result with their molar extinction coefficients being typically < 10 mol^{-1} dm^3 cm^{-1}. The common approach to overcoming the poor absorptivity of these ions is by the use an organic molecule with a high molar extinction coefficient held in close proximity to the ion. The chromophore harvests the incoming radiation and then transfers this energy to the lanthanide ion via its triplet state in a process known as the antenna effect[1]. A convenient means of ensuring the chromophore is in close proximity to the Ln^{3+} ion is by the covalent attachment to a chelate which coordinates to the lanthanide. A chelate is usually chosen to encapsulate the ion since it then serves the further purpose of protecting the ion from the solvent, the excited states of the lanthanide ions being readily deactivated by O-H oscillators in the solvent.

Since the emission from different Ln^{3+} ions appears in different regions of the spectrum, a suitable chromophore system could be used for a number of purposes simply by changing the coordinated Ln^{3+} ion. For example by using the lanthanides which emit in the visible (Eu^{3+} and Tb^{3+}) in fluoroimmunoassays, and by exploiting the emission from the near infrared emitters Yb^{3+} and Er^{3+} for use in light amplification.

In this chapter the photochemistry and photophysics of a series of lanthanide ions coordinated to the MRI contrast agent ethoxybenzyl-DTPA, shown in fig. 7-1 are investigated.

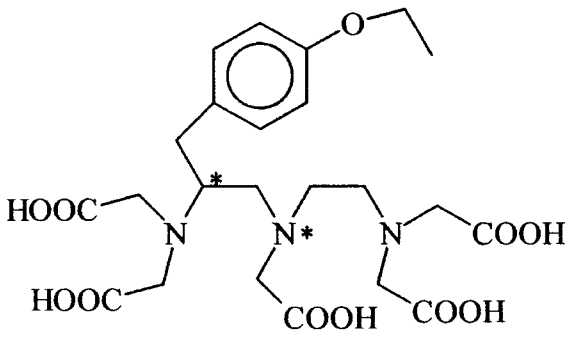

Figure 7-1 *Molecular structure of the chromophore-chelate used in this chapter, L, * = centre of chirality*

Absualeh and Meares[2] investigated the related chromophores of indole, *para*-benzyl, *para*-methoxybenzyl, and *para*-cyanobenzyl bound to the chelate EDTA which was in turn coordinated to the ions La^{3+}, Tb^{3+}, Eu^{3+}, Sm^{3+}, Dy^{3+} and Yb^{3+}. They studied the fluorescence and phosphorescence emission from the ligand and the luminescence seen from the Ln^{3+} ion, and indicated the importance of both electron transfer (eT) and energy transfer (ET) processes in these systems. By studying their particular series of aromatic chromophores, the oxidation potential could be varied without a corresponding change in the energy levels of the ligand. The sensitised emission of the lanthanide and the quenching of the aromatic fluorescence by the lanthanide were observed as a function of the oxidation potential of the aromatic group. Their results show that the two most easily reduced lanthanide ions, Eu^{3+} and Yb^{3+} are the most effective quenchers of the fluorescence intensity of the aromatic ligand, and that the cyanobenzyl ligand, which is hardest to oxidise is the least quenched by the Yb^{3+} ion. Also, the sensitised emission intensity observed was in the order $Tb^{3+} > Dy^{3+} > Sm^{3+} > Eu^{3+}$ (in the order hardest to easiest Ln^{3+} ion to reduce). The significant quenching of the fluorescence from the aromatic group observed in the Eu^{3+} and Yb^{3+} chelates compared to the other lanthanide complexes suggested the involvement of a different deactivation mechanism of the S_1 state in these chelates. Absualeh and Meares concluded that since Eu^{3+} and Yb^{3+} are the most readily reduced species, electron transfer from the aromatic group to these ions was considered as a likely mechanism for the quenching. They determined the free energy for

electron transfer and found that the values obtained were in strong agreement with the observed intensity of emission from the chromophore and the Ln^{3+} ions.

It had previously been proposed by Horrocks *et al.*[3] that quenching of tryptophan fluorescence in some protein Eu^{3+} complexes is due to efficient dipole-dipole energy transfer. Later, however, Horrocks *et al.*[4] proposed a mechanism for an electron transfer quenching of tryptophan (Trp) emission by Eu^{3+} and Yb^{3+} ions which involved the formation of an intermediate radical cation and Ln^{2+} species.

$$Trp, Eu^{3+} \rightarrow Trp^*, Eu^{3+} \rightarrow Trp^{+\cdot}, Eu^{2+} \rightarrow Trp, Eu^{3+}$$
$$Trp, Yb^{3+} \rightarrow Trp^*, Yb^{3+} \rightarrow Trp^{+\cdot}, Yb^{2+} \rightarrow Trp, Yb^{3+*} \rightarrow Trp, Yb^{3+}$$

After the second, back electron transfer step, the tryptophan may leave the Yb^{3+} ion in its excited $^2F_{5/2}$ state, since this is lower in energy than the $Trp^{+\cdot}$, Yb^{2+} state, but since the $^5D_0$ state of Eu^{3+*} is higher in energy than the $Trp^{+\cdot}$, Eu^{2+} state Eu^{3+} cannot be sensitised. The processes involved are shown schematically in fig. 7-2.

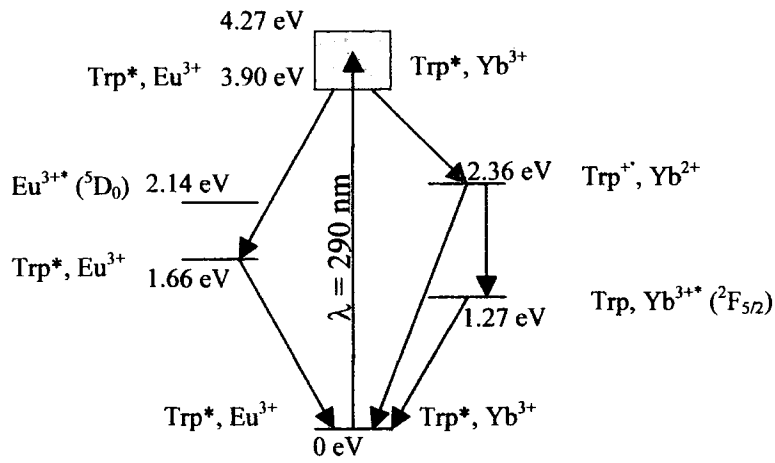

***Figure 7-2** Schematic representation of the energy levels and processes involved in the Trp, Eu^{3+}/Yb^{3+} systems. Adapted from J. Am. Chem. Soc.*, **1997**, *119*, 5972

7.2 Results and discussion

7.2.1 Introduction

The carbon atom marked * in fig. 7-1 represents a centre of chirality, with the enantiomerically pure *S* form being studied here. Upon complexation with Ln^{3+} ions

however, the nitrogen atom marked * also becomes chiral. The *R* and *S* enantiomers exist in a 65:35 ratio, are metastable, and they can be separated by HPLC in phosphate buffer at pH 7.5 on an ODS Hypersil 5 column[5]. Schmitt-Willich *et al.*[5] investigated the kinetics of isomerisation of the 2 isomers and obtained a value of 75.3 kJ mol^{-1} for the activation energy of the interconversion rate between the two isomers. This value indicates that at room temperature the two isomers do not readily interconvert.

7.2.2 Absorption properties

A typical absorption spectrum is shown in fig. 7-3. The molar extinction coefficient of the chromophore was determined to be 800 ± 50 mol^{-1} dm^3 cm^{-1} at 275 nm (cf. 700 mol^{-1} dm^3 cm^{-1} for the 4-methoxytoluene group[6])

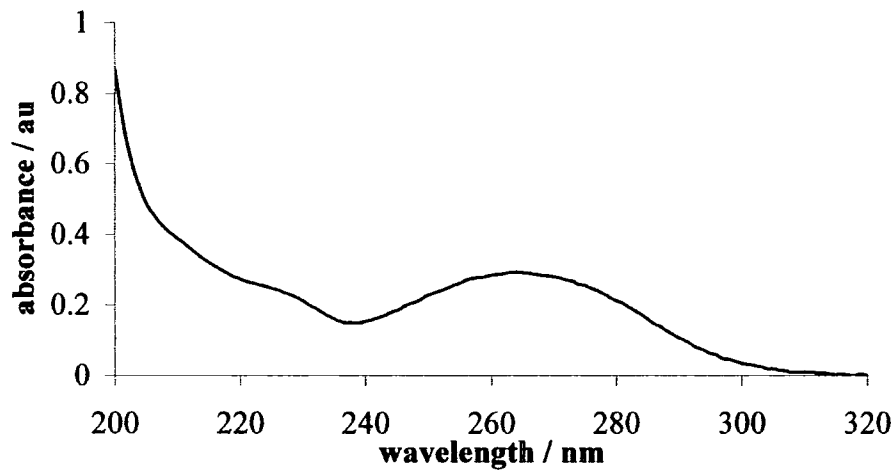

***Figure 7-3** Absorption spectrum of TbL in H_2O*

7.2.3 Emission from the ligand

The chromophore L has a broad emission band in the 280 – 330 nm region of the spectrum with λ_{max} = 305 nm.

Table 7-1 displays the results of the quantum yield measurements of the ligand fluorescence.

	H_2O		D_2O	
LnL	**aerated**	**degassed**	**aerated**	**degassed**
Eu	0.00032	0.00038	0.0073	0.0074
Yb	0.0037	0.0050	0.022	0.016
Dy	0.074	0.079	0.15	0.15
Nd	0.048	0.048	0.082	0.080
Sm	0.014	0.015	0.078	0.074
Gd	0.058	0.058	0.088	0.094
Tb	0.039	0.040	0.074	0.077
La	0.10	0.098	0.15	0.15

Table 7-1 *Fluorescence quantum yield data (± 10 %) for L emission*

From the quantum yield data it can be seen that degassing the solutions has little effect on the emission intensity of the chromophore.

The fluorescence emission from the ligand of the Eu^{3+} and Yb^{3+} chelates is quenched most extensively. These two ions are the most readily reduced ($Ln^{3+/2+}$ E^{θ} = -0.35 eV (Eu) and - 1.05eV (Yb)). The chromophore emission quantum yield is next lowest for the third most easily reduced ion, Sm^{3+}.

Interestingly, the emission from the Gd^{3+} chelate is also reduced compared to the emission from the La^{3+} complex and represents a distinctive case. The Gd^{3+} emissive state is at 32400 cm^{-1}, with an energy gap < 1500 cm^{-1} from the excited singlet state of the ligand, well within the limits for back energy transfer[7]. It is suggested that the mechanism of energy transfer following excitation to the excited singlet is transfer to the Gd^{3+} $^6P_{7/2}$ state. From there, the energy is transferred back to the ligand (in its triplet state), which is subsequently deactivated in the usual way by non-radiative processes. This is represented schematically in fig. 7-4.

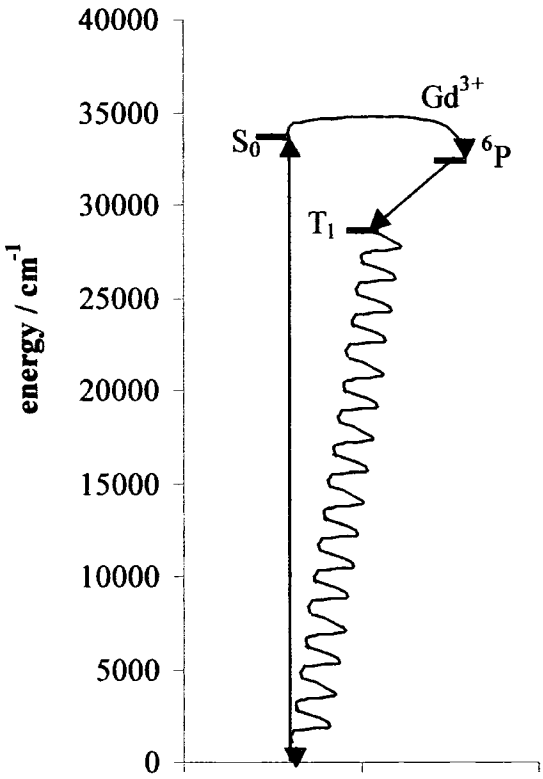

Figure 7-4 *Schematic representation of the proposed energy transfer mechanism occurring in the GdL complex*

The LaL complex has the highest quantum yield of emission because of the lack of any energy transfer from the chromophore to the La^{3+} ion. The La^{3+} ion does not have any electrons in the f orbitals, thus the lack of electronic energy levels below the S_1 and T_1 states of the chromophore means that it is unable to act as an acceptor. For this reason, it is often used as a model in energy transfer studies as a probe of the triplet state properties of the antenna[8].

There is a large difference in the quantum yield values for the lanthanum complex in H_2O and D_2O. The sensitivity of lanthanide(III) ion emission to non-radiative deactivation by vibronic coupling to the O-H vibrational levels is well documented[9], although, the related quenching of organic molecules is less so. Beeby *et al.*[10] reported on the similar quenching effects from the solvent on the photophysical properties of molecular species. The mechanism is analogous, the reduction in the vibrational overlap integral on X-H frequencies, and the vibrational levels of the molecule may act as either promoting or accepting modes of the excited and relaxed states respectively, so that changing the

vibrational frequencies alters the rate constant of non radiative processes. This analogous mechanism occurs in the LnL complex and accounts for the differences in Φ_{H2O} and Φ_{D2O}.

7.2.3.1 Transient species

The decay of the transient species was observed from the GdL complex in degassed H_2O following a flash photolysis experiment with λ_{em} = 400 nm. When the solution was aerated, the signal was no longer distinguishable, i.e. it is likely that this is the triplet-triplet absorption, the triplet states being highly susceptible to quenching by O_2. The emission from lanthanide(III) ions is unaffected by the presence of dissolved molecular oxygen. The lifetime of the triplet state was determined to be 10 μs.

7.2.4 Lanthanide emission

7.2.4.1 Steady state emission

The Nd^{3+}, Sm^{3+}, Eu^{3+}, Tb^{3+}, Dy^{3+}, and Yb^{3+} ions all show characteristic line-like emission associated with the f-f transitions of the Ln^{3+} ion, though with varying intensity following excitation of the ligand absorption band at 275 nm.

Table 7-2 displays the results of the quantum yield measurements of lanthanide luminescence.

	H_2O		D_2O	
Ln^{3+} ion	**aerated**	**degassed**	**aerated**	**degassed**
Eu	0.0013	0.0039	0.0025	0.021
Dy	0.0010	0.0089	0.039	0.029
Sm	0.0014	0.0038	0.013	0.013
Tb	0.048	0.055	0.10	0.11

***Table 7-2** Emission quantum yield data (± 10 %) for Ln^{3+} metal centred emission, λ_{ex} = 265 nm*

The quantum yields of the Nd^{3+} and Yb^{3+} ions were not recorded due to a lack of suitable standards in the near-IR region.

From the quantum yield data it can be seen that the emission intensity increases slightly upon degassing the solutions. The luminescence from Ln^{3+} ions is known to be insensitive

to the presence of dissolved molecular oxygen. Therefore, the results most likely reflects either a back energy transfer process from the metal to the triplet state of the chromophore, which is then subject to deactivation, or more probably, that there is a relatively slow energy transfer process from the ligand triplet state to the Ln^{3+} ions.

7.2.4.2 Electron transfer reactions

In the case of the Yb^{3+} complex, weak emission from the chromophore was observed at 980 nm, and although a quantum yield of metal emission was not recorded, it is likely to be low in accordance with other Yb^{3+} complexes studied in this laboratory. It is suggested that sensitised emission occurs by an electron transfer mechanism. The free energy change (ΔG)[11] can be estimated from the electrode potentials of the donor and acceptor and the excitation energy of the donor, which when solvent effects are neglected, can be given by equation 7-1.

$$\Delta G_{eT} = E(D^{+\bullet}/D) - E_D^* - E(A^{+\bullet}/A) \qquad 7\text{-}1$$

ΔG_{eT} = free energy change of electron transfer reaction

$E(D^{+\bullet}/D)$ = electrode potential of donor / V

E_D^* = excitation energy of donor / kJ mol^{-1}

$E(A^{+\bullet}/A)$ = electrode potential of acceptor / V

The forward eT reaction, ΔG_{eT} = -1.24 eV

$$L, Yb^{3+} \rightarrow L^{+\bullet}, Yb^{2+}$$

for the backward eT reaction, ΔG_{eT} = - 2.81 eV.

$$L^{+\bullet}, Yb^{2+} \rightarrow L, Yb^{3+}$$

Therefore the energy of this process, 2.81 eV is greater than the $^2F_{5/2}$ emissive state (1.27 eV) thus, the Yb^{3+} ion may be re-formed in either its ground or excited state. The fraction of excited Yb^{3+} formed in the upper $^5F_{5/2}$ state results in the Yb^{3+} near-IR luminescence.

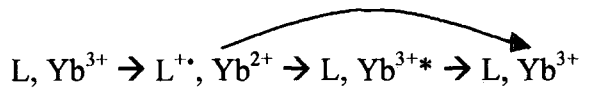

$$L, Yb^{3+} \rightarrow L^{+\bullet}, Yb^{2+} \rightarrow L, Yb^{3+*} \rightarrow L, Yb^{3+}$$

The low ligand emission is due to eT quenching of the excited singlet state.

In the case of the Eu^{3+} complex, an eT mechanism explains why very little sensitised emission from the $^5D_0$ excited state of the Eu^{3+} ion is seen. The ΔG_{eT} for the forward reaction is -1.94 eV, and for the back eT reaction is - 2.11 eV. This energy is lower than the energy of the emissive $^5D_0$ state (2.14 eV), and hence the emissive state cannot be formed by back eT. Thus, Eu^{3+} efficiently quenches the ligand fluorescence and is not itself photosensitised by the eT process. Such a process has been discussed by Horrocks *et al.* in their study of sensitised emission of Ln ions by cod parvalbumin.

$$L, Eu^{3+} \rightarrow L^{+\bullet}, Eu^{2+} \rightarrow L, Eu^{3+}$$

7.2.4.3 Sensitised emission via energy transfer

Nd^{3+}, Dy^{3+}, Sm^{3+}, and Tb^{3+} ions all show sensitised emission which can be assumed to take place via the ligand triplet state by a typical energy transfer mechanism seen in Ln^{3+} complexes[12].

Of all the ions, Tb^{3+} shows the most efficient sensitisation, which could be due to a combination of factors, the main of these being that Tb^{3+} has a high efficiency of emission, unlike the other Ln^{3+} ions. Also, no competing eT reactions, a higher energy gap between the ground and excited $^5D_4$ state resulting in less efficient quenching via coupling to solvent vibrational levels, and a more favourable $T_1 \rightarrow Ln^{3+*}$ pathway as a result of the $^5D_4$ level being the nearest in energy to the chromophore triplet state than the other Ln^{3+} excited energy levels.

7.2.4.4 Time resolved emission

The Ln^{3+} lifetimes are shown in table 7-3.

	τ / ns Nd^{3+}	τ / μs Sm^{3+}	τ / ms Tb^{3+}	τ / μs Dy^{3+}	τ / μs Yb^{3+}
H_2O aerated	84	8.2	1.6	9.9	0.6
H_2O degassed	360	9.5	1.6	9.7	0.6
D_2O aerated	82	54	3.5	72	9.7
D_2O degassed	420	47	3.4	72	9.4

Table 7-3 *Lifetimes (± 10 %) of Ln^{3+} emission*

Emission from the EuL complex upon excitation at 266 nm was shorter than the response time of the instrumental set-up i.e. < 50 ns and could not be recorded. Direct metal excitation of Eu^{3+} gave lifetime values of 2.63 ms and 0.63 ms in D_2O and H_2O respectively.

From the lifetimes, it was possible to determine q, the number of bound water molecules. The values are shown in table 7-4.

Nd^{3+}	Sm^{3+}	Tb^{3+}	Eu^{3+}	Dy^{3+}	Yb^{3+}
1.5	1.9	1.3	1.3	1.1	1.4

Table 7-4 *q-values (± 0.5) for the metal complexes (uncorrected for the weaker effect of outer sphere water molecules)*

The q-values for all the ions indicate between 1 and 2 bound water molecules are present in the complexes. DTPA complexes typically have been shown[13] to have values of ~ 1. There is a large error associated with the q value of ± 0.5.

7.2.5 *Summary of energy transfer processes*

A schematic representation of the energy and electron transfer processes which occur in this complex is illustrated in figure 7-5.

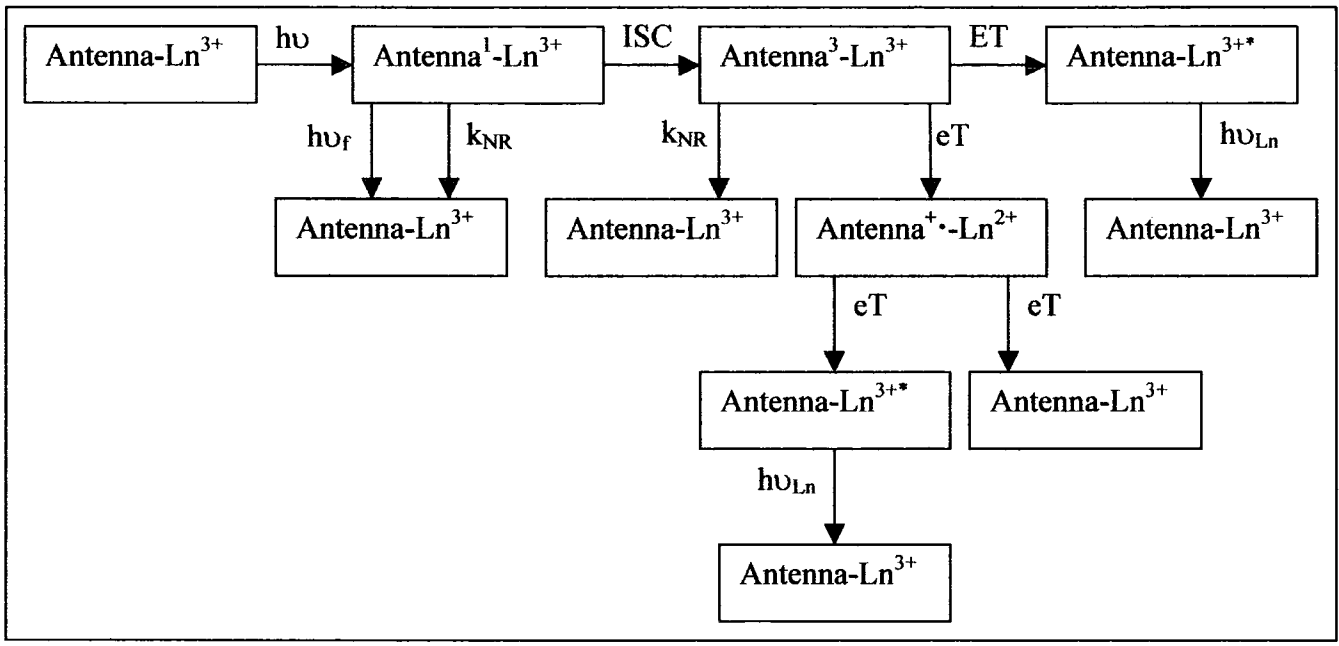

Figure 7-5 *Schematic representation of the energy and electron transfer processes that can occur in the LnL complexes.*

7.2.6 *Low temperature luminescence*

By investigating the emission properties of a Ln^{3+} complex at low temperature (77 K), any thermally activated processes which contribute to the energy transfer process are reduced. For example, back energy transfer quenching mechanisms are minimised at low temperature.

The total emission from EuL as a function of temperature was followed in both a 1:4 EtOH:MeOH mix and in a H_2O solution. Although there is an increase in emission intensity with decreasing temperature in the 1:4 EtOH:MeOH mix it is not as pronounced as in the H_2O sample see fig. 7-6.

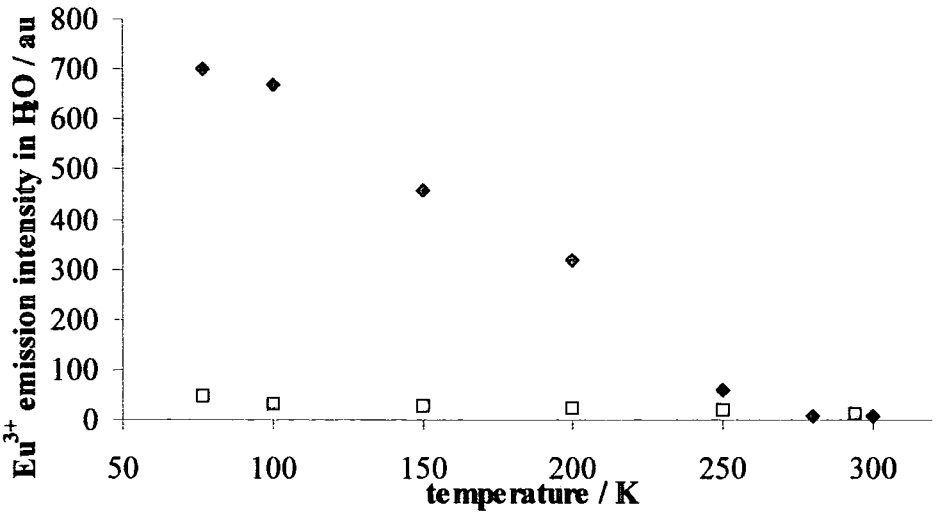

***Figure 7-6** Change in Eu^{3+} emission intensity with temperature in H_2O (black) and 1:4 EtOH:MeOH (grey), λ_{ex} = 265 nm*

A possible explanation for this arises from the type of glass formed by the two solvents at low temperature. H_2O forms a frosty glass upon freezing which increases the scattering of excitation light by the sample. This increases the amount of light getting into the sample, and therefore absorbed, and an increase of observed emission may simply be a reflection of this. The 1:4 EtOH:MeOH solvent mix, by contrast, forms a clear glass at 77 K [6] and has less effect on the optical properties of the sample. This effect has been demonstrated by De Santis *et al.*[14] for a nickel complex. An acetonitrile solution failed to form a glass upon cooling to 77 K so that the optical properties of the sample were affected, when using a glass of 95:5 EtOH:H_2O however, they were able to attribute unambiguously an increase in fluorescence emission upon cooling to the presence of an electron transfer quenching mechanism occurring in a Ni^{3+}/Ni^{2+} couple.

The low temperature measurements of the lanthanum complex showed a broad band centred at ~ 455 nm due to emission from the chromophore triplet state and from this the triplet energy was determined to be 27000 cm^{-1}. The lifetime of the phosphorescence was determined to be 0.42 ms (± 10 %).

7.3 Conclusions

It has been demonstrated that the emission of both the ethoxybenzyl group and the Ln^{3+} ion in ethoxybenzyl-DTPA complexes is dependent on the redox properties of the Ln^{3+} ion. The quantum yields of the chromophore and the Ln^{3+} ion were determined in both H_2O and D_2O, and the effects of oxygenation of the solutions investigated. The Ln^{3+} lifetimes were determined, also in H_2O and D_2O, and allowed the determination of q, the number of bound water molecules revealing values in the range 1 - 2. In the complexes where the Ln^{3+} ion is easily reduced, it was found that the chromophore donates an electron to the Ln^{3+} ion upon excitation to give radical cation species. The back electron transfer reaction can yield the Ln^{3+} ion in either its ground or excited state, depending on the thermodynamics of the process. In the complexes where the Ln^{3+} ions are not so easily reduced, the energy transfer mechanism occurs as expected, probably via a Dexter type mechanism. The efficiency of Ln^{3+} emission is dependent on a number of factors, in particular the efficiency of energy transfer, and the degree of coupling between the Ln^{3+} excited state and solvent/ligand high frequency oscillators.

REFERENCES

[1] B. Alpha, R. Ballardini, V. Balzani, J.-M. Lehn, S. Perathoner, N. Sabbatini, Antenna effect in luminescent lanthanide cryptates: A photophysical study, *Photochem. Photobiol.*, **1990**, *52*, 299

[2] A. Absualeh, C. F. Meares, Excitation and de-excitation processes in lanthanide chelates bearing aromatic side chains, *Photochem. Photobiol.*, **1984**, *39*, 763

[3] W. DeW. Horrocks Jr, W. E. Collier, Lanthanide ion luminescence probes, measurement of distance between intrinsic protein fluorophores and bound metal ions: Quantitation of energy transfer between tryptophan and terbium(III) and europium(III) in the calcium binding protein parvalbumin, *J. Am. Chem. Soc.*, **1981**, *103*, 2856

[4] W. D. Horrocks Jr, J. P. Polender, W. D. Smith, R. M. Supkowski, Photosensitised near infrared luminescence of ytterbium(III) in proteins and complexes occurs via an internal redox process, *J. Am. Chem. Soc.*, **1997**, *119*, 5972

[5] H. Schmitt-Willich, M. Brehm, C. L. J. Ewers, G. Michl, A. Müller-Fahrnow, O. Petrov, J. Platzek, B. Radüchel, D. Schülze, Synthesis and physicochemical characterisation of a new gadolinium chelate: the liver specific magnetic resonance imaging contrast agent Gd-EOB-DTPA, *Inorg. Chem.*, **1999**, *38*, 1134

[6] S. L. Murov, I. Carmichael, G. L. Hug, *Handbook of Photochemistry,* **1993**, Marcel Dekker Inc., New York

[7] M. Latva, H. Takalo, V.-M. Mukkala, C. Matchescu, J. C. Roderíguez-Ubis, J. Kankare, Correlation between the lowest triplet state energy level of the ligand and lanthanide(III) luminescence quantum yield, *J. Lumin.*, **1997**, *75*, 149

[8] C. V. P. de Melo, G. Vicentini, P. C. Isolani, J. Zukerman-Schpector, E. E. Casellano, Spectroscopic studies of lanthanide picrate complexes with N,N-dimethylacetamide. Structure of the La compound, *J. Alloys Compd.*, **1998**, *277*, 242

[9] J. L. Kropp, M. W. Windsor, Luminescence and energy transfer in solutions of rare-earth complexes. I. Enhancement of fluorescence of deuterium substitution, *J. Chem. Phys.*, **1965**, *42*, 1599

[10] A. Beeby, A. W. Parker, M. S. C. Simpson, D. Phillips, Deuteration effects on the photophysical properties of molecules, *Photochem. Photobiol. B: Biol.*, **1993**, *17*, 205

[11] M. A. Fox, M. Chanon, Eds., *Photoinduced Electron Transfer*, **1998**, Elsevier, Oxford

[12] B. Yan, H. Zhang, S. Wang, J. Ni, Intramolecular energy transfer mechanism between ligands in ternary rare earth complexes with aromatic carboxylic acids and 1,10-phenanthroline, *J. Photochem. Photobiol. A:Chem*, **1998**, *116*, 209

[13] R. P. Lauffer, Paramagnetic metal complexes as water proton relaxation agents for NMR imaging: theory and design, *Chem. Rev.*, **1987**, *39*, 2769

[14] G. De Santis, L. Fabbrizzi, M. Licchelli, N. Sardone, A. H. Velders, Fluorescence redox switching systems operating through metal centres: the Ni^{III}/Ni^{II} couple, *Chem. Eur. J.*, **1996**, *2*, 1245

SUMMARY

The steady state and time resolved emission spectra of the Tm^{3+} ion in various solvents and chelating systems have been presented.

The mechanism of energy transfer to Eu^{3+} and Tb^{3+} ions from benzophenone has been investigated in detail following kinetic measurements. It has been shown that it is possible to determine the efficiency of energy transfer via calculating the pure radiative lifetime. It has also been shown that a small change to the structure of the ligand (the addition of a CH_2 group) can have an effect on the oscillator strength of the hypersensitive transitions of both Eu^{3+} and Tb^{3+}, and this affects the efficiency of energy transfer.

It has been shown that the efficiency of energy transfer to Eu^{3+} ions can depend on the polarisability of the chromophore, with a tendency for increased Eu^{3+} emission with increased electron donating ability of the chromophore. In the case of a dimethylamino substituted acetophenone, the emission from Eu^{3+} ions is also highly dependent on the solvent.

Energy transfer to bound Eu^{3+} and Tb^{3+} ions in aqueous micelles has been demonstrated from the 2-naphthylacetic acid chromophore solubilised in the core of the surfactant. It is found that the intensity of Ln^{3+} ion emission is dependent upon the length of the carbon chain of the micelle. The efficiency of energy transfer is enhanced above the surfactant CMC.

The presence/absence of energy transfer in an ethoxybenzyl containing chromophore is found to depend on the redox properties of the Ln^{3+} ion. The complexes with the most easily reduced Ln^{3+} ions, Eu^{3+} and Yb^{3+}, are said to undergo an electron transfer reaction upon excitation of the chromophore. The possibility of Ln^{3+} sensitisation depends on the ΔG value of the forward and backward electron transfer reactions, with Yb^{3+} being reformed in its excited state, but Eu^{3+} being reformed in its ground state.

APPENDIX A: THE PHOTOPHYSICAL PROPERTIES OF POTENTIAL EUROPIUM(III) AND TERBIUM(III) ELECTROLUMINESCENT MATERIALS

A.1 Introduction

Since the pioneering work of Tang and VanSlyke[1] on organic electroluminescent (EL) devices, a large amount of work has used the mechanism of EL, i.e. the emission of light by molecules in response to an electric field, with the aim of producing flat panel displays[2,3]. A voltage applied across a thin layer of such a material generates negative and positive charge carriers that migrate from the contacts and emit visible light when they recombine.

Organic EL devices, used as an alternative to inorganic semiconductors and liquid crystal displays offer significant advantages. In particular, they are expected to be cheaper to manufacture, offer the possibility of full colour displays, may be highly efficient, and as emissive materials may have a wide angle of view.

A major problem associated with the use of conjugated polymers or small organic molecules however, is that of obtaining pure colour emission. The emission bands in general have large FWHM of typically 50-200 nm. Due to the higher sensitivity of the eye to colours in the middle of the visible region, the perceived colour, as judged by the Commission Internationale de l'Eclairage (CIE) colour map coordinates, can be affected if even part of the spectrum falls into a different colour region. Thus, filters are often used to remove unwanted radiation, but these reduce the observed intensity of the device.

Due to the transitions occurring within the f- orbitals, lanthanide ions emit light in sharp line-like bands with FWHM < 10 nm; furthermore, the emission from Tb^{3+} and Eu^{3+} ions, in the green and red regions of the electromagnetic spectrum respectively have excellent CIE coordinates. These reasons, together with the long lifetimes associated with these ions, the complexes of Eu^{3+} and Tb^{3+} are considered as viable alternatives for inclusion in EL devices.

To date, the focus of much of the work incorporating Ln^{3+} ions into EL devices has been based on lanthanide β-diketonates and related complexes[4,5,6].

Lanthanide β-diketonates are relatively easily synthesised, and exhibit efficient photoluminescent (PL) sensitised emission[7]. Moreover, the emission from europium(III) β-diketonates is virtually monochromatic[8], due to the large oscillator strength of the $\Delta J = 2$ transition in the asymmetric environment.

This chapter will describe in detail the results obtained on a PL study of some potential EL materials utilising the emission from Eu^{3+} and Tb^{3+} ions.

A.2 Europium(III) tris-(diphenylimidodiphosphinato)

The molecular structure of europium(III) tris-(diphenylimidodiphosphinato) (EuL^1) is shown in fig. A-1.

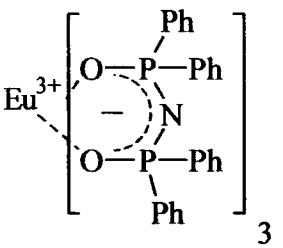

***Figure A-1** The molecular structure of EuL^1*

The imidodiphoshinate ligands form a hydrophobic shell around the Eu^{3+} ion and do not contain any O-H, C-H, or N-H bonds in the binding site that can contribute to the quenching of Ln^{3+} emission. The four phenyl rings associated with each ligand act as antenna units for sensitising the Eu^{3+} ion.

A.2.1 Absorption properties

The absorption spectrum of EuL^1 in CH_2Cl_2 is shown in fig. A-2 where it can be seen that the π–π^* absorption band of the complex extends out to 290 nm, this band corresponds to the $S_0 \rightarrow S_1$ transition of the ligand and has $\lambda_{max} = 271$ nm.

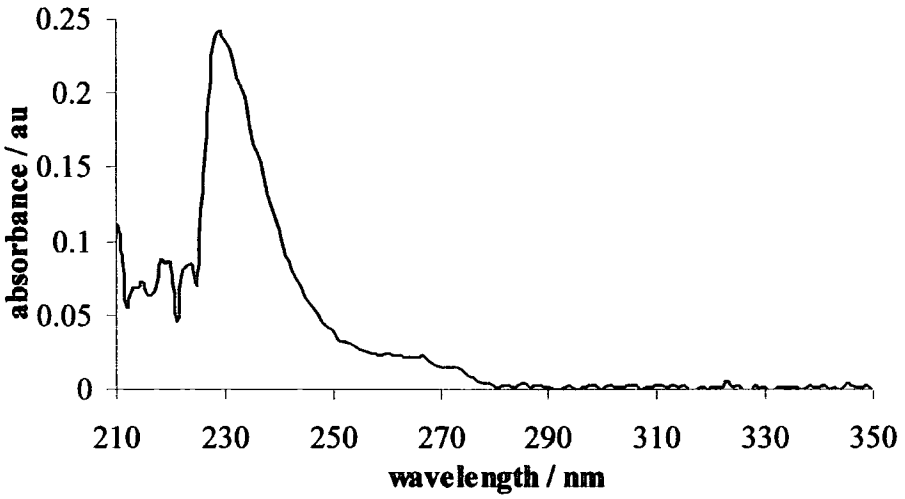

***Figure A-2** The absorption spectrum of EuL^1 in CH_2Cl_2*

A.2.2 Emission and excitation spectra

The excitation spectrum (λ_{em} = 611 nm) of the complex shows a number of sharp bands from 350 – 500 nm associated with the f-f transitions of Eu^{3+}, and a broader band at ~ 270 nm associated with the absorption of the phenyl rings on the ligand. As with the absorption spectrum this band extends to ~ 290 nm. The excitation spectrum proves that energy transfer occurs from the imidodiphosphinate ligand to the Eu^{3+} ion, but that the ion can also be excited directly.

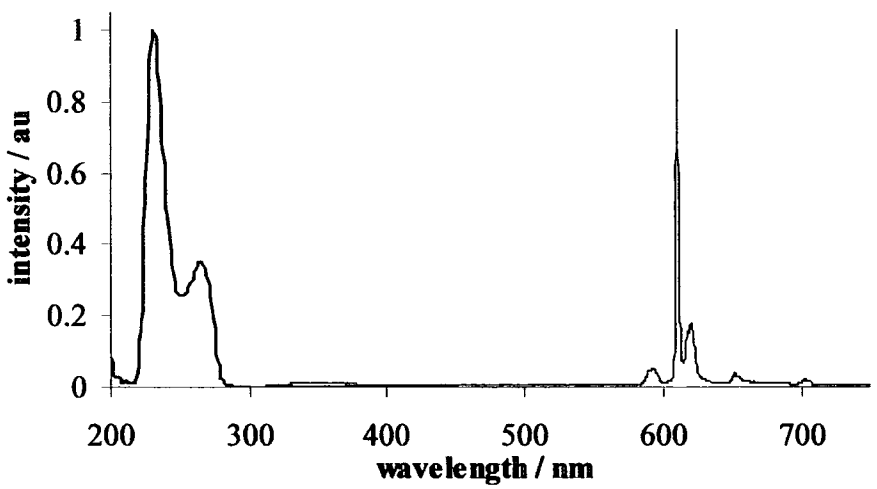

***Figure A-3** The excitation (black) λ_{em} = 611 nm, bandpass = 1 nm, excitation bandpass = 1 nm and emission (grey) spectra of EuL^1 in CH_2Cl_2, λ_{ex} = 277 nm bandpasss = 1 nm, emission bandpass = 1 nm*

The emission spectrum of EuL^1 is dominated by the intense $\Delta J = 2$ hypersensitive transition. The $\Delta J = 2/\Delta J = 1$ ratio is 17.3 representing extreme distortion of the electric field around the ion. This in line with the $\Delta J = 2/\Delta J = 1$ ratios seen in most β-diketonate complexes[9] which typically have values of > 10, although the intensity of hypersensitive transitions can be much greater than this and are known to be up to 200 times more intense than in the aqua ion[10]. The luminescence spectra of the solid state complex are much the same as those seen in solution indicating that the solvent has minimal interaction with the ion. This is to be expected due to the solvent excluding environment imposed by the bulky imidodiphospinate ligands.

A.2.3 Emission quantum yield

The emission quantum yield of EuL^1 in CH_2Cl_2 solution was determined to be 0.03; this value is similar to that determined by Magennis *et al.*[11], although both differ largely from that reported by Christou *et al.*[12] The data are represented in table A-1.

Φ_{tot}	ref
0.03	11
0.013	
0.29	12

***Table A-1** Quantum yield values (± 10 %) determined and literature for EuL^1*

It is possible that the large Φ_{tot} value reported by Christou *et al.* is due to a poor choice of reference material used for the fluorescence quantum yield determination. The quantum yield measured here was using two reliable standards which both emit and absorb radiation in the same spectral region as the sample; rhodamine 101 in acidified ethanol, $\Phi_f = 1.0$, and cresyl violet in methanol, $\Phi_f = 0.54$. Magennis *et al.* used tris(2,2'-bipyridine)ruthenium(II) in H_2O, again a commonly used standard for red emission $\Phi_f = 0.028$. Christou *et al.* however, used the $Eu(TTA)_3$ complex (europium(III)-thenoyltrifluoroacetonate) complex as a standard. It is known that the emission yield of this material is temperature sensitive[13] and is therefore unsuitable for use as a standard in quantum yield measurements.

A.2.4 Time resolved data

The kinetic data show single exponential decays for the complex in acetonitrile solution at room temperature (RT) and in an acetonitrile glass at 77 K. However, the solid state complex shows a single exponential decay at 77 K, and a double exponential decay at RT indicating the presence of 2 components. A summary of the data obtained is shown in table A-2.

	solid		**solution**	
	RT	**77 K**	**RT**	**77 K**
τ_1 / **ms**	0.909	0.981	1.503	1.091
τ_2 / **ms**	0.351			
A1	0.256			
A2	0.744			

Table A-2 *EuL^1 lifetime data (± 10 %)*

A.2.5 Time gated emission spectra

The time gated emission measurements allow the emission spectra of two components with different lifetimes in a sample to be resolved through the differences observed in their emission spectra with time. The spectra obtained for solid state EuL^1 are shown in fig. 8-4.

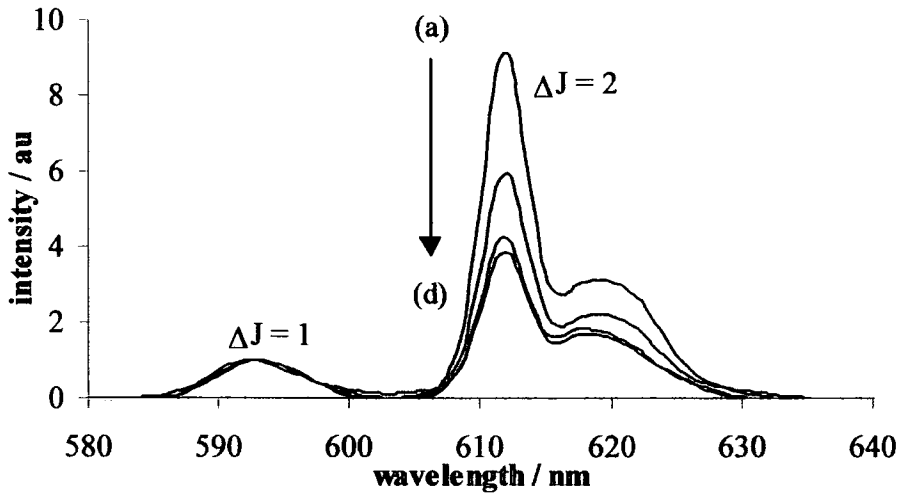

Figure A-4 *Normalised (at λ = 593 nm) time gated emission spectra of solid state EuL[1] (a) τd = 0.1 ms, τg = 0.2 ms, (b) τd = 0.2 ms, τg = 4 ms, (c) τd = 1 ms, τg = 4 ms, (d) τd = 1.5 ms, τg = 4 ms, λ_{ex} = 267 nm bandpass = 15 nm, emission bandpass = 2.5 nm*

There is a clear decrease in the relative intensity of the hypersensitive ΔJ = 2 transition in the longer-lived component compared to the intensity of the ΔJ = 2 transition of the shorter lived component, i.e. the ΔJ = 2/ΔJ = 1 ratio decreases with time. The extreme sensitivity of the ΔJ = 2 transition to the local environment around Eu^{3+} ions results in slightly different Eu^{3+} sites having different emission spectra. The Eu^{3+} ion is also extremely sensitive to quenching by O-H, C-H, and N-H oscillators, so that slightly different sites can also have different emission lifetimes. Time gated emission spectroscopy exploits these two features so that it can be concluded that in this complex there is more than one individual Eu^{3+} site.

A.2.6 Efficiency of energy transfer

The efficiency of the energy transfer processes, $\eta_{ET}.\Phi_T$, can be determined by using equation A-1 since it is possible to estimate η_{Ln} by using the corrected emission spectrum and the observed lifetime for Eu^{3+} emission, see section 4.2.6.

$$\Phi_{tot} = \Phi_T.\eta_{ET}.\eta_{Ln} \qquad \text{A-1}$$

Φ_{tot} = total emission quantum yield

Φ_T = intersystem crossing yield

η_{ET} = efficiency of energy transfer

η_{Ln} = efficiency of lanthanide emission

The product of the efficiency of energy transfer and the intersystem crossing yield was determined for the EuL^1 complex. The summary of results is shown in table A-3.

I_{J1}	0.0558
k_R / s^{-1}	7560
τ_0 / ms	0.13
Φ_{tot}	0.03
τ_{obs} / ms	1.39
η_{Ln}	0.19
$\eta_{ET}.\Phi_T$	0.16

***Table A-3** Summary of the EuL^1 efficiency of energy transfer calculations, values (± 10 %)*

The efficiency of Eu^{3+} emission is quite high (0.978) as a result of the low efficiency of the energy transfer processes (η_{ET} and Φ_T) and the relatively long lived emission observed in this complex. The actual Φ_T value is unknown, but is expected to be < 1.

A.3 Terbium(III) tris-(1-phenyl-3-methyl-4-(2,2-dimethylpropyryl)-5-pyrazolone)-n-(triphenylphosphine oxide)-m-H_2O

The molecular structure of the complex (TbL^1) is shown in fig. A-5.

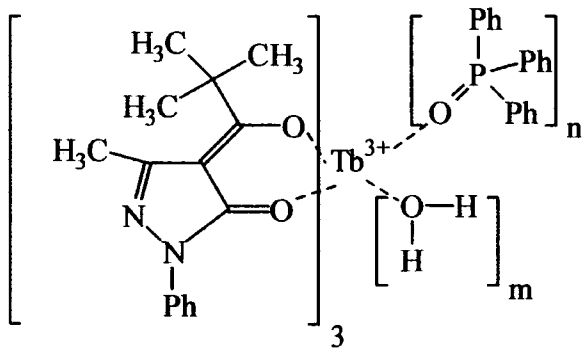

Figure A-5 *Molecular structure of terbium(III) tris-(1-phenyl-3-methyl-4-(2,2-dimethylpropyryl)-5-pyrazolone)-n-(triphenylphosphine oxide)-m-H_2O. n & m = unspecified equivalents. TbL^1*

In a series of papers by Gao *et al.*[14,4,5] a structurally similar Tb^{3+} complex (with an isobutyryl group in the 4-position on the pyrazolone ring) was studied in EL devices. They found an encouraging EL performance (maximum luminance 920 cd/m^2, efficiency 0.51 lm/W), highlighted the potential applicability for complexes of this type and the need for fine tuning the system (both the complex and device structures) to improve the overall EL performance.

A.3.1 Absorption properties

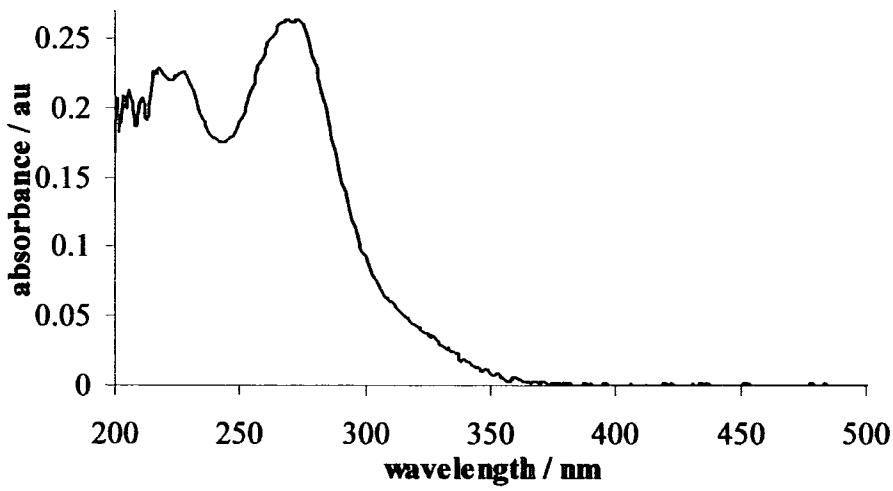

Figure A-6 *Absorption spectrum of TbL^1 in CH_2Cl_2*

The absorption spectrum of TbL^1 in CH_2Cl_2 is shown in fig. A-6. Where it can be seen that λ_{max} = 271 nm, the band being due to the $\pi \rightarrow \pi^*$ absorption of the triphenylphosphine oxide ligand.

A.3.2 Triplet state of triphenylphosphine oxide

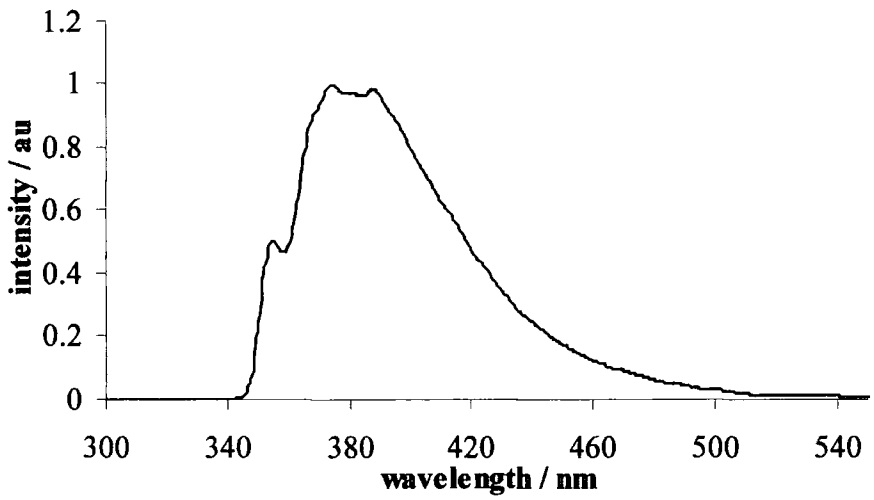

***Figure A-7** Phosphorescence spectrum of TPP in EPA at 77 K, λ_{ex} = 273 nm bandpass = 5 nm, emission bandpass = 5 nm*

The triplet energy of triphenylphosphine oxide, TPP, was determined from the phosphorescence spectrum shown in fig. A-7.

The triplet energy was determined to be 28600 cm^{-1} and is of sufficient energy to sensitise the $^5D_4$ state of Tb^{3+} at 21500 cm^{-1}.

A.3.3 Emission and excitation spectra

The complex is non emissive in CH_2Cl_2 and acetonitrile solutions at RT possibly due to a back energy transfer process occurring from the metal excited state back to the triplet state of the TPP. This process can usually be identified through observed emission upon degassing the solution, though no emission whatsoever was observed at all in this case when the solution was degassed. Also, the triplet energy of TPP is high enough in energy that this process would be energetically unfavourable. Due to the lack of solution state RT emission the quantum yield of this complex could not be determined. When the solution is cooled to a glass at 77 K, the complex emits metal centred green emission. The complex is

emissive at both RT and 77 K in the solid state with no apparent change in the luminescence spectra. The reason for this behaviour is unclear, but could be due to the complex dissociating as the temperature is lowered in solution.

The excitation spectra show a broad band in the uv due to the ligand absorption band, proving that energy transfer occurs.

An example of the typical spectra obtained are shown in fig. A-8.

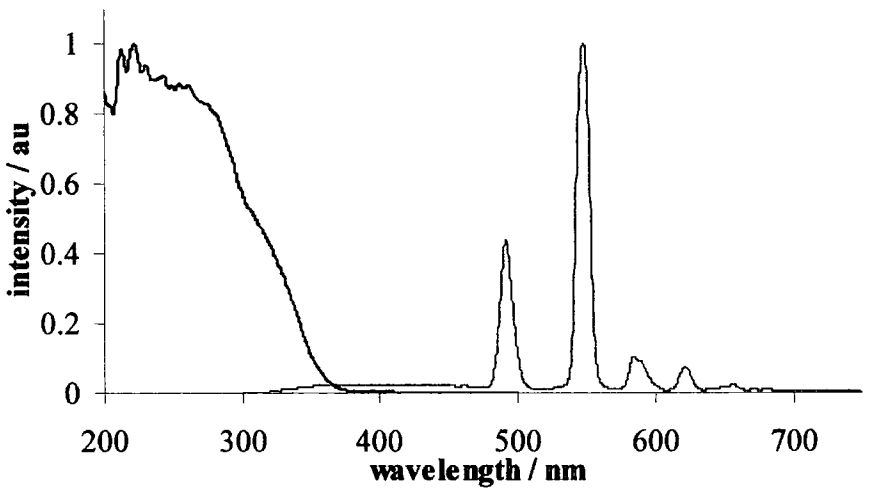

Figure A-8 *Excitation and emission spectra of solid state TbL[1], λ_{ex} = 273 nm bandpass = 2.5 nm, emission bandpass = 2.5 nm*

A.3.4 Time resolved emission

A summary of the lifetimes observed for the TbL^1 complex are given in table A-4.

	solid		solution	
	RT	77K	RT	77K
τ_1 / ms	0.496	0.885	–	1.666
τ_2 / ms	0.119	0.240	–	0.560
A_1	0.414	0.572	–	0.158
A_2	0.586	0.428	–	0.842

Table A-4 *Summary of the lifetime data (± 10 %) for TbL*[1]

The lifetimes follow non exponential decay curves, indicating the presence of a non homogeneous sample. This could be due to the terbium complex having more than one site with different numbers of TPP and H_2O molecules coordinated. Since the terbium ion also has a hypersensitive transition ($^5D_4 \rightarrow {}^7F_5$), time gated emission spectra may be able to resolve the species.

A.3.5 Time gated emission

The time gated emission spectra for the solid state complex are given in fig. A-9.

The spectra obtained show that the hypersensitive $^5D_4 \rightarrow {}^7F_5$ Tb^{3+} transition does show some change in intensity with respect to the other transitions in the spectrum, however, the intensity of the signals obtained at long delay times are weak, so that the emission spectra are more susceptible to noise fluctuations and this could well be the reason for the differences. A further possibility is that the decay has more than two species, and that the decay fitting process is unable to resolve them, in which case there could be a number of different spectra overlaid and changes in the hypersensitive transition would therefore be difficult to determine.

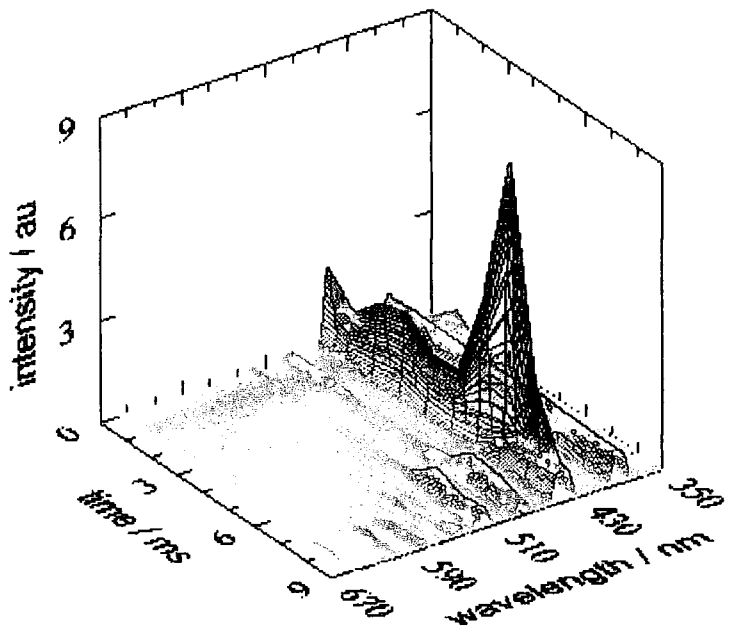

Figure A-9 *Time gated emission spectra, normalised at 492 nm (λ_{ex} = 284 nm, bandpass =10 nm, emission bandpass = 2.5 nm) of solid state TbL[1]. (a) τd = 0.0 ms, τg = 0.1 ms, (b) τd = 0.1 ms, τg = 0.1 ms, (c) τd = 0.2 ms, τg = 0.1 ms, (d) τd = 0.3 ms, τg = 0.1 ms, (e) τd = 0.5 ms, τg = 0.1 ms, (f) τd = 0.7 ms, τg = 0.1 ms, (g) τd = 0.9 ms, τg = 0.1 ms, (h) τd = 1.1 ms, τg = 0.1 ms, (i) τd = 1.3 ms, τg = 1.3 ms*

A.3.6 RT solution state emission

The complex was not emissive in either CH_2Cl_2 or CH_3CN solutions at RT, so that the complex was also studied in four other solvents, DMSO, toluene, acetone, and methanol. It was found that the complex is emissive in the strongly coordinating solvent, DMSO, and showed a single exponential lifetime with τ = 1.45 ms. In toluene, the complex was less emissive, and the lifetime results indicated a value of 0.71 ms. In methanol, the complex was only slightly emissive, with a lifetime < 100 μs, and as with CH_2Cl_2, and CH_3CN, the complex did not emit in acetone.

A.3.7 Thin films

Thin films of TbL^1 on quartz substrates were prepared in which two (A and B) were exposed to an H_2O environment and two (C and D) were exposed to a D_2O environment. The emission lifetimes and the emission quantum yields of the films were recorded in order to ascertain whether the atmospheric environment experienced by the complex affected the properties of the emission. The luminescence spectra obtained for the films were the same as those obtained for the solid state complex, and showed the characteristic Tb^{3+} emission bands. The lifetime results are displayed in table 8-5, and the quantum yield results obtained are displayed in table A-6.

	H_2O		D_2O	
	A	**B**	**C**	**D**
τ_1 / ms	0.149	0.163	0.161	0.172
τ_2 / ms	0.512	0.562	0.566	0.627
A_1	0.575	0.624	0.563	0.583
A_2	0.425	0.376	0.437	0.417

Table A-5 *Lifetime (± 10 %) results of the thin films*

A	B	C	D
14	15	14	13

Table A-6 *Quantum yield results of the thin films. Values are given as percentages, ± 10 %*

The results indicate that the environment has little effect on the properties of the complex in the film, although it appears, anomalously, that the films exposed to D_2O show slightly more quenching than the films exposed to H_2O. The Tb^{3+} ion is well protected from the environment by the bulky substituted pyrazolone ligand, which could hinder the approach of H_2O molecules, and would account for the insensitivity to the atmospheric environment experienced by this complex.

A.4 4,4'-dimethylamino benzophenone: Europium(III) tris(6,6,7,7,8,8,8-heptafluoro-2,2-dimethyloctane-3,5-dione)

A.4.1 Introduction

In 1999 Werts *et al.*[15] demonstrated efficient (Φ_{tot} = 0.20 in degassed benzene) Eu^{3+} sensitised emission by visible light excitation in a push-pull complex with Michler's ketone, (4,4'-bis(*N,N*-dimethylamino)benzophenone) and $Eu(fod)_3$ (europium(III) tris(6,6,7,7,8,8,8-heptafluoro-2,2-dimethyloctane-3,5-dione). This complex is unsuitable for biological applications since it dissociates in polar solvents, but it should be considered as a red emitter in EL devices as the lower excitation energy required is unusual amongst potential lanthanide(III) materials.

In the process of excitation, the electron density of the carbonyl group on Mk increases as it moves from the dimethylamino groups, making the transition solvatochromic.

The molecular structure of the complex is given in fig. A-10.

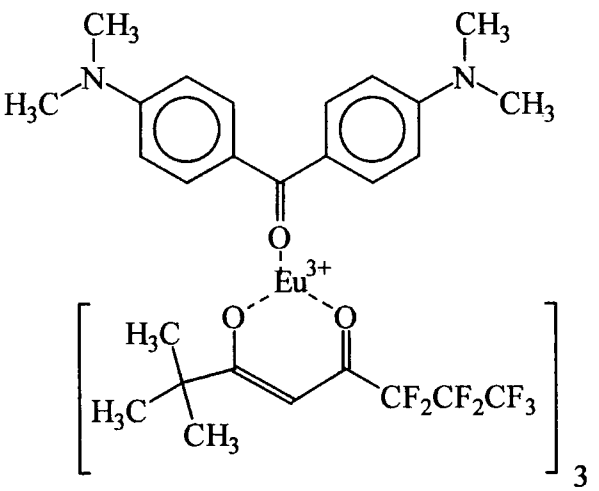

***Figure A-10** Molecular structure of 1:1 Mk:Eu(fod)$_3$, EuL^2*

EuL^2 was studied in 10 x 10^{-3} mol l^{-1} toluene, and 10 x 10^{-3} mol l^{-1} $CHCl_3$ solution, in the solid state, and as films in 6 % PVK (poly(vinylcarbazole)).

A.4.2 Absorption spectra

The absorption spectrum of EuL^2 shows 3 bands, at 299, 358, and 414 nm corresponding to the absorption bands of Mk, $Eu(fod)_3$, and $Mk:Eu(fod)_3$ respectively.

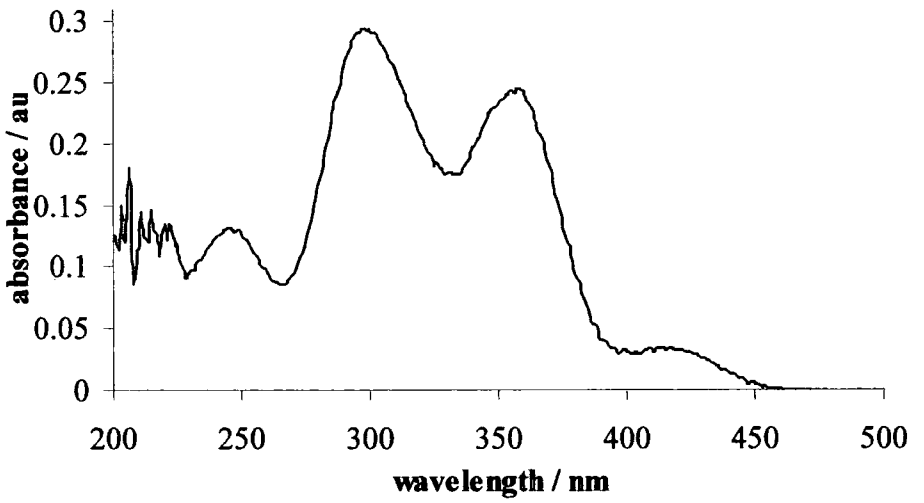

***Figure A-11** Absorption spectrum of EuL^2 in CH_2Cl_2*

The extinction coefficient for this complex at 414 nm in benzene solution as described by Werts *et al.* is 3.04×10^4 mol^{-1} dm^3 cm^{-1}.

A.4.3 Emission and excitation spectra

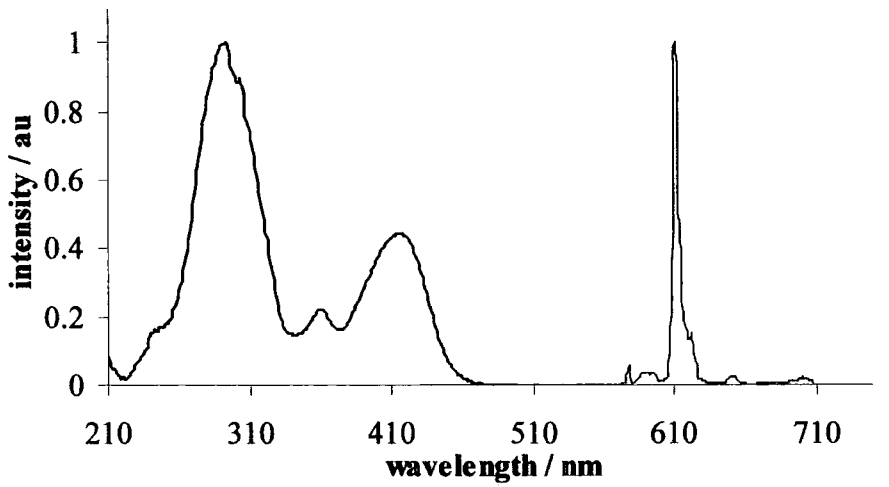

***Figure A-12** Excitation (λ_{em} = 610 nm) and emission (λ_{ex} = 420 nm) spectra of solid state EuL^2, excitation bandpass = 1 nm, emission bandpass = 1 nm*

The excitation spectra show the band at 414 nm as a contributor to the Eu^{3+} emission, with the band at ~ 360 nm showing reduced intensity compared to the absorption spectrum. This band corresponds to the free Michler's ketone molecule, and does not sensitise the Eu^{3+} ions. The band at 414 nm belongs to the Mk:$Eu(fod)_3$ complex, and the band at ~ 300 nm is $Eu(fod)_3$.

The emission spectra show that in this charge-transfer β-diketonate complex, the $\Delta J = 2$ transition dominates the spectrum, with the $\Delta J = 2/\Delta J = 1$ ratio being = 32.

A.4.4 Time resolved data

The lifetimes for all the systems were recorded, and the results are summarised in table A-7.

	solution			**PVK film**		
	$CHCl_3$	**Toluene**	**solid**	**1**	**2**	**3**
τ_1 / ms	0.268	0.263	0.429	0.053	0.040	0.034
τ_2 / ms	-	-	-	0.026	0.023	0.022
A_1	-	-	-	0.46	0.35	0.42
A_2	-	-	-	0.54	0.65	0.58

***Table A-7** Lifetime values for EuL^2 (± 10 %)*

The lifetime values show that the emission is quenched in the PVK films compared to the solid and solution state complexes, this could be due to interactions between the PVK and Eu^{3+} ions.

A.5 Conclusions

The photophysical properties of three potential electroluminescent materials have been presented in various environments.

In the solid state at room temperature, EuL^1 was found to have a double exponential lifetime, indicating the presence of two separate Eu^{3+} emissive sites. Time resolved steady state emission spectra show that the intensity of the hypersensitive $\Delta J = 2$ transition changes with respect to the other transitions in the spectrum at different points along the decay, confirming the presence of more than one site. The emission quantum yield was

determined, and found to be in agreement with the value obtained by Magennis *et al.*

The TbL^1 complex was found to also have a double exponential decay, although in this case the time resolved steady state emission spectra could not resolve them. It was found that the atmospheric environment has little effect on the emission properties of the material. The emission from the TbL^1 complex also showed solvent dependence at room temperature, with the complex being unemissive in dichloromethane and acetonitrile solutions. Although in strongly coordinating solvents such as dimethylsulfoxide, the complex shows metal centred emission.

The EuL^2 complex shows a lower excitation wavelength than most other Ln^{3+} electroluminescent materials. The lifetime data for the complex are presented, and it is shown that the Eu^{3+} lifetime is significantly shorter in a PVK film than in either the solid or solution state complexes.

REFERENCES

[1] C. W. Tang, S. A. VanSlyke, Organic electroluminescent diodes, *Appl. Phys. Lett.*, **1987**, *51*, 913

[2] Y. Shirota, Y. Kuwabara, D. Okuda, R. Okuda, H. Ogawa, H. Inada, T, Wakimoto, H. Nakada, Y. Yonemoto, S. Kawami, K. Imai, Starburst molecules based on π-electron systems as materials for organic electroluminescent devices, *J. Lumin.*, **1997**, *72-74*, 985

[3] J. H. Burroughes, D. D. C. Bradley, A. R. Brown, R. N. Marks, K. Mackay, R. H. Friend, P. L. Burns, A. B. Holmes, Light emitting diodes based on conjugated polymers, *Nature*, 1990, 247, 539

[4] X. C. Gao, H. Cao, C. Huang, B. Li, S. Umitani, Electroluminescence of a novel terbium complex, *Appl. Phys. Lett.*, **1998**, *72*, 2217

[5] X.-C. Gao, H. Cao, C.-H. Huang, S. Umitani, G.-Q Chen, P. Jiang, Photoluminescence and electroluminescence of a series of terbium complexes, *Synth. Metals*, **1999**, *99*, 127

[6] V. Christou, O. V. Salata, T. Q. Ly, S. Cappechi, N. J. Bailey, A. Cowley, A. M. Chippendale, New molecular lanthanide materials for organic electroluminescent devices, *Synth. Metals*, **2000**, *111-112*, 7

[7] A. K. Trikha, L. B. Zinner, K. Zinner, P. C. Isolani, Emission spectra of europium(III) β-diketonate complexes with N-bases, *Polyhedron*, **1998**, *15*, 1651

[8] P. D. Wildes, E. H. White, The dioxetane-sensitised chemiluminescence of lanthanide chelates. A chemical source of "monochromatic" light, *J. Am. Chem. Soc.*, **1971**, 6286

[9] L. R. Melby, N. J. Rose, E. Abramson, J. C. Caris, Synthesis and fluorescence of some trivalent lanthanide complexes, *J. Am. Chem. Soc.*, **1964**, *86*, 5117

[10] R. D. Peacock, The intensities of lanthanide f↔f transitions, *Struct. Bonding*, **1975**, *22*, 82

[11] S. W. Magennis, S. Parsons, A. Corval, J. D. Woolins, Z. Pikramenou, Imidodiphosphinate ligands as antenna units in luminescent lanthanide complexes, *Chem. Commun.*, **1999**, 61

[12] V. Christou, T. Q. Ly, O. V. Salata, S. Cappechi, *Communication*

[13] R. A. Gudmundsen, O. J. Marsh, E. Matovich, Fluorescence of europium thenoyltrifluoroacetonate II. Determination of absolute quantum efficiency, *J. Chem. Phys.*, **1963**, *39*, 272

[14] X.-C. Gao, H. Cao, C.-H. Huang, B.-G. Li, K. Ibrahim, F.-Q. Liu, S. Umitani, Electroluminescence from both a light-emitting layer and hole transport layer: spectral evidence for charge carrier tunnelling injection, *Chem. Phys. Lett.*, **1998**, *297*, 530

[15] M. H. V. Werts, M. A. Duin, J. W. Hofstraat, J. W. Verhoeven, Bathochromacity of Micher's ketone upon coordination with lanthanide(III) β-diketonates enables efficient sensitisation of Eu^{3+} for luminescence under visible light excitation, *Chem. Commun.*, **1999**, 799

APPENDIX B: PUBLICATIONS, SEMINARS ATTENDED

PUBLICATIONS

A. Beeby, L. M. Bushby, D. Maffeo, J. A. G. Williams, The efficient intramolecular sensitisation of terbium(III) and europium(III) ions by benzophenone containing ligands, *J. Chem. Soc., Perkin Trans. 2*, 2000, 1281

A. Beeby, L. M. Bushby, D. Maffeo, J. A. G. Williams, Intramolecular sensitisation of lanthanide(III) luminescence by acetophenone containing ligands: the critical effect of *para*-substituents and solvent, accepted for publication *J. Chem. Soc., Dalton Trans.*, 2001

SEMINARS ATTENDED

1998-1999

October 23 Prof. J. C. Sciano, University of Ottawa, Canada. *In Search of Hypervalent Free Radicals*

October 28 Prof. J. P. S. Badyal, University of Durham, Durham. *Tailoring Solid Surfaces*,

November 3 Dr. C. J. Ludman, University of Durham, Durham. *Bonfire Night Lecture*

November 4 Dr. N. Kaltscoyannis, University College London, London. *Computational Adventures in d and f Element Chemistry*

November 12 Prof. S. Loeb, University of Windsor, Ontario, Canada. *From Macrocycles to Metallo-Supramolecular Chemistry*

November 17 Dr. I. Samuel, University of Durham, Durham. *Polymer Electronics*

December 9 Dr. M. Smith, Warwick Universtiy, Warwick. *Multinuclear Solid-State MagneticResonance Studies of Nanocrystalline Oxides and Glasses*

January 20 Dr. A. Jones, University of Edinburgh, Edinburgh. *Luminescence of Large Molecules: from Conducting Polymers to Coral Reefs*

February 10 Dr. C. Bain, University of Oxford, Oxford. *Surfactant Adsorption and Marangoni Flow at Expanding Liquid Surfaces*

February 17 Dr. B. Horrocks, Newcastle University, Newcastle. *Macroelectrode techniques for the Study of Enzymes and Nucleic Acids at Interfaces*

May 11 Dr. J. Sodeau, University of East Anglia, Norwich. *Ozone Holes and Ozone Hills*

May 12 Dr. D. Bruce, Exeter University, Exeter. *The Synthesis and Characterisation of Liquid-Crystalline Transition Metal Complexes*

1999-2000

October 12 Dr. S. Beckett, Nestle. *Chocolate for the Next Millennium*

October 19 Prof. K. Gloe, TU Dresden, Germany. *Tailor Made Molecules for the Selective Binding of Metal Ions*

November 10 Dr. I. Samuel, University of Durham, Durham. *Improving Organic Light Emitting Diodes by Molecular, Optical and Device Design*

November 18 Dr. G. Siligardi, Kings College, London. *The Use of Circular Dichroism to Detect and Characterise Bimolecular Interactions in Solution*

November 23 Prof. B. Caddy. *Trace Evidence – A Challenge for the Forensic Scientist*

November 24 Prof. T. Jones, Imperial College, London. *Atomic and Molecular Control of Inorganic and Organic Semiconductor Thin Films*

February 15 Prof. D. Philips, Imperial College, London. *A Little Light Relief*

February 23 Dr. N. Clarke, UMIST, Manchester. *The Flow of Polymer Blends*

March 7 Prof. Motherwell, University College, London. *Curiosity and Simplicity – Essential Ingredients for the discovery of New Reactions*

March 20 Prof. S. Marder, University of Arizona, U.S.A. *Design of Molecules for Two-Photon Absorption and their Application to 3D Polymerization and Imaging*

May 3 Prof. R. Hochstrasser, University Pennsylvania, U.S.A. *Ultrafast Molecular and Protein Dynamics seen through their Vibrations*

2000-2001

October 11 Dr. V. Christou, ICL, University of Oxford, Oxford. *Recent Developments in LED Technology: Organolanthanide Phosphors*

October 25 Dr. S. F. Cambell, Former Vice President of Pfizer. *Science, Art, and Drug Discovery – A Personal Perspective*

November 8 Dr. J. P. L. Cox, University of Bath, Bath. *Cosmic: A Universal, DNA-Based Language for Communicating with Aliens and Other Intelligent Lifeforms*

November 29 Prof. T. G. Truscott, University of Keele, Keele. *Life, Death and the Carotenoids*

December 6 Prof. R. Compton, University of Oxford, Oxford. *Dual Activation Approaches to Electroanalysis, Ultrasound, Microwaves, and Laser Activation*

January 10 Prof. S. P. Armes, University of Sussex, Sussex. *Micelles, Reverse Micelles and Shell Cross-Linked Micelles Based on Tertiary Amine Methacrylates*

January 14 Dr. S. Howard, University of Cardiff, Cardiff. *Analysis of Bonding Energy Distribution in Polyatomic Molecules*

January 24 Dr. A. de Mello, Imperial College, London. *Chemical Integrated Circuits: Organic Synthesis and Analysis on a Small Scale*

February 21 Prof. R. Richardson, University of Bristol, Bristol. *Liquid Crystals of All Shapes and Sizes*

April 5 Dr. J. A. G. Williams, University of Durham, Durham. *Luminescent Transition Metal Complexes for Chemical Sensing*

May 2 Prof. R. Perutz, University of York, York. *Escapades with Arenes and Transition Metals from Laser Spectroscopy to Synthetic Applications*